## CITATION REPORT List of articles citing

Standardized nomenclature, symbols, and units for bone histomorphometry: a 2012 update of the report of the ASBMR Histomorphometry Nomenclature Committee

DOI: 10.1002/jbmr.1805 Journal of Bone and Mineral Research, 2013, 28, 2-17.

**Source:** https://exaly.com/paper-pdf/55475876/citation-report.pdf

Version: 2024-04-25

This report has been generated based on the citations recorded by exaly.com for the above article. For the latest version of this publication list, visit the link given above.

The third column is the impact factor (IF) of the journal, and the fourth column is the number of citations of the article.

#	Paper IF	Citations
1847	Actions of osteoporosis treatments on bone histomorphometric remodeling: a two-fold principal component analysis. <b>2013</b> , 24, 3011-9	1
1846	Micro-morphological properties of osteons reveal changes in cortical bone stability during aging, osteoporosis, and bisphosphonate treatment in women. <b>2013</b> , 24, 2671-80	59
1845	The effect of endogenous parathyroid hormone in iliac bone structure and turnover in healthy postmenopausal women. <b>2013</b> , 93, 288-95	1
1844	Low protein intake magnifies detrimental effects of ovariectomy and vitamin D on bone. <b>2013</b> , 93, 184-92	2
1843	Bone microarchitecture of the talus changes with aging. <b>2013</b> , 471, 3663-71	8
1842	Effect of implanted bisphosphonate-enriched cement on the trabecular microarchitecture of bone in a rat model using micro-computed tomography. <b>2013</b> , 37, 1187-93	9
1841	Gelatin hydrogel carrier with the W9-peptide elicits synergistic effects on BMP-2-induced bone regeneration. <b>2013</b> , 55, 217-223	13
1840	Lessons from Bone Histomorphometry on the Mechanisms of Action of Osteoporosis Drugs. <b>2013</b> , 1777-1803	5 о
1839	Bone morphogenetic proteins signal via SMAD and mitogen-activated protein (MAP) kinase pathways at distinct times during osteoclastogenesis. <b>2013</b> , 288, 37230-40	46
1838	(18)F-fluoride positron emission tomography measurements of regional bone formation in hemodialysis patients with suspected adynamic bone disease. <b>2013</b> , 93, 436-47	21
1837	Reversing bone loss by directing mesenchymal stem cells to bone. <b>2013</b> , 31, 2003-14	68
1836	Application of design-based stereology for estimation of absolute volume and surface area of the articular and calcified cartilage compartments of undecalcified human femoral heads. <b>2013</b> , 251, 133-43	9
1835	. 2013,	
1834	Evaluation of Trabecular Microarchitecture of Normal Osteoporotic and Osteopenic Human Vertebrae. <b>2013</b> , 59, 6-15	11
1833	Cortical porosity in children is determined by age-dependent osteonal morphology. <b>2013</b> , 55, 476-86	17
1832	Teriparatide for idiopathic osteoporosis in premenopausal women: a pilot study. <b>2013</b> , 98, 1971-81	64
1831	R-Spondin 1 promotes vibration-induced bone formation in mouse models of osteoporosis. <b>2013</b> , 91, 1421-9	21

1830	Notch signaling in osteocytes differentially regulates cancellous and cortical bone remodeling. <b>2013</b> , 288, 25614-25625	73
1829	Influence of gastrectomy on cortical and cancellous bones in rats. <b>2013</b> , 2013, 381616	5
1828	The role of osteocytes in bone resorption during orthodontic tooth movement. <b>2013</b> , 92, 340-5	51
1827	A mouse model for human osteogenesis imperfecta type VI. <i>Journal of Bone and Mineral Research</i> , <b>2013</b> , 28, 1531-6	41
1826	Nondestructive, epi-illumination surface microscopic characterization of surface discontinuity in bone: a new approach offers a descriptive vocabulary and new insights. <b>2013</b> , 296, 580-9	8
1825	Altered thermogenesis and impaired bone remodeling in Misty mice. <i>Journal of Bone and Mineral Research</i> , <b>2013</b> , 28, 1885-97	46
1824	Absence of Cx43 selectively from osteocytes enhances responsiveness to mechanical force in mice. <b>2013</b> , 31, 1075-81	76
1823	Resorption controls bone anabolism driven by parathyroid hormone (PTH) receptor signaling in osteocytes. <b>2013</b> , 288, 29809-20	37
1822	Seven day insertion rest in whole body vibration improves multi-level bone quality in tail suspension rats. <b>2014</b> , 9, e92312	23
1821	Systemic but no local effects of combined zoledronate and parathyroid hormone treatment in experimental autoimmune arthritis. <b>2014</b> , 9, e92359	8
1820	Plasminogen activator inhibitor-1 is involved in impaired bone repair associated with diabetes in female mice. <b>2014</b> , 9, e92686	36
1819	The effects of a novel hormonal breast cancer therapy, endoxifen, on the mouse skeleton. <b>2014</b> , 9, e98219	5
1818	SH3BP2 gain-of-function mutation exacerbates inflammation and bone loss in a murine collagen-induced arthritis model. <b>2014</b> , 9, e105518	13
1817	A magnesium based phosphate binder reduces vascular calcification without affecting bone in chronic renal failure rats. <b>2014</b> , 9, e107067	29
1816	Effects of different types of jump impact on trabecular bone mass and microarchitecture in growing rats. <b>2014</b> , 9, e107953	16
1815	Raloxifene prevents skeletal fragility in adult female Zucker Diabetic Sprague-Dawley rats. <b>2014</b> , 9, e108262	9
1814	Dimethyloxalylglycine prevents bone loss in ovariectomized C57BL/6J mice through enhanced angiogenesis and osteogenesis. <b>2014</b> , 9, e112744	43
1813	Effects of zoledronic acid on physiologic bone remodeling of condylar part of TMJ: a radiologic and histomorphometric examination in rabbits. <b>2014</b> , 2014, 649026	5

1812	Fibroblast growth factor-2 isoform (low molecular weight/18 kDa) overexpression in preosteoblast cells promotes bone regeneration in critical size calvarial defects in male mice. <b>2014</b> , 155, 965-74		22
1811	FGF-21 and skeletal remodeling during and after lactation in C57BL/6J mice. <b>2014</b> , 155, 3516-26		49
1810	Sirtuin1 (Sirt1) promotes cortical bone formation by preventing Latenin sequestration by FoxO transcription factors in osteoblast progenitors. <b>2014</b> , 289, 24069-78		86
1809	Total body irradiation is permissive for mesenchymal stem cell-mediated new bone formation following local transplantation. <b>2014</b> , 20, 3212-27		14
1808	Recent developments in metabolic bone diseases: a gnathic perspective. <b>2014</b> , 8, 475-81		5
1807	Autophagy in osteoblasts is involved in mineralization and bone homeostasis. <b>2014</b> , 10, 1965-77		214
1806	The effect of estrogen on bone requires ERHn nonhematopoietic cells but is enhanced by ERHn hematopoietic cells. <b>2014</b> , 307, E589-95		13
1805	Pre-suckling calcium supplementation effectively prevents lactation-induced osteopenia in rats. <b>2014</b> , 306, E177-88		13
1804	Negative influence of a long-term high-fat diet on murine bone architecture. <b>2014</b> , 2014, 318924		22
1803	Nongenomic thyroid hormone signaling occurs through a plasma membrane-localized receptor. <b>2014</b> , 7, ra48		97
1802	Effect of ovariectomy on stimulating intracortical remodeling in rats. <b>2014</b> , 2014, 421431		10
1801	Prenatal Exposure to Continuous Constant Light Alters Endochondral Ossification of the Tibiae of Rat Pups. <b>2014</b> , 200, 278-86		2
1800	Early-onset type 2 diabetes impairs skeletal acquisition in the male TALLYHO/JngJ mouse. <b>2014</b> , 155, 3806-16		61
1799	The impact of low-magnitude high-frequency vibration on fracture healing is profoundly influenced by the oestrogen status in mice. <b>2015</b> , 8, 93-104		46
1798	Diet-derived phenolic acids regulate osteoblast and adipocyte lineage commitment and differentiation in young mice. <i>Journal of Bone and Mineral Research</i> , <b>2014</b> , 29, 1043-53	6.3	29
1797	When, how, and why a bone biopsy should be performed in patients with chronic kidney disease. <b>2014</b> , 34, 612-25		45
1796	Tissue-level mechanisms responsible for the increase in bone formation and bone volume by sclerostin antibody. <i>Journal of Bone and Mineral Research</i> , <b>2014</b> , 29, 1424-30	6.3	108
1795	Physiological functions of osteoblast lineage and T cell-derived RANKL in bone homeostasis. Journal of Bone and Mineral Research, <b>2014</b> , 29, 830-42	6.3	51

1794	Oxytocin reverses ovariectomy-induced osteopenia and body fat gain. <b>2014</b> , 155, 1340-52		46
1793	Testosterone dose dependently prevents bone and muscle loss in rodents after spinal cord injury. <b>2014</b> , 31, 834-45		41
1792	Dysapoptosis of osteoblasts and osteocytes increases cancellous bone formation but exaggerates cortical porosity with age. <i>Journal of Bone and Mineral Research</i> , <b>2014</b> , 29, 103-17	6.3	52
1791	Disruption of Lrp4 function by genetic deletion or pharmacological blockade increases bone mass and serum sclerostin levels. <b>2014</b> , 111, E5187-95		83
1790	Identical subchondral bone microarchitecture pattern with increased bone resorption in rheumatoid arthritis as compared to osteoarthritis. <b>2014</b> , 22, 2083-92		18
1789	Influence of physical activity on bone strength in children and adolescents: a systematic review and narrative synthesis. <i>Journal of Bone and Mineral Research</i> , <b>2014</b> , 29, 2161-81	6.3	144
1788	Reproducibility of results in preclinical studies: a perspective from the bone field. <i>Journal of Bone and Mineral Research</i> , <b>2014</b> , 29, 2131-40	6.3	33
1787	Glucocorticoid-induced osteoporosis in growing rats. <b>2014</b> , 95, 362-73		34
1786	Nemo-like kinase regulates postnatal skeletal homeostasis. <b>2014</b> , 229, 1736-43		5
1785	Osteoclast-derived complement component 3a stimulates osteoblast differentiation. <i>Journal of Bone and Mineral Research</i> , <b>2014</b> , 29, 1522-30	6.3	106
1784	Antagonizing the B integrin inhibits angiogenesis and impairs woven but not lamellar bone formation induced by mechanical loading. <i>Journal of Bone and Mineral Research</i> , <b>2014</b> , 29, 1970-80	6.3	10
1783	Soluble guanylate cyclase as a novel treatment target for osteoporosis. <b>2014</b> , 155, 4720-30		30
1782	Bone disease in newly diagnosed lupus nephritis patients. <b>2014</b> , 9, e106728		4
1781	Different approaches for interpretation and reporting of immunohistochemistry analysis results in the bone tissue - a review. <b>2014</b> , 9, 221		277
1780	The effect of erythropoietin on bone. <b>2014</b> , 85, 1-27		6
1779	Endogenous bone regeneration is dependent upon a dynamic oxygen event. <i>Journal of Bone and Mineral Research</i> , <b>2014</b> , 29, 2336-45	6.3	32
1778	High bone mass in mice lacking Cx37 because of defective osteoclast differentiation. <b>2014</b> , 289, 8508-2	:0	49

1776	Increased resistance during jump exercise does not enhance cortical bone formation. <b>2014</b> , 46, 982-9	2
1775	Running exercise alleviates trabecular bone loss and osteopenia in hemizygous Eglobin knockout thalassemic mice. <b>2014</b> , 306, E1406-17	15
1774	Vitamin K-dependent carboxylation of osteocalcin affects the efficacy of teriparatide (PTH(1-34)) for skeletal repair. <b>2014</b> , 64, 95-101	17
1773	Adiponectin receptor 1 regulates bone formation and osteoblast differentiation by GSK-3/Etatenin signaling in mice. <b>2014</b> , 64, 147-54	49
1772	Nano-structural, compositional and micro-architectural signs of cortical bone fragility at the superolateral femoral neck in elderly hip fracture patients vs. healthy aged controls. <b>2014</b> , 55, 19-28	46
1771	Does methamphetamine affect bone metabolism?. <b>2014</b> , 319, 63-8	9
1770	Notch1 and Notch2 expression in osteoblast precursors regulates femoral microarchitecture. <b>2014</b> , 62, 22-8	29
1769	Correlation between absence of bone remodeling compartment canopies, reversal phase arrest, and deficient bone formation in post-menopausal osteoporosis. <b>2014</b> , 184, 1142-1151	29
1768	The resistance of cortical bone tissue to failure under cyclic loading is reduced with alendronate. <b>2014</b> , 64, 57-64	40
1767	Mineralocorticoid receptor function in bone metabolism and its role in glucocorticoid-induced osteopenia. <b>2014</b> , 447, 407-12	24
1766	Techniques in Histomorphometry. <b>2014</b> , 131-148	6
1765	The sclerostin-independent bone anabolic activity of intermittent PTH treatment is mediated by T-cell-produced Wnt10b. <i>Journal of Bone and Mineral Research</i> , <b>2014</b> , 29, 43-54	52
1764	Reversing LRP5-dependent osteoporosis and SOST deficiency-induced sclerosing bone disorders by altering WNT signaling activity. <i>Journal of Bone and Mineral Research</i> , <b>2014</b> , 29, 29-42	53
1763	Increased tartrate-resistant Acid phosphatase expression in osteoblasts and osteocytes in experimental osteoporosis in rats. <b>2014</b> , 94, 510-21	20
1762	Effects of dried plum supplementation on bone metabolism in adult C57BL/6 male mice. <b>2014</b> , 94, 442-53	24
1761	Leptin receptor deficient diabetic (db/db) mice are compromised in postnatal bone regeneration. <b>2014</b> , 356, 195-206	21
1760	Effects of up to 5 years of denosumab treatment on bone histology and histomorphometry: the FREEDOM study extension. <i>Journal of Bone and Mineral Research</i> , <b>2014</b> , 29, 2051-6	47
1759	Accuracy of trabecular structure by HR-pQCT compared to gold standard IT in the radius and tibia of patients with osteoporosis and long-term bisphosphonate therapy. <b>2014</b> , 25, 1595-606	27

1758	Pediatric solid organ transplantation and osteoporosis: a descriptive study on bone histomorphometric findings. <b>2014</b> , 29, 1431-40		16
1757	1,25(OH) Dunduces a mineralization defect and loss of bone mineral density in genetic hypercalciuric stone-forming rats. <b>2014</b> , 94, 531-43		14
1756	Bone loss during partial weight bearing (1/6th gravity) is mitigated by resistance and aerobic exercise in mice. <b>2014</b> , 99, 71-77		3
1755	TNF-Eupregulates sclerostin expression in obese mice fed a high-fat diet. <b>2014</b> , 229, 640-50		67
1754	Bone histomorphometry of transiliac paired bone biopsies after 6 or 12 months of treatment with oral strontium ranelate in 387 osteoporotic women: randomized comparison to alendronate.  Journal of Bone and Mineral Research, 2014, 29, 618-28	6.3	48
1753	The C-terminal domain of chondroadherin: a new regulator of osteoclast motility counteracting bone loss. <i>Journal of Bone and Mineral Research</i> , <b>2014</b> , 29, 1833-46	6.3	14
1752	Deletion of a single Etatenin allele in osteocytes abolishes the bone anabolic response to loading. Journal of Bone and Mineral Research, <b>2014</b> , 29, 705-15	6.3	93
1751	Acceleration of bone regeneration by local application of lithium: Wnt signal-mediated osteoblastogenesis and Wnt signal-independent suppression of osteoclastogenesis. <b>2014</b> , 90, 397-405		53
1750	Inhibition of cathepsin K increases modeling-based bone formation, and improves cortical dimension and strength in adult ovariectomized monkeys. <i>Journal of Bone and Mineral Research</i> , <b>2014</b> , 29, 1847-58	6.3	49
1749	ETCP granules mixed with reticulated hyaluronic acid induce an increase in bone apposition. <b>2014</b> , 9, 015001		12
1748	Protective effects of necrostatin-1 on glucocorticoid-induced osteoporosis in rats. <b>2014</b> , 144 Pt B, 455-6	52	17
1747	Mechanism and function of monoclonal antibodies targeting siglec-15 for therapeutic inhibition of osteoclastic bone resorption. <b>2014</b> , 289, 6498-6512		47
1746	Temporal changes in systemic and local expression of bone turnover markers during six months of sclerostin antibody administration to ovariectomized rats. <b>2014</b> , 67, 305-13		69
1745	DPP IV inhibitor treatment attenuates bone loss and improves mechanical bone strength in male diabetic rats. <b>2014</b> , 307, E447-55		51
1744	Morbid obesity attenuates the skeletal abnormalities associated with leptin deficiency in mice. <b>2014</b> , 223, M1-15		25
1743	Stk11 (Lkb1) deletion in the osteoblast lineage leads to high bone turnover, increased trabecular bone density and cortical porosity. <b>2014</b> , 69, 98-108		12
1742	The influence of age on adaptive bone formation and bone resorption. <b>2014</b> , 35, 9290-301		79
1741	Increased osteopontin contributes to inhibition of bone mineralization in FGF23-deficient mice. Journal of Bone and Mineral Research, <b>2014</b> , 29, 693-704	6.3	67

1740	Development, validation and characterization of a novel mouse model of Adynamic Bone Disease (ABD). <b>2014</b> , 68, 57-66		8
1739	Influence of aromatase inhibition on the bone-protective effects of testosterone. <i>Journal of Bone and Mineral Research</i> , <b>2014</b> , 29, 2405-13	6.3	23
1738	Effect of sclerostin antibody treatment in a mouse model of severe osteogenesis imperfecta. <b>2014</b> , 66, 182-8		73
1737	Effect of sequential treatments with alendronate, parathyroid hormone (1-34) and raloxifene on cortical bone mass and strength in ovariectomized rats. <b>2014</b> , 67, 257-68		21
1736	PTH1-34 alleviates radiotherapy-induced local bone loss by improving osteoblast and osteocyte survival. <b>2014</b> , 67, 33-40		58
1735	Chronic kidney disease and osteoporosis: evaluation and management. <b>2014</b> , 3, 542		36
1734	Does collagen trigger the recruitment of osteoblasts into vacated bone resorption lacunae during bone remodeling?. <b>2014</b> , 67, 181-8		34
1733	Retinaldehyde dehydrogenase 1 deficiency inhibits PPAREmediated bone loss and marrow adiposity. <b>2014</b> , 67, 281-91		7
1732	The role of CT analyses of the sternal end of the clavicle and the first costal cartilage in age estimation. <b>2014</b> , 128, 825-39		22
1731	Tsc2 is a molecular checkpoint controlling osteoblast development and glucose homeostasis. <b>2014</b> , 34, 1850-62		45
1730	Improved trabecular bone structure of 20-month-old male spontaneously hypertensive rats. <b>2014</b> , 95, 282-91		7
1729	Lanthanum carbonate stimulates bone formation in a rat model of renal insufficiency with low bone turnover. <b>2014</b> , 32, 484-93		6
1728	Cathepsin S controls adipocytic and osteoblastic differentiation, bone turnover, and bone microarchitecture. <b>2014</b> , 64, 281-7		23
1727	CLCN7 and TCIRG1 mutations differentially affect bone matrix mineralization in osteopetrotic individuals. <i>Journal of Bone and Mineral Research</i> , <b>2014</b> , 29, 982-91	6.3	25
1726	Mineral bone disorder in chronic kidney disease: head-to-head comparison of the 5/6 nephrectomy and adenine models. <b>2014</b> , 15, 69		33
1725	Prostate cancer cells preferentially home to osteoblast-rich areas in the early stages of bone metastasis: evidence from in vivo models. <i>Journal of Bone and Mineral Research</i> , <b>2014</b> , 29, 2688-96	6.3	87
1724	Engineered nanomedicine for myeloma and bone microenvironment targeting. <b>2014</b> , 111, 10287-92		204
1723	Reduced trabecular bone mass and strength in mice overexpressing G#1 protein in cells of the osteoblast lineage. <b>2014</b> , 59, 211-22		8

1722	Generation of the first autosomal dominant osteopetrosis type II (ADO2) disease models. <b>2014</b> , 59, 66-75	25
1721	Bone disease in CKD: a focus on osteoporosis diagnosis and management. <b>2014</b> , 64, 290-304	77
1720	Beneficial effects of a N-terminally modified GIP agonist on tissue-level bone material properties. <b>2014</b> , 63, 61-8	30
1719	Aging diminishes lamellar and woven bone formation induced by tibial compression in adult C57BL/6. <b>2014</b> , 65, 83-91	70
1718	Effects of teriparatide on cortical histomorphometric variables in postmenopausal women with or without prior alendronate treatment. <b>2014</b> , 59, 139-47	63
1717	A comparative study of the bone metabolic response to dried plum supplementation and PTH treatment in adult, osteopenic ovariectomized rat. <b>2014</b> , 58, 151-9	37
1716	Hepatic lipase is expressed by osteoblasts and modulates bone remodeling in obesity. <b>2014</b> , 62, 90-8	6
1715	Effect of combined teriparatide and monthly minodronic acid therapy on cancellous bone mass in ovariectomized rats: a bone histomorphometry study. <b>2014</b> , 64, 88-94	8
1714	Osteoporosis update: proceedings of the 2013 Santa Fe Bone Symposium. <b>2014</b> , 17, 330-43	7
1713	Mineralizing surface is the main target of mechanical stimulation independent of age: 3D dynamic in vivo morphometry. <b>2014</b> , 66, 15-25	77
1712	Molecular evidence of osteoblast dysfunction in elderly men with osteoporotic hip fractures. <b>2014</b> , 57, 114-21	14
1711	Bisphosphonate-osteoclasts: changes in osteoclast morphology and function induced by antiresorptive nitrogen-containing bisphosphonate treatment in osteoporosis patients. <b>2014</b> , 59, 37-43	80
1710	Hypoxia-inducible factor-1#estricts the anabolic actions of parathyroid hormone. <b>2014</b> , 2, 14005	16
1709	Nrf2 is required for normal postnatal bone acquisition in mice. <b>2014</b> , 2, 14033	29
1708	Chronic kidney disease and the skeleton. <b>2014</b> , 2, 14044	28
1707	SH3BP2 cherubism mutation potentiates TNF-Induced osteoclastogenesis via NFATc1 and TNF-Imediated inflammatory bone loss. <i>Journal of Bone and Mineral Research</i> , <b>2014</b> , 29, 2618-35	45
1706	Histomorphometric Assessment of Cancellous and Cortical Bone Material Distribution in the Proximal Humerus of Normal and Osteoporotic Individuals: Significantly Reduced Bone Stock in the Metaphyseal and Subcapital Regions of Osteoporotic Individuals. <b>2015</b> , 94, e2043	16
1705	Myelosuppressive therapies significantly increase pro-inflammatory cytokines and directly cause bone loss. <i>Journal of Bone and Mineral Research</i> , <b>2015</b> , 30, 886-97	34

1704	PTH Signaling During Exercise Contributes to Bone Adaptation. <i>Journal of Bone and Mineral Research</i> , <b>2015</b> , 30, 1053-63	6.3	36
1703	Establishing biomechanical mechanisms in mouse models: practical guidelines for systematically evaluating phenotypic changes in the diaphyses of long bones. <i>Journal of Bone and Mineral Research</i> , <b>2015</b> , 30, 951-66	6.3	154
1702	Thiazide-sensitive Na+ -Cl- cotransporter (NCC) gene inactivation results in increased duodenal Ca2+ absorption, enhanced osteoblast differentiation and elevated bone mineral density. <i>Journal of Bone and Mineral Research</i> , <b>2015</b> , 30, 116-27	6.3	19
1701	Modifications to nano- and microstructural quality and the effects on mechanical integrity in Paget's disease of bone. <i>Journal of Bone and Mineral Research</i> , <b>2015</b> , 30, 264-73	6.3	40
1700	Gender-Specific Differences in the Skeletal Response to Continuous PTH in Mice Lacking the IGF1 Receptor in Mature Osteoblasts. <i>Journal of Bone and Mineral Research</i> , <b>2015</b> , 30, 1064-76	6.3	10
1699	Bone volume fraction and fabric anisotropy are better determinants of trabecular bone stiffness than other morphological variables. <i>Journal of Bone and Mineral Research</i> , <b>2015</b> , 30, 1000-8	6.3	93
1698	The Effects of Combined Treatment with Naringin and Treadmill Exercise on Osteoporosis in Ovariectomized Rats. <b>2015</b> , 5, 13009		28
1697	Effective Small Interfering RNA Therapy to Treat CLCN7-dependent Autosomal Dominant Osteopetrosis Type 2. <b>2015</b> , 4, e248		14
1696	Hypoxia-reperfusion affects osteogenic lineage and promotes sickle cell bone disease. <b>2015</b> , 126, 2320	-8	31
1695	Administration of soluble activin receptor 2B increases bone and muscle mass in a mouse model of osteogenesis imperfecta. <b>2015</b> , 3, 14042		36
1694	Effect of vitamin K2 on the development of stress-induced osteopenia in a growing senescence-accelerated mouse prone 6 strain. <b>2015</b> , 10, 843-850		3
1693	Skin wound trauma, following high-dose radiation exposure, amplifies and prolongs skeletal tissue loss. <b>2015</b> , 81, 487-494		5
1692	Optineurin Negatively Regulates Osteoclast Differentiation by Modulating NF- <b>B</b> and Interferon Signaling: Implications for Paget's Disease. <b>2015</b> , 13, 1096-1102		46
1691	Prolonged performance of a high repetition low force task induces bone adaptation in young adult rats, but loss in mature rats. <b>2015</b> , 72, 204-17		17
1690	High-fat diet-induced obesity triggers alveolar bone loss and spontaneous periodontal disease in growing mice. <b>2015</b> , 3, 1		39
1689	The bone-sparing effects of estrogen and WNT16 are independent of each other. <b>2015</b> , 112, 14972-7		32
1688	Effects of Deletion of ER#n Osteoblast-Lineage Cells on Bone Mass and Adaptation to Mechanical Loading Differ in Female and Male Mice. <i>Journal of Bone and Mineral Research</i> , <b>2015</b> , 30, 1468-80	6.3	38
1687	High-dose therapy improves the bone remodelling compartment canopy coverage and bone formation in multiple myeloma. <b>2015</b> , 171, 355-65		3

1686	Dysregulated TGF-Isignaling alters bone microstructure in a mouse model of Loeys-Dietz syndrome. <b>2015</b> , 33, 1447-54		7	
1685	Reversible Deterioration in Hypophosphatasia Caused by Renal Failure With Bisphosphonate Treatment. <i>Journal of Bone and Mineral Research</i> , <b>2015</b> , 30, 1726-37	6.3	40	
1684	Neural Crest-Specific TSC1 Deletion in Mice Leads to Sclerotic Craniofacial Bone Lesion. <i>Journal of Bone and Mineral Research</i> , <b>2015</b> , 30, 1195-205	6.3	27	
1683	Blockage of Src by Specific siRNA as a Novel Therapeutic Strategy to Prevent Destructive Repair in Steroid-Associated Osteonecrosis in Rabbits. <i>Journal of Bone and Mineral Research</i> , <b>2015</b> , 30, 2044-57	6.3	25	
1682	Calcilytic Ameliorates Abnormalities of Mutant Calcium-Sensing Receptor (CaSR) Knock-In Mice Mimicking Autosomal Dominant Hypocalcemia (ADH). <i>Journal of Bone and Mineral Research</i> , <b>2015</b> , 30, 1980-93	6.3	40	
1681	Stable Incretin Mimetics Counter Rapid Deterioration of Bone Quality in Type 1 Diabetes Mellitus. <b>2015</b> , 230, 3009-18		50	
1680	High doses of caffeine reduce in⊡ivo osteogenic activity in prepubertal rats. <b>2015</b> , 227, 10-20		10	
1679	Osteoblast-Specific Loss of IGF1R Signaling Results in Impaired Endochondral Bone Formation During Fracture Healing. <i>Journal of Bone and Mineral Research</i> , <b>2015</b> , 30, 1572-84	6.3	40	
1678	Paradoxical effects of partial leptin deficiency on bone in growing female mice. 2015, 298, 2018-29		11	
1677	Young Coconut Juice Supplementation Results in Greater Bone Mass and Bone Formation Indices in Ovariectomized Rats: A Preliminary Study. <b>2015</b> , 29, 1950-5		5	
1676	Disturbances in Bone Largely Predict Aortic Calcification in an Alternative Rat Model Developed to Study Both Vascular and Bone Pathology in Chronic Kidney Disease. <i>Journal of Bone and Mineral Research</i> , <b>2015</b> , 30, 2313-24	6.3	15	
1675	Intramembranous bone regeneration differs among common inbred mouse strains following marrow ablation. <b>2015</b> , 33, 1374-81		5	
1674	Ergonomic task reduction prevents bone osteopenia in a rat model of upper extremity overuse. <b>2015</b> , 53, 206-21		11	
1673	Nanogel-crosslinked nanoparticles increase the inhibitory effects of W9 synthetic peptide on bone loss in a murine bone resorption model. <b>2015</b> , 10, 3459-73		8	
1672	Effects of Combined Exposure to Lead and High-Fat Diet on Bone Quality in Juvenile Male Mice. <b>2015</b> , 123, 935-43		32	
1671	Effects of dexamethasone, celecoxib, and methotrexate on the histology and metabolism of bone tissue in healthy Sprague Dawley rats. <b>2015</b> , 10, 1245-53		21	
1670	Skeletal Assessments in the Nonhuman Primate. <b>2015</b> , 605-625		3	
1669	3D Porous Architecture of Stacks of ETCP Granules Compared with That of Trabecular Bone: A microCT, Vector Analysis, and Compression Study. <b>2015</b> , 6, 161		13	

1668	St. John's Wort (Hypericum perforatum) stimulates human osteoblastic MG-63 cell proliferation and attenuates trabecular bone loss induced by ovariectomy. <b>2015</b> , 9, 459-65	11
1667	Cyclooxygenase-2 suppresses the anabolic response to PTH infusion in mice. <b>2015</b> , 10, e0120164	9
1666	Protection against T1DM-Induced Bone Loss by Zinc Supplementation: Biomechanical, Histomorphometric, and Molecular Analyses in STZ-Induced Diabetic Rats. <b>2015</b> , 10, e0125349	30
1665	Impaired Fracture Healing Caused by Deficiency of the Immunoreceptor Adaptor Protein DAP12. <b>2015</b> , 10, e0128210	11
1664	Differential Effects of Dabigatran and Warfarin on Bone Volume and Structure in Rats with Normal Renal Function. <b>2015</b> , 10, e0133847	33
1663	Mechanical Loading Synergistically Increases Trabecular Bone Volume and Improves Mechanical Properties in the Mouse when BMP Signaling Is Specifically Ablated in Osteoblasts. <b>2015</b> , 10, e0141345	24
1662	Establishment of an Animal Model of Bisphosphonate-Related Osteonecrosis of the Jaws in Spontaneously Diabetic Torii Rats. <b>2015</b> , 10, e0144355	11
1661	Application of AMOR in craniofacial rabbit bone bioengineering. <b>2015</b> , 2015, 628769	7
1660	Association of MRS-Based Vertebral Bone Marrow Fat Fraction with Bone Strength in a Human In Vitro Model. <b>2015</b> , 2015, 152349	26
1659	Modifications in bone matrix of estrogen-deficient rats treated with intermittent PTH. <b>2015</b> , 2015, 454162	10
1658	Activation of Nfatc2 in osteoblasts causes osteopenia. <b>2015</b> , 230, 1689-95	11
1657	Characterization of bone turnover and energy metabolism in a rat model of primary and secondary osteoporosis. <b>2015</b> , 67, 287-96	9
1656	DLK1 Regulates Whole-Body Glucose Metabolism: A Negative Feedback Regulation of the Osteocalcin-Insulin Loop. <b>2015</b> , 64, 3069-80	32
1655	Teriparatide and bone turnover and formation in a hemodialysis patient with low-turnover bone disease: a case report. <b>2015</b> , 65, 933-6	25
1654	Regional Heterogeneity in the Configuration of the Intracortical Canals of the Femoral Shaft. <b>2015</b> , 97, 327-35	23
1653	Bone microstructural defects and osteopenia in hemizygous IVSII-654 knockin thalassemic mice: sex-dependent changes in bone density and osteoclast function. <b>2015</b> , 309, E936-48	10
1652	Are Biochemical Markers of Bone Turnover Representative of Bone Histomorphometry in 370 Postmenopausal Women?. <b>2015</b> , 100, 4662-8	55
1651	The inhibitory effects of a RANKL-binding peptide on articular and periarticular bone loss in a murine model of collagen-induced arthritis: a bone histomorphometric study. <b>2015</b> , 17, 251	23

## (2015-2015)

1650	Loss of bone strength in HLA-B27 transgenic rats is characterized by a high bone turnover and is mainly osteoclast-driven. <b>2015</b> , 75, 183-91	7	
1649	Loss of Runx2 in committed osteoblasts impairs postnatal skeletogenesis. <i>Journal of Bone and Mineral Research</i> , <b>2015</b> , 30, 71-82	34	
1648	HIF-1#egulates bone formation after osteogenic mechanical loading. <b>2015</b> , 73, 98-104	21	
1647	Bone histomorphometry before and after long-term treatment with cinacalcet in dialysis patients with secondary hyperparathyroidism. <b>2015</b> , 87, 846-56	125	
1646	Comparison of osteoconductive properties of three different Etricalcium phosphate graft materials: a pilot histomorphometric study in a pig model. <b>2015</b> , 43, 175-80	14	
1645	Effect of in vivo loading on bone composition varies with animal age. <b>2015</b> , 63, 48-58	18	
1644	Repositioning Potential of PAK4 to Osteoclastic Bone Resorption. <i>Journal of Bone and Mineral Research</i> , <b>2015</b> , 30, 1494-507	6	
1643	Osteoblast menin regulates bone mass in vivo. <b>2015</b> , 290, 3910-24	21	
1642	The 🗚 binding domain of chondroadherin inhibits breast cancer-induced bone metastases and impairs primary tumour growth: a preclinical study. <b>2015</b> , 358, 67-75	12	
1641	Cortical and trabecular bone in pediatric end-stage kidney disease. <b>2015</b> , 30, 497-502	9	
1640	Oncostatin m, an inflammatory cytokine produced by macrophages, supports intramembranous bone healing in a mouse model of tibia injury. <b>2015</b> , 185, 765-75	79	
1639	Modulation of bone's sensitivity to low-intensity vibrations by acceleration magnitude, vibration duration, and number of bouts. <b>2015</b> , 26, 1417-28	10	
1638	Siglec-15 is a potential therapeutic target for postmenopausal osteoporosis. <b>2015</b> , 71, 217-26	34	
1637	Exercise training, creatine supplementation, and bone health in ovariectomized rats. <b>2015</b> , 26, 1395-404	7	
1636	Mesenchymal stem cell expression of stromal cell-derived factor-1 daugments bone formation in a model of local regenerative therapy. <b>2015</b> , 33, 174-84	10	
1635	A special healing pattern in stable metaphyseal fractures. <b>2015</b> , 86, 238-42	29	
1634	Adverse Effects of Osteocytic Constitutive Activation of Ecatenin on Bone Strength and Bone Growth. <i>Journal of Bone and Mineral Research</i> , <b>2015</b> , 30, 1184-94	31	
1633	Bisphosphonate-associated atypical sub-trochanteric femur fractures: paired bone biopsy quantitative histomorphometry before and after teriparatide administration. <b>2015</b> , 44, 477-482	26	

1632	Intermittent administration of teriparatide enhances graft bone healing and accelerates spinal fusion in rats with glucocorticoid-induced osteoporosis. <b>2015</b> , 15, 298-306	32
1631	Loss of SH3 domain-binding protein 2 function suppresses bone destruction in tumor necrosis factor-driven and collagen-induced arthritis in mice. <b>2015</b> , 67, 656-67	23
1630	Impact of radiation history, gender and age on bone quality in sites for orthodontic skeletal anchorage device placement. <b>2015</b> , 199, 67-72	2
1629	Osteocytes mediate the anabolic actions of canonical Wnt/Etatenin signaling in bone. 2015, 112, E478-86	167
1628	Suppression of autophagy in osteocytes does not modify the adverse effects of glucocorticoids on cortical bone. <b>2015</b> , 75, 18-26	37
1627	Effects of saliva on early post-tooth extraction tissue repair in rats. <b>2015</b> , 23, 241-50	6
1626	Poly(amido amine)-based multilayered thin films on 2D and 3D supports for surface-mediated cell transfection. <b>2015</b> , 205, 181-9	7
1625	Cortical bone histomorphometry in male femoral neck: the investigation of age-association and regional differences. <b>2015</b> , 96, 295-306	15
1624	Odanacatib for the treatment of postmenopausal osteoporosis: development history and design and participant characteristics of LOFT, the Long-Term Odanacatib Fracture Trial. <b>2015</b> , 26, 699-712	105
1623	Small changes in bone structure of female ∄ nicotinic acetylcholine receptor knockout mice. <b>2015</b> , 16, 5	11
1622	Mechanical loading causes site-specific anabolic effects on bone following exposure to ionizing radiation. <b>2015</b> , 81, 260-269	13
1621	Sialic acid-binding immunoglobulin-like lectin 15 (Siglec-15) mediates periarticular bone loss, but not joint destruction, in murine antigen-induced arthritis. <b>2015</b> , 79, 65-70	19
1620	Effects of low dose FGF-2 and BMP-2 on healing of calvarial defects in old mice. <b>2015</b> , 64, 62-9	48
1619	Subchondral bone turnover, but not bone volume, is increased in early stage osteoarthritic lesions in the human hip joint. <b>2015</b> , 23, 2167-2173	31
1618	MicroRNA-29a mitigates glucocorticoid induction of bone loss and fatty marrow by rescuing Runx2 acetylation. <b>2015</b> , 81, 80-88	57
1617	Icariin protects against titanium particle-induced osteolysis and inflammatory response in a mouse calvarial model. <b>2015</b> , 60, 92-9	76
1616	Intact bone vitality and increased accumulation of nonmineralized bone matrix in biopsy specimens of juvenile osteochondritis dissecans: a histological analysis. <b>2015</b> , 43, 1337-47	22
1615	Osteopetrorickets due to Snx10 deficiency in mice results from both failed osteoclast activity and loss of gastric acid-dependent calcium absorption. <b>2015</b> , 11, e1005057	20

1614	Mast cell promotion of T cell-driven antigen-induced arthritis despite being dispensable for antibody-induced arthritis in which T cells are bypassed. <b>2015</b> , 67, 903-13	47
1613	A DNA segment spanning the mouse Tnfsf11 transcription unit and its upstream regulatory domain rescues the pleiotropic biologic phenotype of the RANKL null mouse. <i>Journal of Bone and Mineral</i> 6.3 <i>Research</i> , <b>2015</b> , 30, 855-68	13
1612	FGF23 neutralization improves bone quality and osseointegration of titanium implants in chronic kidney disease mice. <b>2015</b> , 5, 8304	29
1611	Combination treatment with whole body vibration and a kidney-tonifying herbal Fufang prevent osteoporosis in ovariectomized rats. <b>2015</b> , 7, 57-65	4
1610	Bone alkaline phosphatase isoforms in hemodialysis patients with low versus non-low bone turnover: a diagnostic test study. <b>2015</b> , 66, 99-105	19
1609	Calcium gluconate supplementation is effective to balance calcium homeostasis in patients with gastrectomy. <b>2015</b> , 26, 987-95	24
1608	Synchrotron X-ray phase nano-tomography-based analysis of the lacunar-canalicular network morphology and its relation to the strains experienced by osteocytes in situ as predicted by case-specific finite element analysis. <b>2015</b> , 14, 267-82	60
1607	The biological effects of tocotrienol on bone: a review on evidence from rodent models. <b>2015</b> , 9, 2049-61	36
1606	Age- and Sex-Specific Bone Structure Patterns Portend Bone Fragility in Radii and Tibiae in Relation to Osteodensitometry: A High-Resolution Peripheral Quantitative Computed Tomography Study in 385 Individuals. <b>2015</b> , 70, 1269-75	37
1605	Loss of milk fat globule-epidermal growth factor 8 (MFG-E8) in mice leads to low bone mass and accelerates ovariectomy-associated bone loss by increasing osteoclastogenesis. <b>2015</b> , 76, 107-14	13
1604	Marrow adiposity assessed on transiliac crest biopsy samples correlates with noninvasive measurement of marrow adiposity by proton magnetic resonance spectroscopy ((1)H-MRS) at the spine but not the femur. <b>2015</b> , 26, 2471-8	26
1603	Transcription factor Hes1 modulates osteoarthritis development in cooperation with calcium/calmodulin-dependent protein kinase 2. <b>2015</b> , 112, 3080-5	56
1602	Loss of BMPR2 leads to high bone mass due to increased osteoblast activity. <b>2015</b> , 128, 1308-15	36
1601	Prevention of glucocorticoid induced bone changes with beta-ecdysone. <b>2015</b> , 74, 48-57	26
1600	Effect of Combined Teriparatide and Monthly Risedronate Therapy on Cancellous Bone Mass in Orchidectomized Rats: A Bone Histomorphometry Study. <b>2015</b> , 97, 23-31	3
1599	Bindarit, an inhibitor of monocyte chemotactic protein synthesis, protects against bone loss induced by chikungunya virus infection. <b>2015</b> , 89, 581-93	85
1598	Gastrodin: an ancient Chinese herbal medicine as a source for anti-osteoporosis agents via reducing reactive oxygen species. <b>2015</b> , 73, 132-44	46
1597	Erythropoietin directly stimulates osteoclast precursors and induces bone loss. <b>2015</b> , 29, 1890-900	71

1596	Porosity imaged by a vector projection algorithm correlates with fractal dimension measured on 3D models obtained by microCT. <b>2015</b> , 258, 24-30	6
1595	Long bone maturation is driven by pore closing: A quantitative tomography investigation of structural formation in young C57BL/6 mice. <b>2015</b> , 22, 92-102	15
1594	Novel rat model of nonunion fracture with vascular deficit. <b>2015</b> , 46, 649-54	13
1593	Mesenchymal stromal cell implantation for stimulation of long bone healing aggravates Staphylococcus aureus induced osteomyelitis. <b>2015</b> , 21, 165-77	29
1592	Impaired bone homeostasis in amyotrophic lateral sclerosis mice with muscle atrophy. <b>2015</b> , 290, 8081-94	24
1591	The effects of atorvastatin on the prevention of osteoporosis and dyslipidemia in the high-fat-fed ovariectomized rats. <b>2015</b> , 96, 541-51	15
1590	Monitoring in vivo (re)modeling: a computational approach using 4D microCT data to quantify bone surface movements. <b>2015</b> , 75, 210-21	49
1589	Hedgehog signaling mediates woven bone formation and vascularization during stress fracture healing. <b>2015</b> , 81, 524-532	27
1588	Hyperthyroidism and Hypothyroidism in Male Mice and Their Effects on Bone Mass, Bone Turnover, and the Wnt Inhibitors Sclerostin and Dickkopf-1. <b>2015</b> , 156, 3517-27	37
1587	Role of T-cell reconstitution in HIV-1 antiretroviral therapy-induced bone loss. <b>2015</b> , 6, 8282	56
1586	Selective inhibition of TNFR1 reduces osteoclast numbers and is differentiated from anti-TNF in a LPS-driven model of inflammatory bone loss. <b>2015</b> , 464, 1145-1150	17
1585	Comprehensive analysis of translational osteochondral repair: Focus on the histological assessment. <b>2015</b> , 50, 19-36	19
1584	Defective cancellous bone structure and abnormal response to PTH in cortical bone of mice lacking Cx43 cytoplasmic C-terminus domain. <b>2015</b> , 81, 632-643	28
1583	Excessive growth hormone expression in male GH transgenic mice adversely alters bone architecture and mechanical strength. <b>2015</b> , 156, 1362-71	22
1582	Thyrostimulin Regulates Osteoblastic Bone Formation During Early Skeletal Development. <b>2015</b> , 156, 3098-113	33
1581	Genome-Wide Mapping and Interrogation of the Nmp4 Antianabolic Bone Axis. <b>2015</b> , 29, 1269-85	8
1580	Early Effects of Single and Low-Frequency Repeated Administration of Teriparatide, hPTH(1-34), on Bone Formation and Resorption in Ovariectomized Rats. <b>2015</b> , 97, 412-20	8
1579	Topical combined application of dexamethasone, vitamin C, and Esodium glycerophosphate for healing the extraction socket in rabbits. <b>2015</b> , 44, 1317-23	6

1578	NLRP12 provides a critical checkpoint for osteoclast differentiation. <b>2015</b> , 112, 10455-60		17
1577	Enhanced Osteogenesis of Nanosized Cobalt-substituted Hydroxyapatite. <b>2015</b> , 12, 604-612		27
1576	Chronic administration of Glucagon-like peptide-1 receptor agonists improves trabecular bone mass and architecture in ovariectomised mice. <b>2015</b> , 81, 459-467		69
1575	Osteoporotic bone of miR-150-deficient mice: Possibly due to low serum OPG-mediated osteoclast activation. <b>2015</b> , 3, 5-10		11
1574	IL-17A Is Increased in Humans with Primary Hyperparathyroidism and Mediates PTH-Induced Bone Loss in Mice. <b>2015</b> , 22, 799-810		59
1573	Animal model for medication-related osteonecrosis of the jaw with precedent metabolic bone disease. <b>2015</b> , 81, 442-448		20
1572	Glycoprotein130 (Gp130)/interleukin-6 (IL-6) signalling in osteoclasts promotes bone formation in periosteal and trabecular bone. <b>2015</b> , 81, 343-351		34
1571	Animal Models for Evaluation of Bone Implants and Devices: Comparative Bone Structure and Common Model Uses. <b>2015</b> , 52, 842-50		98
1570	Igfbp2 Deletion in Ovariectomized Mice Enhances Energy Expenditure but Accelerates Bone Loss. <b>2015</b> , 156, 4129-40		21
1569	Bone Marrow Stress Decreases Osteogenic Progenitors. <b>2015</b> , 97, 476-86		6
1569 1568	Bone Marrow Stress Decreases Osteogenic Progenitors. 2015, 97, 476-86  Effect of alendronate on the mandible and long bones: an experimental study in vivo. 2015, 78, 618-25		6
1568	Effect of alendronate on the mandible and long bones: an experimental study in vivo. <b>2015</b> , 78, 618-25  Fatostatin, an SREBP inhibitor, prevented RANKL-induced bone loss by suppression of osteoclast		6
1568 1567	Effect of alendronate on the mandible and long bones: an experimental study in vivo. <b>2015</b> , 78, 618-25  Fatostatin, an SREBP inhibitor, prevented RANKL-induced bone loss by suppression of osteoclast differentiation. <b>2015</b> , 1852, 2432-41  KCNK1 inhibits osteoclastogenesis by blocking the Ca2+ oscillation and JNK-NFATc1 signaling axis.		6
1568 1567 1566	Effect of alendronate on the mandible and long bones: an experimental study in vivo. <b>2015</b> , 78, 618-25  Fatostatin, an SREBP inhibitor, prevented RANKL-induced bone loss by suppression of osteoclast differentiation. <b>2015</b> , 1852, 2432-41  KCNK1 inhibits osteoclastogenesis by blocking the Ca2+ oscillation and JNK-NFATc1 signaling axis. <b>2015</b> , 128, 3411-9  Bone Density After Teriparatide Discontinuation in Premenopausal Idiopathic Osteoporosis. <b>2015</b> ,		6 12 11
1568 1567 1566 1565	Effect of alendronate on the mandible and long bones: an experimental study in vivo. 2015, 78, 618-25  Fatostatin, an SREBP inhibitor, prevented RANKL-induced bone loss by suppression of osteoclast differentiation. 2015, 1852, 2432-41  KCNK1 inhibits osteoclastogenesis by blocking the Ca2+ oscillation and JNK-NFATc1 signaling axis. 2015, 128, 3411-9  Bone Density After Teriparatide Discontinuation in Premenopausal Idiopathic Osteoporosis. 2015, 100, 4208-14  Treatment with curcumin alleviates sublesional bone loss following spinal cord injury in rats. 2015,	6.3	6 12 11 30
1568 1567 1566 1565	Effect of alendronate on the mandible and long bones: an experimental study in vivo. 2015, 78, 618-25  Fatostatin, an SREBP inhibitor, prevented RANKL-induced bone loss by suppression of osteoclast differentiation. 2015, 1852, 2432-41  KCNK1 inhibits osteoclastogenesis by blocking the Ca2+ oscillation and JNK-NFATc1 signaling axis. 2015, 128, 3411-9  Bone Density After Teriparatide Discontinuation in Premenopausal Idiopathic Osteoporosis. 2015, 100, 4208-14  Treatment with curcumin alleviates sublesional bone loss following spinal cord injury in rats. 2015, 765, 209-16  Sclerostin inhibition prevents spinal cord injury-induced cancellous bone loss. <i>Journal of Bone and</i>	6.3 6.3	6 12 11 30 9

1560	The kynurenine pathway of tryptophan degradation is activated during osteoblastogenesis. <b>2015</b> , 33, 111-21		50
1559	mTORC2 signaling promotes skeletal growth and bone formation in mice. <i>Journal of Bone and Mineral Research</i> , <b>2015</b> , 30, 369-78	6.3	64
1558	Clinical Skeletal Syndromes Associated with Parathyroid Disorders in Chronic Kidney Disease. <b>2015</b> , 65	3-669	
1557	A joined role of canopy and reversal cells in bone remodelinglessons from glucocorticoid-induced osteoporosis. <b>2015</b> , 73, 16-23		38
1556	Comparison of three methods of calculating strain in the mouse ulna in exogenous loading studies. <b>2015</b> , 48, 53-8		5
1555	Lipocalin 2: a new mechanoresponding gene regulating bone homeostasis. <i>Journal of Bone and Mineral Research</i> , <b>2015</b> , 30, 357-68	6.3	52
1554	A novel splice mutation in PLS3 causes X-linked early onset low-turnover osteoporosis. <i>Journal of Bone and Mineral Research</i> , <b>2015</b> , 30, 510-8	6.3	49
1553	Core binding factor of osteoblasts maintains cortical bone mass via stabilization of Runx2 in mice. <i>Journal of Bone and Mineral Research</i> , <b>2015</b> , 30, 715-22	6.3	24
1552	Development of new criteria for cortical bone histomorphometry in femoral neck: intra- and inter-observer reproducibility. <b>2015</b> , 33, 109-18		6
1551	Double incretin receptor knock-out (DIRKO) mice present with alterations of trabecular and cortical micromorphology and bone strength. <b>2015</b> , 26, 209-18		34
1550	Morphology, Morphometry and Spatial Distribution of Secondary Osteons in Equine Femur. <b>2015</b> , 44, 328-32		13
1549	Pre-clinical characterization of tissue engineering constructs for bone and cartilage regeneration. <b>2015</b> , 43, 681-96		20
1548	Unwrapping microcomputed tomographic images for measuring cortical osteolytic lesions in the 5T2 murine model of myeloma treated by bisphosphonate. <b>2015</b> , 68, 107-114		2
1547	Effect of Urocortin on strength and microarchitecture of osteopenic rat femur. <b>2015</b> , 33, 154-60		5
1546	Effects of salvianolate on bone metabolism in glucocorticoid-treated lupus-prone B6.MRL-Fas (lpr) /J mice. <b>2016</b> , 10, 2535-46		18
1545	Effects of 8-Prenylnaringenin and Whole-Body Vibration Therapy on a Rat Model of Osteopenia. <b>2016</b> , 2016, 6893137		10
1544	Osteoporosis and Bone Biology. <b>2016</b> , 1323-1364		5
1543	Hypothalamic Leptin Gene Therapy Reduces Bone Marrow Adiposity in ob/ob Mice Fed Regular and High-Fat Diets. <b>2016</b> , 7, 110		21

1542	Novel Osteointegrative Sr-Substituted Apatitic Cements Enriched with Alginate. 2016, 9,	17
1541	Effects of Proton Pump Inhibitor Administration and Intake of a Combination of Yogurt and Galactooligosaccharides on Bone and Mineral Metabolism in Rats. <b>2016</b> , 8,	3
1540	A Non-Destructive Method for Distinguishing Reindeer Antler (Rangifer tarandus) from Red Deer Antler (Cervus elaphus) Using X-Ray Micro-Tomography Coupled with SVM Classifiers. <b>2016</b> , 11, e0149658	3
1539	Apatite Formation and Biocompatibility of a Low Young's Modulus Ti-Nb-Sn Alloy Treated with Anodic Oxidation and Hot Water. <b>2016</b> , 11, e0150081	14
1538	Semaphorin 4D Promotes Skeletal Metastasis in Breast Cancer. <b>2016</b> , 11, e0150151	32
1537	Governing Equations of Tissue Modelling and Remodelling: A Unified Generalised Description of Surface and Bulk Balance. <b>2016</b> , 11, e0152582	8
1536	Bone Canopies in Pediatric Renal Osteodystrophy. <b>2016</b> , 11, e0152871	3
1535	Deficiency of Causes Bone Loss by Inhibiting Bone Resorption and Bone Formation through the TGF-II Pathway. <b>2016</b> , 6, 2183-2195	28
1534	Reduced Bone Density and Cortical Bone Indices in Female Adiponectin-Knockout Mice. <b>2016</b> , 157, 3550-61	25
1533	Acute Phosphate Restriction Impairs Bone Formation and Increases Marrow Adipose Tissue in Growing Mice. <i>Journal of Bone and Mineral Research</i> , <b>2016</b> , 31, 2204-2214	19
1532	Improved Mobilization of Exogenous Mesenchymal Stem Cells to Bone for Fracture Healing and Sex Difference. <b>2016</b> , 34, 2587-2600	28
1531	Transcriptional Modulator Ifrd1 Regulates Osteoclast Differentiation through Enhancing the NF-B/NFATc1 Pathway. <b>2016</b> , 36, 2451-63	15
1530	The effects of implant topography on osseointegration under estrogen deficiency induced osteoporotic conditions: Histomorphometric, transcriptional and ultrastructural analysis. <b>2016</b> , 42, 351-363	39
1529	Suppression of p38EMAPK Signaling in Osteoblast Lineage Cells Impairs Bone Anabolic Action of Parathyroid Hormone. <i>Journal of Bone and Mineral Research</i> , <b>2016</b> , 31, 985-93	11
1528	The Transcriptional Modulator Interferon-Related Developmental Regulator 1 in Osteoblasts Suppresses Bone Formation and Promotes Bone Resorption. <i>Journal of Bone and Mineral Research</i> , 6.3 <b>2016</b> , 31, 573-84	19
1527	Deletion of Rac in Mature Osteoclasts Causes Osteopetrosis, an Age-Dependent Change in Osteoclast Number, and a Reduced Number of Osteoblasts In Vivo. <i>Journal of Bone and Mineral</i> 6.3 <i>Research</i> , <b>2016</b> , 31, 864-73	25
1526	Effects of Daily or Cyclic Teriparatide on Bone Formation in the Iliac Crest in Women on No Prior Therapy and in Women on Alendronate. <i>Journal of Bone and Mineral Research</i> , <b>2016</b> , 31, 1518-26	29
1525	Prophylactic pamidronate partially protects from glucocorticoid-induced bone loss in the mdx mouse model of Duchenne muscular dystrophy. <b>2016</b> , 90, 168-80	6

1524	Odanacatib Restores Trabecular Bone of Skeletally Mature Female Rabbits With Osteopenia but Induces Brittleness of Cortical Bone: A Comparative Study of the Investigational Drug With PTH, Estrogen, and Alendronate. <i>Journal of Bone and Mineral Research</i> , <b>2016</b> , 31, 615-29	6.3	9	
1523	Strontium Ranelate Reduces the Fracture Incidence in a Growing Mouse Model of Osteogenesis Imperfecta. <i>Journal of Bone and Mineral Research</i> , <b>2016</b> , 31, 1003-14	6.3	10	
1522	Beta Adrenergic Receptor Stimulation Suppresses Cell Migration in Association with Cell Cycle Transition in Osteoblasts-Live Imaging Analyses Based on FUCCI System. <b>2016</b> , 231, 496-504		4	
1521	Deferoxamine released from poly(lactic-co-glycolic acid) promotes healing of osteoporotic bone defect via enhanced angiogenesis and osteogenesis. <b>2016</b> , 104, 2515-27		38	
1520	Skeletal inflammation and attenuation of Wnt signaling, Wnt ligand expression, and bone formation in atherosclerotic ApoE-null mice. <b>2016</b> , 310, E762-73		23	
1519	Effect of cadmium on bone tissue in growing animals. <b>2016</b> , 68, 391-7		34	
1518	Trabecular network arrangement within the human patella: how osteoarthritis remodels the 3D trabecular structure. <b>2016</b> ,			
1517	FIAT Deletion Increases Bone Mass But Does Not Prevent High-Fat-Diet-Induced Metabolic Complications. <b>2017</b> , 158, 264-276		1	
1516	Effects of Chronic Estrogen Administration in the Ventromedial Nucleus of the Hypothalamus (VMH) on Fat and Bone Metabolism in Ovariectomized Rats. <b>2016</b> , 157, 4930-4942		8	
1515	The role of membrane ERBignaling in bone and other major estrogen responsive tissues. <b>2016</b> , 6, 2947.	3	41	
1514	Bone histomorphometric changes in children with rheumatic disorders on chronic glucocorticoids. <b>2016</b> , 14, 58		12	
1513	Dicer ablation in osteoblasts by Runx2 driven cre-loxP recombination affects bone integrity, but not glucocorticoid-induced suppression of bone formation. <b>2016</b> , 6, 32112		17	
1512	Lack of hepcidin ameliorates anemia and improves growth in an adenine-induced mouse model of chronic kidney disease. <b>2016</b> , 311, F877-F889		35	
1511	Histomorphometric analysis of minimodeling in the vertebrae in postmenopausal patients treated with anti-osteoporotic agents. <b>2016</b> , 5, 286-291		7	
1510	Bone micro-architectural analysis of mandible and tibia in ovariectomised rats: A quantitative structural comparison between undecalcified histological sections and micro-CT. <b>2016</b> , 5, 253-62		16	
1509	Minodronic acid ameliorates vertebral bone strength by increasing bone mineral density in 9-month treatment of ovariectomized cynomolgus monkeys. <b>2016</b> , 88, 157-164		4	
1508	Sostdc1 deficiency accelerates fracture healing by promoting the expansion of periosteal mesenchymal stem cells. <b>2016</b> , 88, 20-30		25	
1507	Vector analysis of porosity evidences bone loss at the epiphysis in the BTX rat model of disuse osteoporosis. <b>2016</b> , 65, 3-8		3	

1506	Room temperature housing results in premature cancellous bone loss in growing female mice: implications for the mouse as a preclinical model for age-related bone loss. <b>2016</b> , 27, 3091-101	40
1505	Non-osteoporotic women with low-trauma fracture present altered birefringence in cortical bone. <b>2016</b> , 84, 104-112	12
1504	Improvement of cancellous bone microstructure in patients on teriparatide following alendronate pretreatment. <b>2016</b> , 89, 16-24	18
1503	Effect of Sodium Fluoride on Bone Biomechanical and Histomorphometric Parameters and on Insulin Signaling and Insulin Sensitivity in Ovariectomized Rats. <b>2016</b> , 173, 144-53	5
1502	Intramedullary Mg2Ag nails augment callus formation during fracture healing in mice. <b>2016</b> , 36, 350-60	52
1501	Neuropeptide Y mediates glucocorticoid-induced osteoporosis and marrow adiposity in mice. <b>2016</b> , 27, 2777-2789	20
1500	A new stable GIP-Oxyntomodulin hybrid peptide improved bone strength both at the organ and tissue levels in genetically-inherited type 2 diabetes mellitus. <b>2016</b> , 87, 102-13	22
1499	Apolipoprotein A-1 regulates osteoblast and lipoblast precursor cells in mice. <b>2016</b> , 96, 763-72	18
1498	Sprouty2 regulates endochondral bone formation by modulation of RTK and BMP signaling. <b>2016</b> , 88, 170-179	9
1497	LGR4 acts as a key receptor for R-spondin 2 to promote osteogenesis through Wnt signaling pathway. <b>2016</b> , 28, 989-1000	42
1496	Effects of long term treatment with high doses of odanacatib on bone mass, bone strength, and remodeling/modeling in newly ovariectomized monkeys. <b>2016</b> , 88, 113-124	15
1495	Peptide-induced de novo bone formation after tooth extraction prevents alveolar bone loss in a murine tooth extraction model. <b>2016</b> , 782, 89-97	8
1494	Effects of long-term administration of pantoprazole on bone mineral density in young male rats. <b>2016</b> , 68, 1060-4	12
1493	Long term bone alterations in aged rats suffering type 1 diabetes. <b>2016</b> , 85, 9-12	
1492	WITHDRAWN: Prolyl hydroxylase domain proteins regulate bone mass through their expression in osteoblasts. <b>2016</b> ,	
1491	RANKL (Receptor Activator of NFB Ligand) Produced by Osteocytes Is Required for the Increase in B Cells and Bone Loss Caused by Estrogen Deficiency in Mice. <b>2016</b> , 291, 24838-24850	57
1490	Effect of dietary calcium deficiency and altered diet hardness on the jawbone growth: A micro-CT and bone histomorphometric study in rats. <b>2016</b> , 72, 200-210	11
1489	Odanacatib, effects of 16-month treatment and discontinuation of therapy on bone mass, turnover and strength in the ovariectomized rabbit model of osteopenia. <b>2016</b> , 93, 86-96	11

1488	Fibrinogen scaffolds with immunomodulatory properties promote in vivo bone regeneration. <b>2016</b> , 111, 163-178		43
1487	Finite Element-Based Mechanical Assessment of Bone Quality on the Basis of In Vivo Images. <b>2016</b> , 14, 374-385		26
1486	Aspirin prevents bone loss with little mechanical improvement in high-fat-fed ovariectomized rats. <b>2016</b> , 791, 331-338		13
1485	Glucose-dependent insulinotropic polypeptide (GIP) dose-dependently reduces osteoclast differentiation and resorption. <b>2016</b> , 91, 102-12		25
1484	Enzalutamide Reduces the Bone Mass in the Axial But Not the Appendicular Skeleton in Male Mice. <b>2016</b> , 157, 969-77		17
1483	Activation of Wnt Signaling by Mechanical Loading Is Impaired in the Bone of Old Mice. <i>Journal of Bone and Mineral Research</i> , <b>2016</b> , 31, 2215-2226	6.3	81
1482	Peptide drugs accelerate BMP-2-induced calvarial bone regeneration and stimulate osteoblast differentiation through mTORC1 signaling. <b>2016</b> , 38, 717-25		21
1481	Regeneration of mandibular defects using adipose tissue mesenchymal stromal cells in combination with human serum-derived scaffolds. <b>2016</b> , 44, 1356-65		5
1480	A Longitudinal Study of Skeletal Histomorphometry at 6 and 24 Months Across Four Bone Envelopes in Postmenopausal Women With Osteoporosis Receiving Teriparatide or Zoledronic Acid in the SHOTZ Trial. <i>Journal of Bone and Mineral Research</i> , <b>2016</b> , 31, 1429-39	6.3	40
1479	Ginsenosides Rg3 attenuates glucocorticoid-induced osteoporosis through regulating BMP-2/BMPR1A/Runx2 signaling pathway. <b>2016</b> , 256, 188-97		20
1478	Evolution of bone disease after kidney transplantation: A prospective histomorphometric analysis of trabecular and cortical bone. <b>2016</b> , 21, 55-61		14
1477	Ancient Human Bone Microstructure in Medieval England: Comparisons between Two Socio-Economic Groups. <b>2016</b> , 299, 42-59		29
1476	Fat and Sucrose Intake Induces Obesity-Related Bone Metabolism Disturbances: Kinetic and Reversibility Studies in Growing and Adult Rats. <i>Journal of Bone and Mineral Research</i> , <b>2016</b> , 31, 98-115	6.3	20
1475	1,25-Dihydroxyvitamin D Alone Improves Skeletal Growth, Microarchitecture, and Strength in a Murine Model of XLH, Despite Enhanced FGF23 Expression. <i>Journal of Bone and Mineral Research</i> , <b>2016</b> , 31, 929-39	6.3	43
1474	The role of bone biopsy for the diagnosis of renal osteodystrophy: a short overview and future perspectives. <b>2016</b> , 29, 617-26		12
1473	BMP signaling is required for adult skeletal homeostasis and mediates bone anabolic action of parathyroid hormone. <b>2016</b> , 92, 132-144		18
1472	Cutaneous skeletal hypophosphatemia syndrome: clinical spectrum, natural history, and treatment. <b>2016</b> , 27, 3615-3626		31
1471	Only minor differences in renal osteodystrophy features between wild-type and sclerostin knockout mice with chronic kidney disease. <b>2016</b> , 90, 828-34		17

1470	Role of ERMISS in the Effect of Estradiol on Cancellous and Cortical Femoral Bone in Growing Female Mice. <b>2016</b> , 157, 2533-44	17
1469	microRNA-21 Contributes to Orthodontic Tooth Movement. <b>2016</b> , 95, 1425-1433	53
1468	The Primary Cilium as a Strain Amplifying Microdomain for Mechanotransduction at the Cell Membrane. <b>2016</b> , 3-27	1
1467	Can Intestinal Phosphate Binding or Inhibition of Hydroxyapatite Growth in the Vascular Wall Halt the Progression of Established Aortic Calcification in Chronic Kidney Disease?. <b>2016</b> , 99, 525-534	5
1466	Protein Phosphatase PP5 Controls Bone Mass and the Negative Effects of Rosiglitazone on Bone through Reciprocal Regulation of PPAR[[Peroxisome Proliferator-activated Receptor ]] and RUNX2 (Runt-related Transcription Factor 2). <b>2016</b> , 291, 24475-24486	18
1465	Prolyl hydroxylase domain proteins regulate bone mass through their expression in osteoblasts. <b>2016</b> , 594, 125-130	4
1464	Promotion of osteointegration under diabetic conditions by tantalum coating-based surface modification on 3-dimensional printed porous titanium implants. <b>2016</b> , 148, 440-452	38
1463	First-time systematic postoperative clinical assessment of a minimally invasive approach for lumbar ventrolateral vertebroplasty in the large animal model sheep. <b>2016</b> , 16, 1263-1275	14
1462	Exploring the Bone Proteome to Help Explain Altered Bone Remodeling and Preservation of Bone Architecture and Strength in Hibernating Marmots. <b>2016</b> , 89, 364-76	10
1461	Non-Lethal Type VIII Osteogenesis Imperfecta Has Elevated Bone Matrix Mineralization. <b>2016</b> , 101, 3516-25	18
1460	FAK Promotes Osteoblast Progenitor Cell Proliferation and Differentiation by Enhancing Wnt Signaling. <i>Journal of Bone and Mineral Research</i> , <b>2016</b> , 31, 2227-2238	44
1459	Specific bone region localization of osteolytic versus osteoblastic lesions in a patient-derived xenograft model of bone metastatic prostate cancer. <b>2016</b> , 3, 229-239	3
1458	Deletion of BMP receptor type IB decreased bone mass in association with compromised osteoblastic differentiation of bone marrow mesenchymal progenitors. <b>2016</b> , 6, 24256	23
1457	Antibodies for the Treatment of Bone Diseases: Clinical Data. <b>2016</b> , 239-255	
1456	Intrinsic mechanical behavior of femoral cortical bone in young, osteoporotic and bisphosphonate-treated individuals in low- and high energy fracture conditions. <b>2016</b> , 6, 21072	44
1455	Disruption of c-Kit Signaling in Kit(W-sh/W-sh) Growing Mice Increases Bone Turnover. <b>2016</b> , 6, 31515	9
1454	Prolyl Hydroxylase Domain-Containing Protein 2 (Phd2) Regulates Chondrocyte Differentiation and Secondary Ossification in Mice. <b>2016</b> , 6, 35748	10
1453	Low bone mass and changes in the osteocyte network in mice lacking autophagy in the osteoblast lineage. <b>2016</b> , 6, 24262	58

1452	SIKs control osteocyte responses to parathyroid hormone. <b>2016</b> , 7, 13176	79
1451	Gut microbiota induce IGF-1 and promote bone formation and growth. <b>2016</b> , 113, E7554-E7563	287
1450	Allogeneic Mesenchymal Stem Cell Therapy Promotes Osteoblastogenesis and Prevents Glucocorticoid-Induced Osteoporosis. <b>2016</b> , 5, 1238-46	52
1449	GDF11 decreases bone mass by stimulating osteoclastogenesis and inhibiting osteoblast differentiation. <b>2016</b> , 7, 12794	97
1448	How the European eel (Anguilla anguilla) loses its skeletal framework across lifetime. <b>2016</b> , 283,	10
1447	Mesenchymal progenitors in osteopenias of diverse pathologies: differential characteristics in the common shift from osteoblastogenesis to adipogenesis. <b>2016</b> , 6, 30186	47
1446	Elevated GI expression in osteoblast lineage cells promotes osteoclastogenesis and leads to enhanced trabecular bone accrual in response to pamidronate. <b>2016</b> , 310, E811-20	2
1445	Murine Hind Limb Long Bone Dissection and Bone Marrow Isolation. 2016,	83
1444	Microgravity Stress: Bone and Connective Tissue. <b>2016</b> , 6, 645-86	29
1443	IGF-1 Regulates Vertebral Bone Aging Through Sex-Specific and Time-Dependent Mechanisms. <i>Journal of Bone and Mineral Research</i> , <b>2016</b> , 31, 443-54	27
1442	Adynamic Bone Decreases Bone Toughness During Aging by Affecting Mineral and Matrix. <i>Journal of Bone and Mineral Research</i> , <b>2016</b> , 31, 369-79	20
1441	Circadian Clock Regulates Bone Resorption in Mice. <i>Journal of Bone and Mineral Research</i> , <b>2016</b> , 31, 13446555	50
1440	The Actin-Binding Protein Cofilin and Its Interaction With Cortactin Are Required for Podosome Patterning in Osteoclasts and Bone Resorption In Vivo and In Vitro. <i>Journal of Bone and Mineral Research</i> , <b>2016</b> , 31, 1701-12	24
1439	Variation in osteon histomorphometrics and their impact on age-at-death estimation in older individuals. <b>2016</b> , 262, 282.e1-6	25
1438	Bone lesions in a Late Pleistocene assemblage of the insular deer Candiacervus sp.II from Liko cave (Crete, Greece). <b>2016</b> , 14, 36-45	7
1437	Daily leptin blunts marrow fat but does not impact bone mass in calorie-restricted mice. <b>2016</b> , 229, 295-306	22
1436	Peripubertal Caffeine Exposure Impairs Longitudinal Bone Growth in Immature Male Rats in a Dose- and Time-Dependent Manner. <b>2016</b> , 19, 73-84	4
1435	Effects of odanacatib on bone matrix mineralization in rhesus monkeys are similar to those of alendronate. <b>2016</b> , 5, 62-69	2

## (2016-2016)

1434	Bone marrow lesions in hip osteoarthritis are characterized by increased bone turnover and enhanced angiogenesis. <b>2016</b> , 24, 1745-1752	41
1433	Postnatal Etatenin deletion from Dmp1-expressing osteocytes/osteoblasts reduces structural adaptation to loading, but not periosteal load-induced bone formation. <b>2016</b> , 88, 138-145	18
1432	Data in support of the bone analysis of NOD-SCID mice treated with zoledronic acid and prednisolone. <b>2016</b> , 7, 1486-90	2
1431	A correlative imaging based methodology for accurate quantitative assessment of bone formation in additive manufactured implants. <b>2016</b> , 27, 112	11
1430	Overexpression of G#1 in Osteoblast Lineage Cells Suppresses the Osteoanabolic Response to Intermittent PTH and Exercise. <b>2016</b> , 99, 423-34	3
1429	Rictor/mTORC2 loss in osteoblasts impairs bone mass and strength. <b>2016</b> , 90, 50-8	18
1428	CCL20/CCR6 Signaling Regulates Bone Mass Accrual in Mice. <i>Journal of Bone and Mineral Research</i> , <b>2016</b> , 31, 1381-90	13
1427	Canonical Notch activation in osteocytes causes osteopetrosis. <b>2016</b> , 310, E171-82	32
1426	Elevated Lifetime Lead Exposure Impedes Osteoclast Activity and Produces an Increase in Bone Mass in Adolescent Mice. <b>2016</b> , 149, 277-88	23
1425	DMP-1-mediated Ghr gene recombination compromises skeletal development and impairs skeletal response to intermittent PTH. <b>2016</b> , 30, 635-52	19
1424	Positive effects of bisphosphonates on bone and muscle in a mouse model of Duchenne muscular dystrophy. <b>2016</b> , 26, 73-84	15
1423	Inhibition of titanium-particle-induced inflammatory osteolysis after local administration of dopamine and suppression of osteoclastogenesis via D2-like receptor signaling pathway. <b>2016</b> , 80, 1-10	62
1422	Hajdu Cheney Mouse Mutants Exhibit Osteopenia, Increased Osteoclastogenesis, and Bone Resorption. <b>2016</b> , 291, 1538-1551	55
1421	Effects of Sclerostin Antibody on the Healing of Femoral Fractures in Ovariectomised Rats. <b>2016</b> , 98, 263-74	18
1420	Effect of Teriparatide on Bone Formation in the Human Femoral Neck. <b>2016</b> , 101, 1498-505	26
1419	Combined exposure to big endothelin-1 and mechanical loading in bovine sternal cores promotes osteogenesis. <b>2016</b> , 85, 115-22	7
1418	Differential Effects of Teriparatide and Denosumab on Intact PTH and Bone Formation Indices: AVA Osteoporosis Study. <b>2016</b> , 101, 1353-63	42
1417	Osteogenic response and osteoprotective effects in vivo of a nanostructured titanium surface with antibacterial properties. <b>2016</b> , 27, 52	9

1416	Elcatonin prevents bone loss caused by skeletal unloading by inhibiting preosteoclast fusion through the unloading-induced high expression of calcitonin receptors in bone marrow cells. <b>2016</b> , 85, 70-80	13
1415	Comparative study of two types of herbal capsules with different species for the prevention of ovariectomised-induced osteoporosis in rats. <b>2016</b> , 4, 14-27	12
1414	A threshold of mechanical strain intensity for the direct activation of osteoblast function exists in a murine maxilla loading model. <b>2016</b> , 15, 1091-100	7
1413	Teriparatide for osteoporosis: importance of the full course. <b>2016</b> , 27, 2395-410	97
1412	Calcitriol Suppression of Parathyroid Hormone Fails to Improve Skeletal Properties in an Animal Model of Chronic Kidney Disease. <b>2016</b> , 43, 20-31	6
1411	Material heterogeneity in cancellous bone promotes deformation recovery after mechanical failure. <b>2016</b> , 113, 2892-7	31
1410	MEKK2 mediates an alternative Etatenin pathway that promotes bone formation. <b>2016</b> , 113, E1226-35	36
1409	Deterioration of teeth and alveolar bone loss due to chronic environmental high-level fluoride and low calcium exposure. <b>2016</b> , 20, 2361-2370	9
1408	Osteoblast-Specific Overexpression of Human WNT16 Increases Both Cortical and Trabecular Bone Mass and Structure in Mice. <b>2016</b> , 157, 722-36	26
1407	Early reversal cells in adult human bone remodeling: osteoblastic nature, catabolic functions and interactions with osteoclasts. <b>2016</b> , 145, 603-15	42
1406	A multiscale mechanobiological model of bone remodelling predicts site-specific bone loss in the femur during osteoporosis and mechanical disuse. <b>2016</b> , 15, 43-67	37
1405	Inflammation and the bone-vascular axis in end-stage renal disease. <b>2016</b> , 27, 489-97	27
1404	Src siRNA prevents corticosteroid-associated osteoporosis in a rabbit model. <b>2016</b> , 83, 190-196	7
1403	Conditional Deletion of Prolyl Hydroxylase Domain-Containing Protein 2 (Phd2) Gene Reveals Its Essential Role in Chondrocyte Function and Endochondral Bone Formation. <b>2016</b> , 157, 127-40	16
1402	Parathyroid hormone 1 receptor is essential to induce FGF23 production and maintain systemic mineral ion homeostasis. <b>2016</b> , 30, 428-40	51
1401	In vivo effects of two novel ALN-EP4a conjugate drugs on bone in the ovariectomized rat model for reversing postmenopausal bone loss. <b>2016</b> , 27, 797-808	7
1400	Rapamycin reduces severity of senile osteoporosis by activating osteocyte autophagy. <b>2016</b> , 27, 1093-1101	54
1399	Activation of Protein Kinase A in Mature Osteoblasts Promotes a Major Bone Anabolic Response. <b>2016</b> , 157, 112-26	10

Long-term vitamin D deficiency in older adult C57BL/6 mice does not affect bone structure, remodeling and mineralization. <b>2016</b> , 164, 344-352	12
Raloxifene improves skeletal properties in an animal model of cystic chronic kidney disease. <b>2016</b> , 89, 95-104	16
Sclerostin-antibody treatment of glucocorticoid-induced osteoporosis maintained bone mass and strength. <b>2016</b> , 27, 283-294	80
Differences in vertebral, tibial, and iliac cancellous bone metabolism in ovariectomized rats. <b>2016</b> , 34, 291-302	10
Biomarkers for Bisphosphonate-Related Osteonecrosis of the Jaw. <b>2016</b> , 18, 281-91	22
Comparison of parathyroid hormone and strontium ranelate in combination with whole-body vibration in a rat model of osteoporosis. <b>2017</b> , 35, 31-39	12
Comparison of tissue transglutaminase 2 and bone biological markers osteocalcin, osteopontin and sclerostin expression in human osteoporosis and osteoarthritis. <b>2017</b> , 49, 683-693	11
Effects of Sex and Notch Signaling on the Osteocyte Cell Pool. <b>2017</b> , 232, 363-370	10
Different bone remodeling levels of trabecular and cortical bone in response to changes in Wnt/Etatenin signaling in mice. <b>2017</b> , 35, 812-819	34
Abaloparatide: Recombinant human PTHrP (1-34) anabolic therapy for osteoporosis. <b>2017</b> , 97, 53-60	13
Unique local bone tissue characteristics in iliac crest bone biopsy from adolescent idiopathic scoliosis with severe spinal deformity. <b>2017</b> , 7, 40265	11
Effects of suppressed bone remodeling by minodronic acid and alendronate on bone mass, microdamage accumulation, collagen crosslinks and bone mechanical properties in the lumbar vertebra of ovariectomized cynomolgus monkeys. <b>2017</b> , 97, 184-191	12
Iliac crest histomorphometry and skeletal heterogeneity in men. 2017, 6, 9-16	10
Leptin stimulates bone formation in ob/ob mice at doses having minimal impact on energy metabolism. <b>2017</b> , 232, 461-474	39
Intrinsic material property differences in bone tissue from patients suffering low-trauma osteoporotic fractures, compared to matched non-fracturing women. <b>2017</b> , 97, 233-242	17
A Conditional Knockout Mouse Model Reveals a Critical Role of PKD1 in Osteoblast Differentiation and Bone Development. <b>2017</b> , 7, 40505	16
Biodegradable Magnesium Screws Accelerate Fibrous Tissue Mineralization at the Tendon-Bone Insertion in Anterior Cruciate Ligament Reconstruction Model of Rabbit. <b>2017</b> , 7, 40369	23
Bone Mass and Strength are Significantly Improved in Mice Overexpressing Human WNT16 in Osteocytes. <b>2017</b> , 100, 361-373	8
	Raioxifene improves skeletal properties in an animal model of cystic chronic kidney disease. 2016, 89, 95-104  Sclerostin-antibody treatment of glucocorticoid-induced osteoporosis maintained bone mass and strength. 2016, 27, 283-294  Differences in vertebral, tibial, and iliac cancellous bone metabolism in ovariectomized rats. 2016, 34, 291-302  Biomarkers for Bisphosphonate-Related Osteonecrosis of the Jaw. 2016, 18, 281-91  Comparison of parathyroid hormone and strontium ranelate in combination with whole-body vibration in a rat model of osteoporosis. 2017, 35, 31-39  Comparison of tissue transglutaminase 2 and bone biological markers osteocalcin, osteopontin and sclerostin expression in human osteoporosis and osteoarthritis. 2017, 49, 683-693  Effects of Sex and Notch Signaling on the Osteocyte Cell Pool. 2017, 232, 363-370  Different bone remodeling levels of trabecular and cortical bone in response to changes in Wnt/£tatenin signaling in mice. 2017, 35, 812-819  Abaloparatide: Recombinant human PTHrP (1-34) anabolic therapy for osteoporosis. 2017, 97, 53-60  Unique local bone tissue characteristics in iliac crest bone biopsy from adolescent idiopathic scollosis with severe spinal deformity. 2017, 7, 40265  Effects of suppressed bone remodeling by minodronic acid and alendronate on bone mass, microdamage accumulation, collagen crosslinks and bone mechanical properties in the lumbar vertebra of ovariectomized cynomologus monkeys. 2017, 97, 184-191  Iliac crest histomorphometry and skeletal heterogeneity in men. 2017, 6, 9-16  Leptin stimulates bone formation in ob/ob mice at doses having minimal impact on energy metabolism. 2017, 232, 461-474  Intrinsic material property differences in bone tissue from patients suffering low-trauma osteoporotic fractures, compared to matched non-fracturing women. 2017, 97, 233-242  A Conditional Knockout Mouse Model Reveals a Critical Role of PKD1 in Osteoblast Differentiation and Bone Development. 2017, 7, 40569

1380	Inhibition of osteoclast differentiation and collagen antibody-induced arthritis by CTHRC1. <b>2017</b> , 97, 153-167		16
1379	IGF-1 Receptor Expression on Circulating Osteoblast Progenitor Cells Predicts Tissue-Based Bone Formation Rate and Response to Teriparatide in Premenopausal Women With Idiopathic Osteoporosis. <i>Journal of Bone and Mineral Research</i> , <b>2017</b> , 32, 1267-1273	6.3	8
1378	Bone Structure and Turnover Status in Postmenopausal Women with Atypical Femur Fracture After Prolonged Bisphosphonate Therapy. <b>2017</b> , 100, 235-243		11
1377	A histomorphometric study of the cancellous spinal process bone in adolescent idiopathic scoliosis. <b>2017</b> , 26, 1600-1609		7
1376	Asymmetric bone remodeling in mandibular and maxillary tori. 2017, 21, 2781-2788		3
1375	Fkbp10 Deletion in Osteoblasts Leads to Qualitative Defects in Bone. <i>Journal of Bone and Mineral Research</i> , <b>2017</b> , 32, 1354-1367	6.3	11
1374	Tomography-Based Quantification of Regional Differences in Cortical Bone Surface Remodeling and Mechano-Response. <b>2017</b> , 100, 255-270		26
1373	Impaired rib bone mass and quality in end-stage cystic fibrosis patients. <b>2017</b> , 98, 9-17		9
1372	miR-21 deficiency inhibits osteoclast function and prevents bone loss in mice. <b>2017</b> , 7, 43191		71
1371	A novel in silico method to quantify primary stability of screws in trabecular bone. <b>2017</b> , 35, 2415-2424		14
1370	Coupling of Bone Resorption and Formation in Real Time: New Knowledge Gained From Human Haversian BMUs. <i>Journal of Bone and Mineral Research</i> , <b>2017</b> , 32, 1395-1405	6.3	64
1369	VDR in Osteoblast-Lineage Cells Primarily Mediates Vitamin D Treatment-Induced Increase in Bone Mass by Suppressing Bone Resorption. <i>Journal of Bone and Mineral Research</i> , <b>2017</b> , 32, 1297-1308	6.3	41
1368	Intermittent Ibandronate Maintains Bone Mass, Bone Structure, and Biomechanical Strength of Trabecular and Cortical Bone After Discontinuation of Parathyroid Hormone Treatment in Ovariectomized Rats. <b>2017</b> , 101, 65-74		5
1367	Proceedings of the 2016 Santa Fe Bone Symposium: New Concepts in the Management of Osteoporosis and Metabolic Bone Diseases. <b>2017</b> , 20, 134-152		5
1366	Klotho expression in long bones regulates FGF23 production during renal failure. <b>2017</b> , 31, 2050-2064		31
1365	Loss of menin in osteoblast lineage affects osteocyte-osteoclast crosstalk causing osteoporosis. <b>2017</b> , 24, 672-682		32
1364	Role of estrogen receptor signaling in skeletal response to leptin in female mice. <b>2017</b> , 233, 357-367		13
1363	What Animal Models Have Taught Us About the Safety and Efficacy of Bisphosphonates in Chronic Kidney Disease. <b>2017</b> , 15, 171-177		6

## (2017-2017)

1362	Icariin protects against glucocorticoid induced osteoporosis, increases the expression of the bone enhancer DEC1 and modulates the PI3K/Akt/GSK3/Acatenin integrated signaling pathway. <b>2017</b> , 136, 109-121	35
1361	Connexin43 and Runx2 Interact to Affect Cortical Bone Geometry, Skeletal Development, and Osteoblast and Osteoclast Function. <i>Journal of Bone and Mineral Research</i> , <b>2017</b> , 32, 1727-1738	31
1360	NGF-TrkA signaling in sensory nerves is required for skeletal adaptation to mechanical loads in mice. <b>2017</b> , 114, E3632-E3641	79
1359	Renal Osteodystrophy-Time for Common Nomenclature. <b>2017</b> , 15, 187-193	10
1358	Human type H vessels are a sensitive biomarker of bone mass. <b>2017</b> , 8, e2760	53
1357	Administration frequency as well as dosage of PTH are associated with development of cortical porosity in ovariectomized rats. <b>2017</b> , 5, 17002	23
1356	Role of Osteoblast Gi Signaling in Age-Related Bone Loss in Female Mice. <b>2017</b> , 158, 1715-1726	4
1355	Trabecular resorption patterns of cement-bone interlock regions in total knee replacements. <b>2017</b> , 35, 2773-2780	8
1354	Chronic Mild Stress Causes Bone Loss via an Osteoblast-Specific Glucocorticoid-Dependent Mechanism. <b>2017</b> , 158, 1939-1950	12
1353	Eldecalcitol, an Active Vitamin D Derivative, Prevents Trabecular Bone Loss and Bone Fragility in Type I Diabetic Model Rats. <b>2017</b> , 101, 433-444	7
1352	Low-dose BMP-2 is sufficient to enhance the bone formation induced by an injectable, PLGA fiber-reinforced, brushite-forming cement in a sheep defect model of lumbar osteopenia. <b>2017</b> , 17, 1699-171	I <sup>16</sup>
1351	Inhibiting the osteocyte-specific protein sclerostin increases bone mass and fracture resistance in multiple myeloma. <b>2017</b> , 129, 3452-3464	117
1350	Hypodynamia Alters Bone Quality and Trabecular Microarchitecture. <b>2017</b> , 100, 332-340	14
1349	A Direct Comparison of the Effects of the Antiretroviral Drugs Stavudine, Tenofovir and the Combination Lopinavir/Ritonavir on Bone Metabolism in a Rat Model. <b>2017</b> , 101, 422-432	4
1348	10 years of denosumab treatment in postmenopausal women with osteoporosis: results from the phase 3 randomised FREEDOM trial and open-label extension. <b>2017</b> , 5, 513-523	419
1347	An Essential Physiological Role for MCT8 in Bone in Male Mice. <b>2017</b> , 158, 3055-3066	11
1346	Osteoblast-specific deletion of Hrpt2/Cdc73 results in high bone mass and increased bone turnover. <b>2017</b> , 98, 68-78	6
1345	Disruption of the Aldehyde Dehydrogenase 2 Gene Results in No Increase in Trabecular Bone Mass Due to Skeletal Loading in Association with Impaired Cell Cycle Regulation Through p21 Expression in the Bone Marrow Cells of Mice. <b>2017</b> , 101, 328-340	9

1344	Sclerostin activity plays a key role in the negative effect of glucocorticoid signaling on osteoblast function in mice. <b>2017</b> , 5, 17013	13
1343	Sustained Notch2 signaling in osteoblasts, but not in osteoclasts, is linked to osteopenia in a mouse model of Hajdu-Cheney syndrome. <b>2017</b> , 292, 12232-12244	20
1342	Oral administration of kaempferol inhibits bone loss in rat model of ovariectomy-induced osteopenia. <b>2017</b> , 69, 1113-1119	19
1341	Genetic deletion of Sost or pharmacological inhibition of sclerostin prevent multiple myeloma-induced bone disease without affecting tumor growth. <b>2017</b> , 31, 2686-2694	72
1340	A comparative study of bone biopsies from the iliac crest, the tibial bone, and the lumbar spine. <b>2017</b> , 18, 134	7
1339	Long-term supplementation with young coconut juice does not prevent bone loss but rather alleviates body weight gain in ovariectomized rats. <b>2017</b> , 6, 585-591	3
1338	Bone Formation Is Coupled to Resorption Via Suppression of Sclerostin Expression by Osteoclasts. <i>Journal of Bone and Mineral Research</i> , <b>2017</b> , 32, 2074-2086	42
1337	Integrin-Linked Kinase Regulates Bone Formation by Controlling Cytoskeletal Organization and Modulating BMP and Wnt Signaling in Osteoprogenitors. <i>Journal of Bone and Mineral Research</i> , 6.3 <b>2017</b> , 32, 2087-2102	30
1336	Klotho Lacks an FGF23-Independent Role in Mineral Homeostasis. <i>Journal of Bone and Mineral Research</i> , <b>2017</b> , 32, 2049-2061	24
1335	Bone Mass Is Compromised by the Chemotherapeutic Trabectedin in Association With Effects on Osteoblasts and Macrophage Efferocytosis. <i>Journal of Bone and Mineral Research</i> , <b>2017</b> , 32, 2116-2127 6.3	16
1334	Decreased trabecular bone deterioration of proximal tibiae and lumbar vertebrae in postmenopausal women with osteoarthritis. <b>2017</b> , 13, 3355-3359	2
1333	The integration of orthodontic miniscrews under mechanical loading: a pre-clinical study in rabbit. <b>2017</b> , 39, 519-527	3
1332	Open source software for semi-automated histomorphometry of bone resorption and formation parameters. <b>2017</b> , 99, 69-79	48
1331	The Pharmacological Profile of a Novel Highly Potent Bisphosphonate, OX14 (1-Fluoro-2-(Imidazo-[1,2-Pyridin-3-yl)-Ethyl-Bisphosphonate). <i>Journal of Bone and Mineral</i> 6.3 Research, <b>2017</b> , 32, 1860-1869	18
1330	Osteocyte Protein Expression Is Altered in Low-Turnover Osteoporosis Caused by Mutations in WNT1 and PLS3. <b>2017</b> , 102, 2340-2348	14
1329	Deletion of Adseverin in Osteoclasts Affects Cell Structure But Not Bone Metabolism. <b>2017</b> , 101, 207-216	1
1328	Klotho expression in osteocytes regulates bone metabolism and controls bone formation. <b>2017</b> , 92, 599-611	57
1327	Effect of Sequential Treatment with Bisphosphonates After Teriparatide in Ovariectomized Rats: A Direct Comparison Between Risedronate and Alendronate. <b>2017</b> , 101, 102-110	2

1326	Zoledronic acid improves bone histomorphometry in a murine model of Rett syndrome. <b>2017</b> , 99, 1-7		5
1325	Zinc supplementation reduces RANKL/OPG ratio and prevents bone architecture alterations in ovariectomized and type 1 diabetic rats. <b>2017</b> , 40, 48-56		14
1324	Cathepsin K Controls Cortical Bone Formation by Degrading Periostin. <i>Journal of Bone and Mineral Research</i> , <b>2017</b> , 32, 1432-1441	6.3	42
1323	Bone Resorption Is Regulated by Circadian Clock in Osteoblasts. <i>Journal of Bone and Mineral Research</i> , <b>2017</b> , 32, 872-881	6.3	56
1322	Efficacy and safety of osteoporosis medications in a rat model of late-stage chronic kidney disease accompanied by secondary hyperparathyroidism and hyperphosphatemia. <b>2017</b> , 28, 1481-1490		12
1321	Hairy and Enhancer of Split-Related With YRPW Motif-Like (HeyL) Is Dispensable for Bone Remodeling in Mice. <b>2017</b> , 118, 1819-1826		7
1320	CRMP4 Inhibits Bone Formation by Negatively Regulating BMP and RhoA Signaling. <i>Journal of Bone and Mineral Research</i> , <b>2017</b> , 32, 913-926	6.3	9
1319	Syntaxin 4a Regulates Matrix Vesicle-Mediated Bone Matrix Production by Osteoblasts. <i>Journal of Bone and Mineral Research</i> , <b>2017</b> , 32, 440-448	6.3	3
1318	Bisphosphonate Withdrawal: Effects on Bone Formation and Bone Resorption in Maturing Male Mice. <i>Journal of Bone and Mineral Research</i> , <b>2017</b> , 32, 814-820	6.3	10
1317	Effects of chronic lead exposure on bone mineral properties in femurs of growing rats. <b>2017</b> , 377, 64-7	2	16
1317	Effects of chronic lead exposure on bone mineral properties in femurs of growing rats. <b>2017</b> , 377, 64-7  Defective signaling, osteoblastogenesis and bone remodeling in a mouse model of connexin 43  C-terminal truncation. <b>2017</b> , 130, 531-540	2	16 42
,	Defective signaling, osteoblastogenesis and bone remodeling in a mouse model of connexin 43 C-terminal truncation. <b>2017</b> , 130, 531-540	2	
1316	Defective signaling, osteoblastogenesis and bone remodeling in a mouse model of connexin 43 C-terminal truncation. <b>2017</b> , 130, 531-540	6.3	
1316 1315	Defective signaling, osteoblastogenesis and bone remodeling in a mouse model of connexin 43 C-terminal truncation. <b>2017</b> , 130, 531-540  Effects of electromagnetic fields on bone loss in hyperthyroidism rat model. <b>2017</b> , 38, 137-150  PTHrP-Derived Peptides Restore Bone Mass and Strength in Diabetic Mice: Additive Effect of		4 <sup>2</sup>
1316 1315 1314	Defective signaling, osteoblastogenesis and bone remodeling in a mouse model of connexin 43 C-terminal truncation. 2017, 130, 531-540  Effects of electromagnetic fields on bone loss in hyperthyroidism rat model. 2017, 38, 137-150  PTHrP-Derived Peptides Restore Bone Mass and Strength in Diabetic Mice: Additive Effect of Mechanical Loading. <i>Journal of Bone and Mineral Research</i> , 2017, 32, 486-497  Teriparatide treatment in a heart transplant patient with a chronic kidney disease and a		7 24
1316 1315 1314 1313	Defective signaling, osteoblastogenesis and bone remodeling in a mouse model of connexin 43 C-terminal truncation. 2017, 130, 531-540  Effects of electromagnetic fields on bone loss in hyperthyroidism rat model. 2017, 38, 137-150  PTHrP-Derived Peptides Restore Bone Mass and Strength in Diabetic Mice: Additive Effect of Mechanical Loading. Journal of Bone and Mineral Research, 2017, 32, 486-497  Teriparatide treatment in a heart transplant patient with a chronic kidney disease and a low-turnover bone disease: a case report. 2017, 28, 1149-1152  Bone histomorphometry in de novo renal transplant recipients indicates a further decline inlbone		42 7 24
1316 1315 1314 1313 1312	Defective signaling, osteoblastogenesis and bone remodeling in a mouse model of connexin 43 C-terminal truncation. 2017, 130, 531-540  Effects of electromagnetic fields on bone loss in hyperthyroidism rat model. 2017, 38, 137-150  PTHrP-Derived Peptides Restore Bone Mass and Strength in Diabetic Mice: Additive Effect of Mechanical Loading. Journal of Bone and Mineral Research, 2017, 32, 486-497  Teriparatide treatment in a heart transplant patient with a chronic kidney disease and a low-turnover bone disease: a case report. 2017, 28, 1149-1152  Bone histomorphometry in de novo renal transplant recipients indicates a further decline infbone resorption 1 year posttransplantation. 2017, 91, 469-476  Time course of disassociation of bone formation signals with bone mass and bone strength in		<ul><li>42</li><li>7</li><li>24</li><li>7</li><li>26</li></ul>

1308	Daily parathyroid hormone administration enhances bone turnover and preserves bone structure after severe immobilization-induced bone loss. <b>2017</b> , 5, e13446	11
1307	Small leucine rich proteoglycans, a novel link to osteoclastogenesis. <b>2017</b> , 7, 12627	27
1306	Chronic psychosocial stress disturbs long-bone growth in adolescent mice. <b>2017</b> , 10, 1399-1409	13
1305	Application of Histopathology and Bone Histomorphometry for Understanding Test Article-Related Bone Changes and Assessing Potential Bone Liabilities. <b>2017</b> , 253-278	3
1304	Effect of the antidiabetic agent pioglitazone on bone metabolism in rats. 2017, 135, 22-28	7
1303	Role of Anatomic Pathology in Skeletal Evaluations: Applying INHAND Diagnostic Criteria. <b>2017</b> , 45, 845-850	2
1302	Clcn7 as a new mouse model of Albers-Schibberg disease. <b>2017</b> , 105, 253-261	6
1301	Exposure to Low-Dose X-Ray Radiation Alters Bone Progenitor Cells and Bone Microarchitecture. <b>2017</b> , 188, 433-442	14
1300	Update on the role of bone biopsy in the management of patients with CKD-MBD. <b>2017</b> , 30, 645-652	24
1299	Spontaneous mutation of Dock7 results in lower trabecular bone mass and impaired periosteal expansion in aged female Misty mice. <b>2017</b> , 105, 103-114	9
1298	An Antibody to Notch2 Reverses the Osteopenic Phenotype of Hajdu-Cheney Mutant Male Mice. <b>2017</b> , 158, 730-742	23
1297	Evaluation of loading parameters for murine axial tibial loading: Stimulating cortical bone formation while reducing loading duration. <b>2018</b> , 36, 682-691	23
1296	Automatic registration of 2D histological sections to 3D microCT volumes: Trabecular bone. <b>2017</b> , 105, 173-183	3
1295	Specific inhibition of NLRP3 in chikungunya disease reveals a role for inflammasomes in alphavirus-induced inflammation. <b>2017</b> , 2, 1435-1445	54
1294	Etelcalcetide (AMG 416), a peptide agonist of the calcium-sensing receptor, preserved cortical bone structure and bone strength in subtotal nephrectomized rats with established secondary hyperparathyroidism. <b>2017</b> , 105, 163-172	12
1293	Patient-specific in silico models can quantify primary implant stability in elderly human bone. <b>2018</b> , 36, 954-962	5
1292	Kynurenine, a Tryptophan Metabolite That Accumulates With Age, Induces Bone Loss. <i>Journal of Bone and Mineral Research</i> , <b>2017</b> , 32, 2182-2193	61
1291	Comparison of calcimimetic R568 and calcitriol in mineral homeostasis in the Hyp mouse, a murine homolog of X-linked hypophosphatemia. <b>2017</b> , 103, 224-232	7

1290	Rad GTPase is essential for the regulation of bone density and bone marrow adipose tissue in mice. <b>2017</b> , 103, 270-280	$\epsilon$	6
1289	An appropriate Wnt/Ecatenin expression level during the remodeling phase is required for improved bone fracture healing in mice. <b>2017</b> , 7, 2695	3	32
1288	A novel role for dopamine signaling in the pathogenesis of bone loss from the atypical antipsychotic drug risperidone in female mice. <b>2017</b> , 103, 168-176	2	22
1287	Effects of the basic multicellular unit and lamellar thickness on osteonal fatigue life. <b>2017</b> , 60, 116-123	4	1
1286	Sclerostin Blockade and Zoledronic Acid Improve Bone Mass and Strength in Male Mice With Exogenous Hyperthyroidism. <b>2017</b> , 158, 3765-3777	1	10
1285	Relationships between age and microarchitectural descriptors of iliac trabecular bone determined by microCT. <b>2017</b> , 101, 64-70	1	[
1284	PLS3 sequencing in childhood-onset primary osteoporosis identifies two novel disease-causing variants. <b>2017</b> , 28, 3023-3032	2	24
1283	Histomorphometric Parameters of the Growth Plate and Trabecular Bone in Wild-Type and Trefoil Factor Family 3 (Tff3)-Deficient Mice Analyzed by Free and Open-Source Image Processing Software. <b>2017</b> , 23, 818-825	3	3
1282	Dietary magnesium supplementation prevents and liteverses vascular and soft tissue calcifications in uremic rats. <b>2017</b> , 92, 1084-1099	$\epsilon$	67
1281	Commensal Gut Microbiota Immunomodulatory Actions in Bone Marrow and Liver have Catabolic Effects on Skeletal Homeostasis in Health. <b>2017</b> , 7, 5747	٥	55
1280	Calcium and vitamin-D deficiency marginally impairs fracture healing but aggravates posttraumatic bone loss in osteoporotic mice. <b>2017</b> , 7, 7223	2	23
1279	Development of an efficient screening system to identify novel bone metabolism-related genes using the exchangeable gene trap mutagenesis mouse models. <b>2017</b> , 7, 40692	2	2
1278	The CRH-Transgenic Cushingoid Mouse Is a Model of Glucocorticoid-Induced Osteoporosis. <b>2017</b> , 1, 46-57	1	Ĺ
1277	Treatment With a Soluble Bone Morphogenetic Protein Type 1A Receptor (BMPR1A) Fusion Protein Increases Bone Mass and Bone Formation in Mice Subjected to Hindlimb Unloading. <b>2017</b> , 1, 66-72	1	10
1276	Metformin Affects Cortical Bone Mass and Marrow Adiposity in Diet-Induced Obesity in Male Mice. <b>2017</b> , 158, 3369-3385	3	36
1275	Mast Cells Are Critical Regulators of Bone Fracture-Induced Inflammation and Osteoclast Formation and Activity. <i>Journal of Bone and Mineral Research</i> , <b>2017</b> , 32, 2431-2444	3	35
1274	PLS3 Deletions Lead to Severe Spinal Osteoporosis and Disturbed Bone Matrix Mineralization. <i>Journal of Bone and Mineral Research</i> , <b>2017</b> , 32, 2394-2404	2	23
1273	Acceleration of Fracture Healing by Overexpression of Basic Fibroblast Growth Factor in the Mesenchymal Stromal Cells. <b>2017</b> , 6, 1880-1893	3	33

1272	Histomorphometric and osteocytic characteristics of cortical bone in male subtrochanteric femoral shaft. <b>2017</b> , 231, 708-717		5
1271	Activated FGFR3 promotes bone formation via accelerating endochondral ossification in mouse model of distraction osteogenesis. <b>2017</b> , 105, 42-49		10
<b>127</b> 0	Differential responses of mechanosensitive osteocyte proteins in fore- and hindlimbs of hindlimb-unloaded rats. <b>2017</b> , 105, 26-34		17
1269	Osteoblasts remotely supply lung tumors with cancer-promoting SiglecF neutrophils. 2017, 358,		172
1268	Catabolic Effects of Human PTH (1-34) on Bone: Requirement of Monocyte Chemoattractant Protein-1 in Murine Model of Hyperparathyroidism. <b>2017</b> , 7, 15300		17
1267	Inducible Activation of FGFR2 in Adult Mice Promotes Bone Formation After Bone Marrow Ablation. <i>Journal of Bone and Mineral Research</i> , <b>2017</b> , 32, 2194-2206	3	8
1266	eIF2Bignaling regulates ischemic osteonecrosis through endoplasmic reticulum stress. <b>2017</b> , 7, 5062		21
1265	Severe bone loss and multiple fractures in SCN8A-related epileptic encephalopathy. <b>2017</b> , 103, 136-143		9
1264	Vertebral bone microarchitecture and osteocyte characteristics of three toothed whale species with varying diving behaviour. <b>2017</b> , 7, 1604		12
1263	GDF5 significantly augments the bone formation induced by an injectable, PLGA fiber-reinforced, brushite-forming cement in a sheep defect model of lumbar osteopenia. <b>2017</b> , 17, 1685-1698		7
1262	Osteoblastic heparan sulfate glycosaminoglycans control bone remodeling by regulating Wnt signaling and the crosstalk between bone surface and marrow cells. <b>2017</b> , 8, e2902		30
1261	Vitamin D regulates osteocyte survival and perilacunar remodeling in human and murine bone. <b>2017</b> , 103, 78-87		46
1260	Quantitative histological grading methods to assess subchondral bone and synovium changes subsequent to medial meniscus transection in the rat. <b>2017</b> , 58, 373-385		9
1259	Cortical bone analysis in a predialysis population: a comparison with a dialysis population. <b>2017</b> , 35, 513-52	21	16
1258	Inflammatory Bowel Disease in a Rodent Model Alters Osteocyte Protein Levels Controlling Bone Turnover. <i>Journal of Bone and Mineral Research</i> , <b>2017</b> , 32, 802-813	.3	36
1257	Effects of abaloparatide-SC (BA058) on bone histology and histomorphometry: The ACTIVE phase 3 trial. <b>2017</b> , 97, 314-319		60
1256	One Year of Abaloparatide, a Selective Activator of the PTH1 Receptor, Increased Bone Formation and Bone Mass in Osteopenic Ovariectomized Rats Without Increasing Bone Resorption. <i>Journal of Bone and Mineral Research</i> , <b>2017</b> , 32, 24-33	.3	55
1255	The development of inter-strain variation in cortical and trabecular traits during growth of the mouse lumbar vertebral body. <b>2017</b> , 28, 1133-1143		3

1254	Not only stiffness, but also yield strength of the trabecular structure determined by non-linear IPE is best predicted by bone volume fraction and fabric tensor. <b>2017</b> , 65, 808-813		30
1253	Repair of calvarial bone defects in mice using electrospun polystyrene scaffolds combined with ETCP or gold nanoparticles. <b>2017</b> , 93, 29-37		13
1252	A Novel ANO5 Mutation Causing Gnathodiaphyseal Dysplasia With High Bone Turnover Osteosclerosis. <i>Journal of Bone and Mineral Research</i> , <b>2017</b> , 32, 277-284	5.3	26
1251	Deletion of FoxO1, 3, and 4 in Osteoblast Progenitors Attenuates the Loss of Cancellous Bone Mass in a Mouse Model of Type 1 Diabetes. <i>Journal of Bone and Mineral Research</i> , <b>2017</b> , 32, 60-69	5.3	21
1250	The effect of experimental osteoporosis on bone regeneration: Part 1, histology findings. <b>2017</b> , 28, e101	-e11(	023
1249	Anabolic Effect of Insulin Therapy on the Bone: Osteoprotegerin and Osteocalcin Up-Regulation in Streptozotocin-Induced Diabetic Rats. <b>2017</b> , 120, 227-234		17
1248	Effects of fluoride on insulin signaling and bone metabolism in ovariectomized rats. <b>2017</b> , 39, 140-146		15
1247	A Novel Hybrid Compound LLP2A-Ale Both Prevented and Rescued the Osteoporotic Phenotype in a Mouse Model of Glucocorticoid-Induced Osteoporosis. <b>2017</b> , 100, 67-79		12
1246	The incorporation of fluoride and strontium in hydroxyapatite affects the composition, structure, and mechanical properties of human cortical bone. <b>2017</b> , 105, 433-442		8
1245	Systemic IL-6 Effector Response in Mediating Systemic Bone Loss Following Inhalation of Organic Dust. <b>2017</b> , 37, 9-19		8
1244	Fluvastatin Inhibits Osteoclast Differentiation and Porphyromonas gingivalis Lipopolysaccharide-Induced Alveolar Bone Erosion in Mice. <b>2017</b> , 88, 390-398		9
1243	Osteoarthritis alters the patellar bones subchondral trabecular architecture. <b>2017</b> , 35, 1982-1989		2
1242	The Circadian Gene Clock Regulates Bone Formation Via PDIA3. <i>Journal of Bone and Mineral Research</i> , <b>2017</b> , 32, 861-871	5.3	25
1241	Enhanced bone formation in sheep vertebral bodies after minimally invasive treatment with a novel, PLGA fiber-reinforced brushite cement. <b>2017</b> , 17, 709-719		23
1240	Suppression of Sclerostin Alleviates Radiation-Induced Bone Loss by Protecting Bone-Forming Cells and Their Progenitors Through Distinct Mechanisms. <i>Journal of Bone and Mineral Research</i> , <b>2017</b> , 32, 360-372	5.3	65
1239	The efficacy of poly-d,l-lactic acid- and hyaluronic acid-coated bone substitutes on implant fixation in sheep. <b>2017</b> , 8, 12-19		9
1238	Impairment of PTX3 expression in osteoblasts: a key element for osteoporosis. 2017, 8, e3125		32
1237	Experimental repetitive mild traumatic brain injury induces deficits in trabecular bone microarchitecture and strength in mice. <b>2017</b> , 5, 17042		4

1236	The HIV co-receptor CCR5 regulates osteoclast function. <b>2017</b> , 8, 2226	26
1235	Unique Regenerative Mechanism to Replace Bone Lost During Dietary Bone Depletion in Weanling Mice. <b>2017</b> , 158, 714-729	O
1234	Effect of anthocyanin-rich bilberry extract on bone metabolism in ovariectomized rats. 2018, 8, 198-204	9
1233	Antioxidant Effect of Fructus Ligustri Lucidi Aqueous Extract in Ovariectomized Rats Is Mediated through Nox4-ROS-NF- <b>B</b> Pathway. <b>2017</b> , 8, 266	24
1232	Total Flavonoids of Drynariae Rhizoma Prevent Bone Loss Induced by Hindlimb Unloading in Rats. <b>2017</b> , 22,	18
1231	Quantification of Bone Fatty Acid Metabolism and Its Regulation by Adipocyte Lipoprotein Lipase. <b>2017</b> , 18,	21
1230	Exenatide Improves Bone Quality in a Murine Model of Genetically Inherited Type 2 Diabetes Mellitus. <b>2017</b> , 8, 327	14
1229	Collagen Sponge Functionalized with Chimeric Anti-BMP-2 Monoclonal Antibody Mediates Repair of Critical-Size Mandibular Continuity Defects in a Nonhuman Primate Model. <b>2017</b> , 2017, 8094152	4
1228	Recipient Glycemic Micro-environments Govern Therapeutic Effects of Mesenchymal Stem Cell Infusion on Osteopenia. <b>2017</b> , 7, 1225-1244	26
1227	Extracorporeal shock waves alone or combined with raloxifene promote bone formation and suppress resorption in ovariectomized rats. <b>2017</b> , 12, e0171276	10
1226	Excessive dietary intake of vitamin A reduces skull bone thickness in mice. <b>2017</b> , 12, e0176217	13
1225	Higher mineralized bone volume is associated with a lower plain X-Ray vascular calcification score in hemodialysis patients. <b>2017</b> , 12, e0179868	6
1224	Renal osteodystrophy in the obesity era: Is metabolic syndrome relevant?. <b>2017</b> , 12, e0180387	2
1223	Low calcium diet increases 4T1 mammary tumor carcinoma cell burden and bone pathology in mice. <b>2017</b> , 12, e0180886	2
1222	Accuracy and reproducibility of mouse cortical bone microporosity as quantified by desktop microcomputed tomography. <b>2017</b> , 12, e0182996	14
1221	Effects of the antiepileptic drugs topiramate and lamotrigine on bone metabolism in rats. <b>2017</b> , 38, 297-305	6
1220	Effects of mechanical repetitive load on bone quality around implants in rat maxillae. <b>2017</b> , 12, e0189893	19
1219	The use of a biphasic calcium phosphate in a maxillary sinus floor elevation procedure: a clinical, radiological, histological, and histomorphometric evaluation with 9- and 12-month healing times. <b>2017</b> , 3, 34	8

1218	Inhibition of GDF8 (Myostatin) accelerates bone regeneration in diabetes mellitus type 2. <b>2017</b> , 7, 9878	26
1217	Image-Based Histological Evaluation of Scaffold-Free 3D Osteoblast Cultures. <b>2017</b> , 2, 42	1
1216	Utilising mobilisation of body reserves to improve the management of phosphorus nutrition of breeder cows. <b>2017</b> , 57, 2280	8
1215	Melphalan modifies the bone microenvironment by enhancing osteoclast formation. <b>2017</b> , 8, 68047-68058	8
1214	Old age causes de novo intracortical bone remodeling and porosity in mice. 2017, 2,	91
1213	The contribution of Micro-CT to the evaluation of trabecular bone at the posterior part of the auricular surface in men. <b>2018</b> , 132, 1231-1239	O
1212	Runx2 overexpression compromises bone quality in acromegalic patients. <b>2018</b> , 25, 269-277	12
1211	Pharmacological Inhibition of the Skeletal IKKIReduces Breast Cancer-Induced Osteolysis. <b>2018</b> , 103, 206-216	7
1 <b>2</b> 10	Lrp1 in osteoblasts controls osteoclast activity and protects against osteoporosis by limiting PDGF-RANKL signaling. <b>2018</b> , 6, 4	24
1209	Increased mechanical loading through controlled swimming exercise induces bone formation and mineralization in adult zebrafish. <b>2018</b> , 8, 3646	49
1208	Trabecular bone microstructure and mineral density in human residual ridge at various intervals over a long period after tooth extraction. <b>2018</b> , 20, 375-383	2
1207	The high bone mass phenotype of Lrp5-mutant mice is not affected by megakaryocyte depletion. <b>2018</b> , 497, 659-666	
1206	Prolonged high force high repetition pulling induces osteocyte apoptosis and trabecular bone loss in distal radius, while low force high repetition pulling induces bone anabolism. <b>2018</b> , 110, 267-283	10
1205	Neutralization of CD40 ligand costimulation promotes bone formation and accretion of vertebral bone mass in mice. <b>2018</b> , 57, 1105-1114	6
1204	Cortical bone loss due to skeletal unloading in aldehyde dehydrogenase 2 gene knockout mice is associated with decreased PTH receptor expression in osteocytes. <b>2018</b> , 110, 254-266	11
1203	Effect of 25-HydroxyVitamin D Deficiency and Its Interaction with Prednisone Treatment on Musculoskeletal Health in Growing Mdx Mice. <b>2018</b> , 103, 311-323	4
1202	Sixty-Two-Year-Old Male Suffering From Uremic Leontiasis Ossea Caused by Severe Secondary Hyperparathyroidism. <b>2018</b> , 2, 240-245	5
1201	Targeting sphingosine-1-phosphate lyase as an anabolic therapy for bone loss. <b>2018</b> , 24, 667-678	62

1200	NOX4 Deletion in Male Mice Exacerbates the Effect of Ethanol on Trabecular Bone and Osteoblastogenesis. <b>2018</b> , 366, 46-57		12
1199	Mutations That Alter the Carboxy-Terminal-Propeptide Cleavage Site of the Chains of Type I Procollagen Are Associated With a Unique Osteogenesis Imperfecta Phenotype. <i>Journal of Bone</i> and Mineral Research, <b>2018</b> , 33, 1260-1271	6.3	20
1198	Microcystin-leucine arginine (MC-LR) induces bone loss and impairs bone micro-architecture by modulating host immunity in mice: Implications for bone health. <b>2018</b> , 238, 792-802		5
1197	Respective role of membrane and nuclear estrogen receptor (ER) In the mandible of growing mice: Implications for ERI nodulation. <i>Journal of Bone and Mineral Research</i> , <b>2018</b> , 33, 1520-1531	6.3	6
1196	WAIF1 Is a Cell-Surface CTHRC1 Binding Protein Coupling Bone Resorption and Formation. <i>Journal of Bone and Mineral Research</i> , <b>2018</b> , 33, 1500-1512	6.3	11
1195	Bone histomorphometry in transiliac biopsies from 48 normal, healthy men. <b>2018</b> , 111, 109-115		8
1194	Alendronate induces osteoclast precursor apoptosis via peroxisomal dysfunction mediated ER stress. <b>2018</b> , 233, 7415-7423		17
1193	Sclerostin vaccination mitigates estrogen deficiency induction of bone mass loss and microstructure deterioration. <b>2018</b> , 112, 24-34		7
1192	Bone adaptation in response to treadmill exercise in young and adult mice. <b>2018</b> , 8, 29-37		18
1191	Bone Strength in Growing Rats Treated with Fluoride: a Multi-dose Histomorphometric, Biomechanical and Densitometric Study. <b>2018</b> , 185, 375-383		3
1190	A Complex Role for Lipocalin 2 in Bone Metabolism: Global Ablation in Mice Induces Osteopenia Caused by an Altered Energy Metabolism. <i>Journal of Bone and Mineral Research</i> , <b>2018</b> , 33, 1141-1153	6.3	21
1189	High-Fat Diet-Induced Obesity Promotes Expansion of Bone Marrow Adipose Tissue and Impairs Skeletal Stem Cell Functions in Mice. <i>Journal of Bone and Mineral Research</i> , <b>2018</b> , 33, 1154-1165	6.3	87
1188	Chronic Exposure to Fluoride During Gestation and Lactation Increases Mandibular Bone Volume of Suckling Rats. <b>2018</b> , 185, 395-403		
1187	High dietary salt intake correlates with modulated Th17-Treg cell balance resulting in enhanced bone loss and impaired bone-microarchitecture in male mice. <b>2018</b> , 8, 2503		32
1186	inhibits bone loss and increases bone heterogeneity in osteoporotic mice via modulating Treg-Th17 cell balance. <b>2018</b> , 8, 46-56		50
1185	CYR61/CCN1 Regulates Sclerostin Levels and Bone Maintenance. <i>Journal of Bone and Mineral Research</i> , <b>2018</b> , 33, 1076-1089	6.3	16
1184	Mathematical modelling of bone adaptation of the metacarpal subchondral bone in racehorses. <b>2018</b> , 17, 877-890		3
1183	Devising tissue ingrowth metrics: a contribution to the computational characterization of engineered soft tissue healing. <b>2018</b> , 13, 035010		5

1182	Estrogen Deficiency-Mediated M2 Macrophage Osteoclastogenesis Contributes to M1/M2 Ratio Alteration in Ovariectomized Osteoporotic Mice. <i>Journal of Bone and Mineral Research</i> , <b>2018</b> , 33, 899-908 <sup>.3</sup>	57
1181	Effects of estrogen status in osteocyte autophagy and its relation to osteocyte viability in alveolar process of ovariectomized rats. <b>2018</b> , 98, 406-415	21
1180	Perimenopausal bone histomorphometry before and after menopause. 2018, 108, 55-61	10
1179	Trabecular bone microarchitecture analysis, a way for an early detection of genetic dwarfism? Case study of a dwarf mother's offspring. <b>2018</b> , 20, 65-71	2
1178	Expression of an active Gemutant in skeletal stem cells is sufficient and necessary for fibrous dysplasia initiation and maintenance. <b>2018</b> , 115, E428-E437	23
1177	The protective effects of triptolide on age-related bone loss in old male rats. <b>2018</b> , 98, 280-285	4
1176	Protein Kinase G Activation Reverses Oxidative Stress and Restores Osteoblast Function and Bone Formation in Male Mice With Type 1 Diabetes. <b>2018</b> , 67, 607-623	33
1175	Occlusal disharmony-induced stress causes osteopenia of the lumbar vertebrae and long bones in mice. <b>2018</b> , 8, 173	6
1174	Perturbed bone composition and integrity with disorganized osteoblast function in zinc receptor/Gpr39-deficient mice. <b>2018</b> , 32, 2507-2518	16
1173	Sclerostin Antibody Reverses Bone Loss by Increasing Bone Formation and Decreasing Bone Resorption in a Rat Model of Male Osteoporosis. <b>2018</b> , 159, 260-271	19
1172	Cx43 overexpression in osteocytes prevents osteocyte apoptosis and preserves cortical bone quality in aging mice. <b>2018</b> , 2, 206-216	28
1171	Healing of fractures in osteoporotic bones in mice treated with bisphosphonates - A transcriptome analysis. <b>2018</b> , 112, 107-119	18
1170	Effect of long-term administration of mangiferin from Belamcanda chinensis on bone metabolism in ovariectomized rats. <b>2018</b> , 46, 12-18	8
1169	Sclerostin Antibody Treatment Stimulates Bone Formation to Normalize Bone Mass in Male Down Syndrome Mice. <b>2018</b> , 2, 47-54	7
1168	Annexin A5 Involvement in Bone Overgrowth at the Enthesis. <i>Journal of Bone and Mineral Research</i> , <b>2018</b> , 33, 1532-1543	3
1167	Alveolar bone loss and mineralization in the pig with experimental periodontal disease. 2018, 4, e00589	3
1166	Metformin prevents the development of severe chronic kidney disease and its associated mineral and bone disorder. <b>2018</b> , 94, 102-113	34
1165	Redox-Dependent Bone Alkaline Phosphatase Dysfunction Drives Part of the Complex Bone Phenotype in Mice Deficient for. <b>2018</b> , 2, 195-205	8

1164	Inducible inactivation: WNT16 regulates cortical bone thickness in adult mice. <b>2018</b> , 237, 113-122	20
1163	Metaplastic woven bone in bone metastases: A Fourier-transform infrared analysis and imaging of bone quality (FTIR). <b>2018</b> , 102, 69-77	5
1162	Bone-related Circulating MicroRNAs miR-29b-3p, miR-550a-3p, and miR-324-3p and their Association to Bone Microstructure and Histomorphometry. <b>2018</b> , 8, 4867	48
1161	Loss of the Hematopoietic Stem Cell Factor GATA2 in the Osteogenic Lineage Impairs Trabecularization and Mechanical Strength of Bone. <b>2018</b> , 38,	8
1160	Steroid-associated osteonecrosis animal model in rats. <b>2018</b> , 13, 13-24	26
1159	Bacillus clausii inhibits bone loss by skewing Treg-Th17 cell equilibrium in postmenopausal osteoporotic mice model. <b>2018</b> , 54, 118-128	29
1158	Bone histomorphometry in the evaluation of osteomalacia. <b>2018</b> , 8, 125-134	35
1157	Zoledronic Acid Induces Site-Specific Structural Changes and Decreases Vascular Area in the Alveolar Bone. <b>2018</b> , 76, 1893-1901	16
1156	Tristetraprolin Is Required for Alveolar Bone Homeostasis. <b>2018</b> , 97, 946-953	9
1155	Raloxifene but not alendronate can compensate the impaired osseointegration in osteoporotic rats. <b>2018</b> , 22, 255-265	19
1154	High fat diet attenuates hyperglycemia, body composition changes, and bone loss in male streptozotocin-induced type 1 diabetic mice. <b>2018</b> , 233, 1585-1600	13
1153	Serum CTX levels and histomorphometric analysis in Src versus RANKL knockout mice. <b>2018</b> , 36, 264-273	6
1152	Micro-CT and FE-SEM enamel analyses of calcium-based agent application after bleaching. <b>2018</b> , 22, 961-970	5
1151	Pharmacological inhibition of tankyrase induces bone loss in mice by increasing osteoclastogenesis. <b>2018</b> , 106, 156-166	23
1150	Osteoblast-Derived Extracellular Vesicles Are Biological Tools for the Delivery of Active Molecules to Bone. <i>Journal of Bone and Mineral Research</i> , <b>2018</b> , 33, 517-533	64
1149	A Novel Diterpenoid Suppresses Osteoclastogenesis and Promotes Osteogenesis by Inhibiting Ifrd1-Mediated and IBEMediated p65 Nuclear Translocation. <i>Journal of Bone and Mineral Research</i> , <b>2018</b> , 33, 667-678	38
1148	The GDF5 mutant BB-1 enhances the bone formation induced by an injectable, poly(l-lactide-co-glycolide) acid (PLGA) fiber-reinforced, brushite-forming cement in a sheep defect model of lumbar osteopenia. <b>2018</b> , 18, 357-369	8
1147	ECatenin Directs Long-Chain Fatty Acid Catabolism in the Osteoblasts of Male Mice. <b>2018</b> , 159, 272-284	20

1146	Standardization of Small Animal Imaging-Current Status and Future Prospects. 2018, 20, 716-731		16
1145	Effects of single or combination therapy of teriparatide and anti-RANKL monoclonal antibody on bone defect regeneration in mice. <b>2018</b> , 106, 1-10		15
1144	Loss of the nutrient sensor TAS1R3 leads to reduced bone resorption. <b>2018</b> , 74, 3-8		6
1143	PFMG1 promotes osteoblast differentiation and prevents osteoporotic bone loss. <b>2018</b> , 32, 838-849		5
1142	Clinical Significance of DXA and HR-pQCT in Autosomal Dominant Osteopetrosis (ADO II). <b>2018</b> , 102, 41-52		8
1141	A novel bone targeting delivery system carrying phytomolecule icaritin for prevention of steroid-associated osteonecrosis in rats. <b>2018</b> , 106, 52-60		18
1140	Deletion of Menin in craniofacial osteogenic cells in mice elicits development of mandibular ossifying fibroma. <b>2018</b> , 37, 616-626		4
1139	New bone formation and trabecular bone microarchitecture of highly porous tantalum compared to titanium implant threads: A pilot canine study. <b>2018</b> , 29, 164-174		25
1138	Effect of zileuton on osteoporotic bone and its healing, expression of bone, and brain genes in rats. <b>2018</b> , 124, 118-130		4
1137	Proteasome inhibitor bortezomib is a novel therapeutic agent for focal radiation-induced osteoporosis. <b>2018</b> , 32, 52-62		19
1136	High Bone Turnover in Mice Carrying a Pathogenic Notch2 Mutation Causing Hajdu-Cheney Syndrome. <i>Journal of Bone and Mineral Research</i> , <b>2018</b> , 33, 70-83	6.3	17
1135	Reduced Serum IGF-1 Associated With Hepatic Osteodystrophy Is a Main Determinant of Low Cortical but Not Trabecular Bone Mass. <i>Journal of Bone and Mineral Research</i> , <b>2018</b> , 33, 123-136	6.3	11
1134	Regulatory T cells are expanded by Teriparatide treatment in humans and mediate intermittent PTH-induced bone anabolism in mice. <b>2018</b> , 19, 156-171		32
1133	Sclerostin deficiency modifies the development of CKD-MBD in mice. <b>2018</b> , 107, 115-123		15
1132	Bone morphogenetic protein signaling through ACVR1 and BMPR1A negatively regulates bone mass along with alterations in bone composition. <b>2018</b> , 201, 237-246		14
1131	Effects of hypothalamic leptin gene therapy on osteopetrosis in leptin-deficient mice. <b>2018</b> , 236, 57-68		7
1130	The Expanding Life and Functions of Osteogenic Cells: From Simple Bone-Making Cells to Multifunctional Cells and Beyond. <i>Journal of Bone and Mineral Research</i> , <b>2018</b> , 33, 199-210	6.3	7
1129	Bone histomorphometry in acromegaly patients with fragility vertebral fractures. <b>2018</b> , 21, 56-64		28

1128	Induced global deletion of glucocorticoid receptor impairs fracture healing. 2018, 32, 2235-2245	16
1127	Distinct Effects of IL-6 Classic and Trans-Signaling in Bone Fracture Healing. <b>2018</b> , 188, 474-490	54
1126	Imbalanced Osteogenesis and Adipogenesis in Mice Deficient in the Chemokine Cxcl12/Sdf1 in the Bone Mesenchymal Stem/Progenitor Cells. <i>Journal of Bone and Mineral Research</i> , <b>2018</b> , 33, 679-690	15
1125	Kit Mutation Prevents Cancellous Bone Loss during Calcium Deprivation. <b>2018</b> , 102, 93-104	1
1124	Reduction of protein phosphatase 2A C⊕romotes in vivo bone formation and adipocyte differentiation. <b>2018</b> , 470, 251-258	4
1123	The chemokine receptor type 4 antagonist, AMD3100, interrupts experimental tooth movement in rats. <b>2018</b> , 86, 35-39	5
1122	Enhancement of bone regeneration with the accordion technique via HIF-1 NEGF activation in a rat distraction osteogenesis model. <b>2018</b> , 12, e1268-e1276	16
1121	Is centrally induced alveolar bone loss in a large animal model preventable by peripheral hormone substitution?. <b>2018</b> , 22, 495-503	1
1120	Effects of combined teriparatide and zoledronic acid on posterior lumbar vertebral fusion in an aged ovariectomized rat model of osteopenia. <b>2018</b> , 36, 937-944	10
1119	An Optimized Approach to Perform Bone Histomorphometry. <b>2018</b> , 9, 666	21
1118	Osteonecrosis of the jaws caused by bisphosphonate treatment and oxidative stress in mice. <b>2019</b> , 17, 1440-1448	6
1117	Targeted disruption of adenosine kinase in myeloid monocyte cells increases osteoclastogenesis and bone resorption in mice. <b>2018</b> , 41, 2177-2184	1
1116	Phloridzin, an Apple Polyphenol, Exerted Unfavorable Effects on Bone and Muscle in an Experimental Model of Type 2 Diabetes in Rats. <b>2018</b> , 10,	19
1115	Wnt1 is an Lrp5-independent bone-anabolic Wnt ligand. <b>2018</b> , 10,	42
1114	Prevalence of glucocorticoid induced osteonecrosis in the mouse is not affected by treatments that maintain bone vascularity. <b>2018</b> , 9, 181-187	6
1113	Differential effects of type 1 diabetes mellitus and subsequent osteoblastic Etatenin activation on trabecular and cortical bone in a mouse model. <b>2018</b> , 50, 1-14	11
1112	Raman Spectroscopic and Microscopic Analysis for Monitoring Renal Osteodystrophy Signatures. <b>2018</b> , 8,	5
1111	Gender-independent efficacy of mesenchymal stem cell therapy in sex hormone-deficient bone loss via immunosuppression and resident stem cell recovery. <b>2018</b> , 50, 1-14	25

1110	High Doses of Partially Prevents Estrogen Deficiency-Induced Bone Loss With Anti-osteoclastogenic Activity Due to Enhanced iNOS/NO Signaling. <b>2018</b> , 9, 1314	5
1109	Irisin Mediates Effects on Bone and Fat via ₩ Integrin Receptors. 2018, 175, 1756-1768.e17	207
1108	Losartan reverses impaired osseointegration in spontaneously hypertensive rats. 2018, 29, 1126-1134	5
1107	Histomorphometry of ectopic mineralization using undecalcified frozen bone sections. <b>2018</b> , 81, 1318-1324	1
1106	Extracellular matrix with defective collagen cross-linking affects the differentiation of bone cells. <b>2018</b> , 13, e0204306	20
1105	Understanding age-induced cortical porosity in women: Is a negative BMU balance in quiescent osteons a major contributor?. <b>2018</b> , 117, 70-82	9
1104	Guided bone regeneration using beta-tricalcium phosphate with and without fibronectin-An experimental study in rats. <b>2018</b> , 29, 1038-1049	5
1103	Examining the influence of PTH(1-34) on tissue strength and composition. <b>2018</b> , 117, 130-137	14
1102	Parathyroid Hormone (PTH) Increases Skeletal Tumour Growth and Alters Tumour Distribution in an In Vivo Model of Breast Cancer. <b>2018</b> , 19,	6
1101	Discovery of a periosteal stem cell mediating intramembranous bone formation. <b>2018</b> , 562, 133-139	214
1101	Discovery of a periosteal stem cell mediating intramembranous bone formation. <b>2018</b> , 562, 133-139  Loss of Gsan osteocytes leads to osteopenia due to sclerostin induced suppression of osteoblast activity. <b>2018</b> , 117, 138-148	214
	Loss of Gs&n osteocytes leads to osteopenia due to sclerostin induced suppression of osteoblast	
1100	Loss of Gs&n osteocytes leads to osteopenia due to sclerostin induced suppression of osteoblast activity. 2018, 117, 138-148  Topical rifampin powder for orthopaedic trauma part II: Topical rifampin allows for spontaneous bone healing in sterile and contaminated wounds. 2018, 36, 3142-3150	11
1100	Loss of Gs&n osteocytes leads to osteopenia due to sclerostin induced suppression of osteoblast activity. 2018, 117, 138-148  Topical rifampin powder for orthopaedic trauma part II: Topical rifampin allows for spontaneous bone healing in sterile and contaminated wounds. 2018, 36, 3142-3150	11
1000	Loss of GsI nosteocytes leads to osteopenia due to sclerostin induced suppression of osteoblast activity. 2018, 117, 138-148  Topical rifampin powder for orthopaedic trauma part II: Topical rifampin allows for spontaneous bone healing in sterile and contaminated wounds. 2018, 36, 3142-3150  Royal jelly does not prevent bone loss but improves bone strength in ovariectomized rats. 2018, 21, 601-606  Loss of cyclin-dependent kinase 1 impairs bone formation, but does not affect the bone-anabolic	11 12 6
1000 1099 1098 1097	Loss of GsHn osteocytes leads to osteopenia due to sclerostin induced suppression of osteoblast activity. 2018, 117, 138-148  Topical rifampin powder for orthopaedic trauma part II: Topical rifampin allows for spontaneous bone healing in sterile and contaminated wounds. 2018, 36, 3142-3150  Royal jelly does not prevent bone loss but improves bone strength in ovariectomized rats. 2018, 21, 601-606  Loss of cyclin-dependent kinase 1 impairs bone formation, but does not affect the bone-anabolic effects of parathyroid hormone. 2018, 293, 19387-19399  Antiresorptive Agents are More Effective in Preventing Titanium Particle-Induced Calvarial	11 12 6
1000 1099 1098 1097 1096	Loss of GsAn osteocytes leads to osteopenia due to sclerostin induced suppression of osteoblast activity. 2018, 117, 138-148  Topical rifampin powder for orthopaedic trauma part II: Topical rifampin allows for spontaneous bone healing in sterile and contaminated wounds. 2018, 36, 3142-3150  Royal jelly does not prevent bone loss but improves bone strength in ovariectomized rats. 2018, 21, 601-606  Loss of cyclin-dependent kinase 1 impairs bone formation, but does not affect the bone-anabolic effects of parathyroid hormone. 2018, 293, 19387-19399  Antiresorptive Agents are More Effective in Preventing Titanium Particle-Induced Calvarial Osteolysis in Ovariectomized Mice Than Anabolic Agents in Short-Term Administration. 2018, 42, E259-E271  Estrogen therapy associated with mechanical vibration improves bone microarchitecture and	11 12 6 7

1092	Impaired osteocyte maturation in the pathogenesis of renal osteodystrophy. 2018, 94, 1002-1012	17
1091	Bone Histomorphometry in Clinical Practice. <b>2018</b> , 310-318	2
1090	Rickets and Osteomalacia. 2018, 684-694	3
1089	Coupling of bone resorption and formation by RANKL reverse signalling. <b>2018</b> , 561, 195-200	221
1088	A Phase III Randomized Placebo-Controlled Trial to Evaluate Efficacy and Safety of Romosozumab in Men With Osteoporosis. <b>2018</b> , 103, 3183-3193	118
1087	Intermittent PTH 1-34 administration improves the marrow microenvironment and endothelium-dependent vasodilation in bone arteries of aged rats. <b>2018</b> , 124, 1426-1437	15
1086	Computer-based automatic classification of trabecular bone pattern can assist radiographic bone quality assessment at dental implant site. <b>2018</b> , 91, 20180437	5
1085	Low temperature decreases bone mass in mice: Implications for humans. <b>2018</b> , 167, 557-568	13
1084	Enhanced angiogenesis and increased bone turnover characterize bone marrow lesions in osteoarthritis at the base of the thumb. <b>2018</b> , 7, 406-413	5
1083	A bone mineralization defect in the Pah model of classical phenylketonuria involves compromised mesenchymal stem cell differentiation. <b>2018</b> , 125, 193-199	11
1082	Spinal manifestations in 12 patients with musculocontractural Ehlers-Danlos syndrome caused by CHST14/D4ST1 deficiency (mcEDS-CHST14). <b>2018</b> , 176, 2331-2341	12
1081	The lateral meningocele syndrome mutation causes marked osteopenia in mice. <b>2018</b> , 293, 14165-14177	23
1080	Osseointegrative effect of rhBMP-2 covalently bound on a titan-plasma-spray-surface after modification with chromosulfuric acid in a large animal bone gap-healing model with the GEtingen minipig. <b>2018</b> , 13, 219	1
1079	Ubiquitin-specific protease USP34 controls osteogenic differentiation and bone formation by regulating BMP2 signaling. <b>2018</b> , 37,	36
1078	Effectiveness of Strontium Ranelate in the Treatment of Rat Model of Legg-Calve-Perthes Disease. <b>2018</b> , 52, 380-386	2
1077	Maternal embryonic leucine zipper kinase inhibitor OTSSP167 has preclinical activity in multiple myeloma bone disease. <b>2018</b> , 103, 1359-1368	10
1076	Continuous PTH in Male Mice Causes Bone Loss Because It Induces Serum Amyloid A. <b>2018</b> , 159, 2759-2776	7
1075	Targeting skeletal endothelium to ameliorate bone loss. <b>2018</b> , 24, 823-833	110

1074	Global deletion of tetraspanin CD82 attenuates bone growth and enhances bone marrow adipogenesis. <b>2018</b> , 113, 105-113		6	
1073	Deterioration of Cortical Bone Microarchitecture: Critical Component of Renal Osteodystrophy Evaluation. <b>2018</b> , 47, 376-384		24	
1072	Resorption of the mandibular residual ridge: A micro-CT and histomorphometrical analysis. <b>2018</b> , 35, 221		2	
1071	Skeletal Response to Soluble Activin Receptor Type IIB in Mouse Models of Osteogenesis Imperfecta. <i>Journal of Bone and Mineral Research</i> , <b>2018</b> , 33, 1760-1772	3	18	
1070	Strontium-releasing fluorapatite glass-ceramic scaffolds: Structural characterization and in vivo performance. <b>2018</b> , 75, 463-471		19	
1069	Increased H3K27ac level of ACE mediates the intergenerational effect of low peak bone mass induced by prenatal dexamethasone exposure in male offspring rats. <b>2018</b> , 9, 638		26	
1068	Magnetic resonance imaging based assessment of bone microstructure as a non-invasive alternative to histomorphometry in patients with chronic kidney disease. <b>2018</b> , 114, 14-21		18	
1067	Late stages of mineralization and their signature on the bone mineral density distribution. <b>2018</b> , 59, 74-80		5	
1066	Conditional mouse models support the role of SLC39A14 (ZIP14) in Hyperostosis Cranialis Interna and in bone homeostasis. <b>2018</b> , 14, e1007321		4	
1065	The Effects of Long-term Administration of rhPTH(1-84) in Hypoparathyroidism by Bone Histomorphometry. <i>Journal of Bone and Mineral Research</i> , <b>2018</b> , 33, 1931-1939	3	20	
1064	Defective autophagy in osteoblasts induces endoplasmic reticulum stress and causes remarkable bone loss. <b>2018</b> , 14, 1726-1741		79	
1063	Effect of a cathepsin K inhibitor on arthritis and bone mineral density in ovariectomized rats with collagen-induced arthritis. <b>2018</b> , 9, 1-10		6	
1062	Bone Histology as an Integrated Tool in the Process of Human Identification. 2018, 201-213		5	
1061	Skeletal accumulation of fluorescently tagged zoledronate is higher in animals with early stage chronic kidney disease. <b>2018</b> , 29, 2139-2146		7	
1060	Osteocytic oxygen sensing controls bone mass through epigenetic regulation of sclerostin. <b>2018</b> , 9, 2557		54	
1059	Differential effects of high fat diet and diet-induced obesity on skeletal acquisition in female C57BL/6J vs. FVB/NJ Mice. <b>2018</b> , 8, 204-214		17	
1058	Tsc1 Regulates the Balance Between Osteoblast and Adipocyte Differentiation Through Autophagy/Notch1/ECatenin Cascade. <i>Journal of Bone and Mineral Research</i> , <b>2018</b> , 33, 2021-2034	3	30	
1057	Inflammation-induced lymphatic architecture and bone turnover changes are ameliorated by irisin treatment in chronic inflammatory bowel disease. <b>2018</b> , 32, 4848-4861		35	

1056	Intravital microscopy of osteolytic progression and therapy response of cancer lesions in the bone. <b>2018</b> , 10,		33
1055	WNT16 overexpression partly protects against glucocorticoid-induced bone loss. <b>2018</b> , 314, E597-E604		14
1054	Siglec-15-targeting therapy increases bone mass in rats without impairing skeletal growth. <b>2018</b> , 116, 172-180		18
1053	To what extent does hyaluronic acid affect healing of xenografts? A histomorphometric study in a rabbit model. <b>2018</b> , 26, e20170004		9
1052	Daily melatonin administration improves osseointegration in pinealectomized rats. <b>2018</b> , 26, e20170470		15
1051	Nuclear factor of activated T cells 2 is required for osteoclast differentiation and function in vitro but not in vivo. <b>2018</b> , 119, 9334-9345		7
1050	Resveratrol counteracts bone loss via mitofilin-mediated osteogenic improvement of mesenchymal stem cells in senescence-accelerated mice. <b>2018</b> , 8, 2387-2406		60
1049	Retinoic Acid Receptor Activity in Mesenchymal Stem Cells Regulates Endochondral Bone, Angiogenesis, and B Lymphopoiesis. <i>Journal of Bone and Mineral Research</i> , <b>2018</b> , 33, 2202-2213	3	17
1048	VWC2 Increases Bone Formation Through Inhibiting Activin Signaling. <b>2018</b> , 103, 663-674		4
1047	Evidence for Ongoing Modeling-Based Bone Formation in Human Femoral Head Trabeculae Forming Minimodeling Structures: A Study in Patients with Fractures and Arthritis. <b>2018</b> , 9, 88		6
1046	Augmented Fibroblast Growth Factor-23 Secretion in Bone Locally Contributes to Impaired Bone Mineralization in Chronic Kidney Disease in Mice. <b>2018</b> , 9, 311		10
1045	Periosteal progenitors contribute to load-induced bone formation in adult mice and require primary cilia to sense mechanical stimulation. <b>2018</b> , 9, 190		27
1044	Bone Toolbox: Biomarkers, Imaging Tools, Biomechanics, and Histomorphometry. <b>2018</b> , 46, 511-529		13
1043	Effects of Long-Term Denosumab on Bone Histomorphometry and Mineralization in Women With Postmenopausal Osteoporosis. <b>2018</b> , 103, 2498-2509		51
1042	Diminished Canonical ECatenin Signaling During Osteoblast Differentiation Contributes to Osteopenia in Progeria. <i>Journal of Bone and Mineral Research</i> , <b>2018</b> , 33, 2059-2070	3	22
1041	Differing Effects of Parathyroid Hormone, Alendronate, and Odanacatib on Bone Formation and on the Mineralization Process in Intracortical and Endocortical Bone of Ovariectomized Rabbits. <b>2018</b> , 103, 625-637		8
1040	Vitamin D and the skeleton. 2018, 3, 68-73		1
1039	Deletion of the Fanconi Anemia C Gene in Mice Leads to Skeletal Anomalies and Defective Bone Mineralization and Microarchitecture. <i>Journal of Bone and Mineral Research</i> , <b>2018</b> , 33, 2007-2020	3	3

1038	FoxO1 expression in osteoblasts modulates bone formation through resistance to oxidative stress in mice. <b>2018</b> , 503, 1401-1408		19
1037	GATA4 represses RANKL in osteoblasts via multiple long-range enhancers to regulate osteoclast differentiation. <b>2018</b> , 116, 78-86		7
1036	Tiludronate and clodronate do not affect bone structure or remodeling kinetics over a 60day randomized trial. <b>2018</b> , 14, 105		9
1035	Postnatal Skeletal Deletion of Dickkopf-1 Increases Bone Formation and Bone Volume in Male and Female Mice, Despite Increased Sclerostin Expression. <i>Journal of Bone and Mineral Research</i> , <b>2018</b> , 33, 1698-1707	6.3	26
1034	Porcupine inhibitors impair trabecular and cortical bone mass and strength in mice. <b>2018</b> , 238, 13-23		21
1033	Cortical and trabecular bone are equally affected in rats with renal failure and secondary hyperparathyroidism. <b>2018</b> , 19, 24		4
1032	LRP1 Suppresses Bone Resorption in Mice by Inhibiting the RANKL-Stimulated NF- <b>B</b> and p38 Pathways During Osteoclastogenesis. <i>Journal of Bone and Mineral Research</i> , <b>2018</b> , 33, 1773-1784	6.3	15
1031	Osteocytic perilacunar/canalicular turnover in hemodialysis patients with high and low serum PTH levels. <b>2018</b> , 113, 68-76		8
1030	Bone Effects of Binge Alcohol Drinking Using Prepubescent Pigs as a Model. <b>2018</b> , 42, 2123-2135		5
1029	Inflammatory bone loss associated with MFG-E8 deficiency is rescued by teriparatide. <b>2018</b> , 32, 3730-37	741	8
	Inflammatory bone loss associated with MFG-E8 deficiency is rescued by teriparatide. <b>2018</b> , 32, 3730-37 Bone Histomorphometry. <b>2018</b> , 959-973	741	8
		741	
1028	Bone Histomorphometry. 2018, 959-973  Analysis of short-term treatment with the phosphodiesterase type 5 inhibitor tadalafil on long bone development in young rats. 2018, 315, E446-E453  The trabecular bone score: Relationships with trabecular and cortical microarchitecture measured.	741	4
1028	Bone Histomorphometry. 2018, 959-973  Analysis of short-term treatment with the phosphodiesterase type 5 inhibitor tadalafil on long bone development in young rats. 2018, 315, E446-E453  The trabecular bone score: Relationships with trabecular and cortical microarchitecture measured	741	5
1028 1027 1026	Bone Histomorphometry. 2018, 959-973  Analysis of short-term treatment with the phosphodiesterase type 5 inhibitor tadalafil on long bone development in young rats. 2018, 315, E446-E453  The trabecular bone score: Relationships with trabecular and cortical microarchitecture measured by HR-pQCT and histomorphometry in patients with chronic kidney disease. 2018, 116, 215-220  Sinus Membrane Elevation with Heterologous Cortical Lamina: A Randomized Study of a New Surgical Technique for Maxillary Sinus Floor Augmentation without Bone Graft. 2018, 11,  The effect of vitamin D and zoledronic acid in bone marrow adiposity in kidney transplant patients:	741	4 5 31
1028 1027 1026	Bone Histomorphometry. 2018, 959-973  Analysis of short-term treatment with the phosphodiesterase type 5 inhibitor tadalafil on long bone development in young rats. 2018, 315, E446-E453  The trabecular bone score: Relationships with trabecular and cortical microarchitecture measured by HR-pQCT and histomorphometry in patients with chronic kidney disease. 2018, 116, 215-220  Sinus Membrane Elevation with Heterologous Cortical Lamina: A Randomized Study of a New Surgical Technique for Maxillary Sinus Floor Augmentation without Bone Graft. 2018, 11,  The effect of vitamin D and zoledronic acid in bone marrow adiposity in kidney transplant patients:	741	4 5 31 18
1028 1027 1026 1025	Bone Histomorphometry. 2018, 959-973  Analysis of short-term treatment with the phosphodiesterase type 5 inhibitor tadalafil on long bone development in young rats. 2018, 315, E446-E453  The trabecular bone score: Relationships with trabecular and cortical microarchitecture measured by HR-pQCT and histomorphometry in patients with chronic kidney disease. 2018, 116, 215-220  Sinus Membrane Elevation with Heterologous Cortical Lamina: A Randomized Study of a New Surgical Technique for Maxillary Sinus Floor Augmentation without Bone Graft. 2018, 11,  The effect of vitamin D and zoledronic acid in bone marrow adiposity in kidney transplant patients: A post hoc analysis. 2018, 13, e0197994  Loss of RANKL in osteocytes dramatically increases cancellous bone mass in the osteogenesis	741	4 5 31 18

1020	Efficacy of targeting bone-specific GIP receptor in ovariectomy-induced bone loss. 2018,	11
1019	R-spondin-2 is a Wnt agonist that regulates osteoblast activity and bone mass. <b>2018</b> , 6, 24	22
1018	Liraglutide exerts a bone-protective effect in ovariectomized rats with streptozotocin-induced diabetes by inhibiting osteoclastogenesis. <b>2018</b> , 15, 5077-5083	16
1017	Effects of the calcineurin inhibitors cyclosporine and tacrolimus on bone metabolism in rats. <b>2018</b> , 39, 131-139	16
1016	Skeletal Consequences of Nephropathic Cystinosis. <i>Journal of Bone and Mineral Research</i> , <b>2018</b> , 33, 18706188	0 14
1015	Mucin 1 (Muc1) Deficiency in Female Mice Leads to Temporal Skeletal Changes During Aging. <b>2018</b> , 2, 341-350	1
1014	Early life vitamin D depletion alters the postnatal response to skeletal loading in growing and mature bone. <b>2018</b> , 13, e0190675	6
1013	Reversal of loss of bone mass in old mice treated with mefloquine. <b>2018</b> , 114, 22-31	9
1012	Oxidation-specific epitopes restrain bone formation. <b>2018</b> , 9, 2193	22
1011	Folliculin Regulates Osteoclastogenesis Through Metabolic Regulation. <i>Journal of Bone and Mineral Research</i> , <b>2018</b> , 33, 1785-1798	15
1010	Osteoporosis; Prevention and Callitamin D Treatment. <b>2019</b> , 270-274	
1009	Evaluation of ostarine as a selective androgen receptor modulator in a rat model of postmenopausal osteoporosis. <b>2019</b> , 37, 243-255	16
1008	Role of pannexin 1 channels in load-induced skeletal response. <b>2019</b> , 1442, 79-90	11
1007	Whole body vibration with rest days could improve bone quality of distal femoral metaphysis by regulating trabecular arrangement. <b>2019</b> , 62, 95-103	2
1006	Hierarchically Porous Hydroxyapatite Hybrid Scaffold Incorporated with Reduced Graphene Oxide for Rapid Bone Ingrowth and Repair. <b>2019</b> , 13, 9595-9606	93
1005	Hormone-Independent Sexual Dimorphism in the Regulation of Bone Resorption by Krox20. <i>Journal of Bone and Mineral Research</i> , <b>2019</b> , 34, 2277-2286	4
1004	Novel ActRIIB ligand trap increases muscle mass and improves bone geometry in a mouse model of severe osteogenesis imperfecta. <b>2019</b> , 128, 115036	14
1003	Calcium Deficiency Rickets in African Adolescents: Cortical Bone Histomorphometry. <b>2019</b> , 3, e10169	4

1002	Burosumab Improved Histomorphometric Measures of Osteomalacia in Adults with X-Linked Hypophosphatemia: A Phase 3, Single-Arm, International Trial. <i>Journal of Bone and Mineral Research</i> , <b>2019</b> , 34, 2183-2191	6.3	41
1001	The Hajdu Cheney mutation sensitizes mice to the osteolytic actions of tumor necrosis factor $\blacksquare$ <b>2019</b> , 294, 14203-14214		7
1000	Proliferation and Activation of Osterix-Lineage Cells Contribute to Loading-Induced Periosteal Bone Formation in Mice. <b>2019</b> , 3, e10227		11
999	Hop2 Interacts with ATF4 to Promote Osteoblast Differentiation. <i>Journal of Bone and Mineral Research</i> , <b>2019</b> , 34, 2287-2300	6.3	7
998	Asiatic Acid Attenuates Bone Loss by Regulating Osteoclastic Differentiation. 2019, 105, 531-545		6
997	Osteoblast-derived NOTUM reduces cortical bone mass in mice and the locus is associated with bone mineral density in humans. <b>2019</b> , 33, 11163-11179		15
996	Sclerostin inhibition alleviates breast cancer-induced bone metastases and muscle weakness. <b>2019</b> , 5,		40
995	Hyaluronic Acid Stimulates Osseointegration of ETCP in Young and Old Ewes. 2019, 105, 487-496		3
994	The L-type amino acid transporter LAT1 inhibits osteoclastogenesis and maintains bone homeostasis through the mTORC1 pathway. <b>2019</b> , 12,		5
993	Postnatal Runx2 deletion leads to low bone mass and adipocyte accumulation in mice bone tissues. <b>2019</b> , 516, 1229-1233		13
992	Absence of Dipeptidyl Peptidase 3 Increases Oxidative Stress and Causes Bone Loss. <i>Journal of Bone and Mineral Research</i> , <b>2019</b> , 34, 2133-2148	6.3	14
991	Skeletal levels of bisphosphonate in the setting of chronic kidney disease are independent of remodeling rate and lower with fractionated dosing. <b>2019</b> , 127, 419-426		4
990	Histological and histomorphometric analysis of bone tissue after guided bone regeneration with non-resorbable membranes vs resorbable membranes and titanium mesh. <b>2019</b> , 21, 693-701		20
989	Profilin 1 Negatively Regulates Osteoclast Migration in Postnatal Skeletal Growth, Remodeling, and Homeostasis in Mice. <b>2019</b> , 3, e10130		5
988	Women With Pregnancy and Lactation-Associated Osteoporosis (PLO) Have Low Bone Remodeling Rates at the Tissue Level. <i>Journal of Bone and Mineral Research</i> , <b>2019</b> , 34, 1552-1561	6.3	18
987	3D analysis of the osteonal and interstitial tissue in human radii cortical bone. <b>2019</b> , 127, 526-536		8
986	Role of the captured retroviral envelope gene in the fusion of osteoclast and giant cell precursors and in bone resorption, analyzed and in knockout mice. <b>2019</b> , 11, 100214		6
985	Conditional Activation of NF-B Inducing Kinase (NIK) in the Osteolineage Enhances Both Basal and Loading-Induced Bone Formation. <i>Journal of Bone and Mineral Research</i> , <b>2019</b> , 34, 2087-2100	6.3	4

984	Glucocorticoid-Induced Bone Fragility Is Prevented in Female Mice by Blocking Pyk2/Anoikis Signaling. <b>2019</b> , 160, 1659-1673		10
983	Positive impact of low-dose, high-energy radiation on bone in partial- and/or full-weightbearing mice. <b>2019</b> , 5, 13		4
982	Targeted genetic screening in mice through haploid embryonic stem cells identifies critical genes in bone development. <b>2019</b> , 17, e3000350		12
981	Treatment of Human Immunodeficiency Virus Infection With Tenofovir Disoproxil Fumarate-Containing Antiretrovirals Maintains Low Bone Formation Rate, But Increases Osteoid Volume on Bone Histomorphometry. <i>Journal of Bone and Mineral Research</i> , <b>2019</b> , 34, 1574-1584	6.3	6
980	Lactobacillus paracasei HII01, xylooligosaccharide and synbiotics improve tibial microarchitecture in obese-insulin resistant rats. <b>2019</b> , 59, 371-379		1
979	DSS-induced colitis produces inflammation-induced bone loss while irisin treatment mitigates the inflammatory state in both gut and bone. <b>2019</b> , 9, 15144		16
978	MicroRNA-29a Counteracts Glucocorticoid Induction of Bone Loss through Repressing TNFSF13b Modulation of Osteoclastogenesis. <b>2019</b> , 20,		10
977	Effects of loratadine, a histamine H receptor antagonist, on the skeletal system of young male rats. <b>2019</b> , 13, 3357-3367		3
976	Outcome of Teriparatide Treatment on Fracture Healing Complications and Symptomatic Bone Marrow Edema in Four Adult Patients With Hypophosphatasia. <b>2019</b> , 3, e10215		10
975	Let-7f-5p regulates TGFBR1 in glucocorticoid-inhibited osteoblast differentiation and ameliorates glucocorticoid-induced bone loss. <b>2019</b> , 15, 2182-2197		15
974	Site-Specific Load-Induced Expansion of Sca-1Prrx1 and Sca-1Prrx1 Cells in Adult Mouse Long Bone Is Attenuated With Age. <b>2019</b> , 3, e10199		7
973	In Vivo Bone Effects of a Novel Bisphosphonate-EP4a Conjugate Drug (C3) for Reversing Osteoporotic Bone Loss in an Ovariectomized Rat Model. <b>2019</b> , 3, e10237		6
972	Predicting Bone Modeling Parameters in Response to Mechanical Loading. <b>2019</b> , 7, 122561-122572		7
971	TGFIInhibition Stimulates Collagen Maturation to Enhance Bone Repair and Fracture Resistance in a Murine Myeloma Model. <i>Journal of Bone and Mineral Research</i> , <b>2019</b> , 34, 2311-2326	6.3	10
970	The period circadian clock 2 gene responds to glucocorticoids and regulates osteogenic capacity. <b>2019</b> , 11, 199-206		5
969	Female-Specific Role of Progranulin to Suppress Bone Formation. <b>2019</b> , 160, 2024-2037		2
968	The RNA demethylase FTO is required for maintenance of bone mass and functions to protect osteoblasts from genotoxic damage. <b>2019</b> , 116, 17980-17989		40
967	Serum bone markers in ROD patients across the spectrum of decreases in GFR: Activin A increases before all other markers?. <b>2019</b> , 91, 222-230		17

966	Effect of alendronate or 8-prenylnaringenin applied as a single therapy or in combination with vibration on muscle structure and bone healing in ovariectomized rats. <b>2019</b> , 11, 100224		6
965	TRPV6 and Ca1.3 Mediate Distal Small Intestine Calcium Absorption Before Weaning. <b>2019</b> , 8, 625-642		13
964	The emerging role of IMD 0354 on bone homeostasis by suppressing osteoclastogenesis and bone resorption, but without affecting bone formation. <b>2019</b> , 10, 654		4
963	Nicotine exposure during pregnancy programs osteopenia in male offspring rats 42-nAChR-p300-ACE pathway. <b>2019</b> , 33, 12972-12982		6
962	A Delphinidin-Enriched Maqui Berry Extract Improves Bone Metabolism and Protects against Bone Loss in Osteopenic Mouse Models. <b>2019</b> , 8,		13
961	Age-related histological changes in calcified cartilage and subchondral bone in femoral heads from healthy humans. <b>2019</b> , 129, 115037		6
960	Disruption of the preB Cell Receptor Complex Leads to Decreased Bone Mass. <b>2019</b> , 10, 2063		4
959	Hydroxyapatite Block Produced by Sponge Replica Method: Mechanical, Clinical and Histologic Observations. <b>2019</b> , 12,		5
958	Bone loss caused by dopaminergic degeneration and levodopa treatment in Parkinson's disease model mice. <b>2019</b> , 9, 13768		16
957	Age- and sex-dependent role of osteocytic pannexin1 on bone and muscle mass and strength. <b>2019</b> , 9, 13903		4
956	Improved Osseointegration of a TiNbSn Alloy with a Low Young's Modulus Treated with Anodic Oxidation. <b>2019</b> , 9, 13985		12
955	Biofunctionalization with a TGFEI Inhibitor Peptide in the Osseointegration of Synthetic Bone Grafts: An In Vivo Study in Beagle Dogs. <b>2019</b> , 12,		4
954	Teriparatide Improves Bone and Lipid Metabolism in a Male Rat Model of Type 2 Diabetes Mellitus. <b>2019</b> , 160, 2339-2352		13
953	Vdr expression in osteoclast precursors is not critical in bone homeostasis. <b>2019</b> , 195, 105478		7
952	Absence of an osteopetrosis phenotype in IKBKG (NEMO) mutation-positive women: A case-control study. <b>2019</b> , 121, 243-254		1
951	Vitamin A decreases the anabolic bone response to mechanical loading by suppressing bone formation. <b>2019</b> , 33, 5237-5247		8
950	Mesenchymal Cell-Derived Juxtacrine Wnt1 Signaling Regulates Osteoblast Activity and Osteoclast Differentiation. <i>Journal of Bone and Mineral Research</i> , <b>2019</b> , 34, 1129-1142	6.3	15
949	Loss of the PTH/PTHrP receptor along the osteoblast lineage limits the anabolic response to exercise. <b>2019</b> , 14, e0211076		11

948	Probiotic Lactobacillus reuteri Prevents Postantibiotic Bone Loss by Reducing Intestinal Dysbiosis and Preventing Barrier Disruption. <i>Journal of Bone and Mineral Research</i> , <b>2019</b> , 34, 681-698	56
947	The adaption of the bony microstructure of the human glenoid cavity as a result of long-term biomechanical loading. <b>2019</b> , 41, 401-408	1
946	Psoralen accelerates bone fracture healing by activating both osteoclasts and osteoblasts. <b>2019</b> , 33, 5399-5410	25
945	The periosteum dilemma in bioarcheology: Normal growth or pathological condition? BD discriminating microscopic approach. <b>2019</b> , 24, 236-243	1
944	Intermittent PTH treatment improves bone and muscle in glucocorticoid treated Mdx mice: A model of Duchenne Muscular Dystrophy. <b>2019</b> , 121, 232-242	11
943	A distinct bone phenotype in ADPKD patients with end-stage renal disease. <b>2019</b> , 95, 412-419	15
942	Effect of Collagen Cross-Link Deficiency on Incorporation of Grafted Bone. 2019, 7,	
941	Deficiency in the phosphatase PHLPP1 suppresses osteoclast-mediated bone resorption and enhances bone formation in mice. <b>2019</b> , 294, 11772-11784	9
940	Osteocyte Death and Bone Overgrowth in Mice Lacking Fibroblast Growth Factor Receptors 1 and 2 in Mature Osteoblasts and Osteocytes. <i>Journal of Bone and Mineral Research</i> , <b>2019</b> , 34, 1660-1675	11
939	Osteoblast-specific expression of Panx3 is dispensable for postnatal bone remodeling. <b>2019</b> , 127, 155-163	6
938	Bone-Forming and Antiresorptive Effects of Romosozumab in Postmenopausal Women With Osteoporosis: Bone Histomorphometry and Microcomputed Tomography Analysis After 2 and 12 Months of Treatment. <i>Journal of Bone and Mineral Research</i> , <b>2019</b> , 34, 1597-1608	54
937	Investigating Osteocytic Perilacunar/Canalicular Remodeling. <b>2019</b> , 17, 157-168	27
936	Specific RANK Cytoplasmic Motifs Drive Osteoclastogenesis. <i>Journal of Bone and Mineral Research</i> , <b>2019</b> , 34, 1938-1951	7
935	Expression of a Degradation-Resistant ECatenin Mutant in Osteocytes Protects the Skeleton From Mechanodeprivation-Induced Bone Wasting. <i>Journal of Bone and Mineral Research</i> , <b>2019</b> , 34, 1964-1975 6.3	8
934	Management of bone disease in cystinosis: Statement from an international conference. <b>2019</b> , 42, 1019-1029	28
933	Reversal of Osteopenia in Ovariectomized Rats by Pentoxifylline: Evidence of Osteogenic and Osteo-Angiogenic Roles of the Drug. <b>2019</b> , 105, 294-307	9
932	Recovery of bone mineralization and quality during asfotase alfa treatment in an adult patient with infantile-onset hypophosphatasia. <b>2019</b> , 127, 67-74	18
931	Paradoxical effects of JZL184, an inhibitor of monoacylglycerol lipase, on bone remodelling in healthy and cancer-bearing mice. <b>2019</b> , 44, 452-466	20

930	Growth Hormone Increases Bone Toughness and Decreases Muscle Inflammation in Glucocorticoid-Treated Mdx Mice, Model of Duchenne Muscular Dystrophy. <i>Journal of Bone and Mineral Research</i> , <b>2019</b> , 34, 1473-1486	3
929	Petunidin, a B-ring 5'Methylated Derivative of Delphinidin, Stimulates Osteoblastogenesis and Reduces sRANKL-Induced Bone Loss. <b>2019</b> , 20,	17
928	Multimodal [F]FDG PET/CT Is a Direct Readout for Inflammatory Bone Repair: A Longitudinal Study in TNF\(\text{Transgenic Mice.}\) Journal of Bone and Mineral Research, <b>2019</b> , 34, 1632-1645	5
927	Dose-related histopathology and bone remodeling characteristics of the knee articular cartilage and subchondral bone induced by glucocorticoids in rats. <b>2019</b> , 17, 4492-4498	
926	VEGFA From Early Osteoblast Lineage Cells (Osterix+) Is Required in Mice for Fracture Healing.  Journal of Bone and Mineral Research, 2019, 34, 1690-1706	17
925	Accumulation of microdamage and low bone mass in the femoral head as a cause of subchondral insufficiency fracture in a patient with osteogenesis imperfecta. <b>2019</b> , 37, 768-772	1
924	Changes in Bone Histomorphometry after Kidney Transplantation. <b>2019</b> , 14, 894-903	23
923	A Composite Chitosan-Reinforced Scaffold Fails to Provide Osteochondral Regeneration. <b>2019</b> , 20,	10
922	A new target to ameliorate the damage of periodontal disease: The role of transient receptor potential vanilloid type-1 in contrast to that of specific cannabinoid receptors in rats. <b>2019</b> , 90, 1325-1335	4
921	Software comparison to analyze bone radiomics from high resolution CBCT scans of mandibular condyles. <b>2019</b> , 48, 20190049	16
920	Novel application and validation of in vivo micro-CT to study bone modelling in 3D. <b>2019</b> , 22 Suppl 1, 90-95	1
919	Sonochemical time standardization for bioactive materials used in periimplantar defects filling. <b>2019</b> , 56, 437-446	5
918	Is bone loss a physiological cost of reproduction in the Great fruit-eating bat Artibeus lituratus?. <b>2019</b> , 14, e0213781	3
917	Teriparatide improves alveolar bone modelling after tooth extraction in orchiectomized rats. <b>2019</b> , 102, 147-154	7
916	Network models for characterization of trabecular bone. <b>2019</b> , 99, 042406	2
915	Naproxen impairs load-induced bone formation, reduces bone toughness, and diminishes woven bone formation following stress fracture in mice. <b>2019</b> , 124, 22-32	13
914	Bone histology for skeletal age-at-death estimation. <b>2019</b> , 145-159	1
913	Sclerostin antibody reduces long bone fractures in the oim/oim model of osteogenesis imperfecta. <b>2019</b> , 124, 137-147	15

912	Abaloparatide improves cortical geometry and trabecular microarchitecture and increases vertebral and femoral neck strength in a rat model of male osteoporosis. <b>2019</b> , 124, 148-157		13
911	Effects of Surgical Angiogenesis on Segmental Bone Reconstruction With Cryopreserved Massive-Structural Allografts in a Porcine Tibia Model. <b>2019</b> , 37, 1698-1708		5
910	Combined Collagen-Induced Arthritis and Organic Dust-Induced Airway Inflammation to Model Inflammatory Lung Disease in Rheumatoid Arthritis. <i>Journal of Bone and Mineral Research</i> , <b>2019</b> , 34, 173	3 <del>5-</del> 374	13 <sup>11</sup>
909	Salt-Assisted Toughening of Protein Hydrogel with Controlled Degradation for Bone Regeneration. <b>2019</b> , 29, 1901314		50
908	Short-term pharmacologic RAGE inhibition differentially affects bone and skeletal muscle in middle-aged mice. <b>2019</b> , 124, 89-102		13
907	Agonist-induced activation of the S1P receptor 2 constitutes a novel osteoanabolic therapy for the treatment of osteoporosis in mice. <b>2019</b> , 125, 1-7		10
906	TG-interacting factor 1 (Tgif1)-deficiency attenuates bone remodeling and blunts the anabolic response to parathyroid hormone. <b>2019</b> , 10, 1354		16
905	Calcimimetics maintain bone turnover in uremic rats despite the concomitant decrease in parathyroid hormone concentration. <b>2019</b> , 95, 1064-1078		18
904	Macrophage migration inhibitory factor (MIF) inhibitor 4-IPP suppresses osteoclast formation and promotes osteoblast differentiation through the inhibition of the NF-B signaling pathway. <b>2019</b> , 33, 7667-7683		16
903	The Role of Dickkopf-1 in Thyroid Hormone-Induced Changes of Bone Remodeling in Male Mice. <b>2019</b> , 160, 664-674		6
902	Matrix remodeling associated 7 promotes differentiation of bone marrow mesenchymal stem cells toward osteoblasts. <b>2019</b> , 234, 18053-18064		4
901	1,25-Dihydroxy vitamin D3 treatment attenuates osteopenia, and improves bone muscle quality in Goto-Kakizaki type 2 diabetes model rats. <b>2019</b> , 64, 184-195		2
900	DMP1 Ablation in the Rabbit Results in Mineralization Defects and Abnormalities in Haversian Canal/Osteon Microarchitecture. <i>Journal of Bone and Mineral Research</i> , <b>2019</b> , 34, 1115-1128	6.3	16
899	Mechanical Competence and Bone Quality Develop During Skeletal Growth. <i>Journal of Bone and Mineral Research</i> , <b>2019</b> , 34, 1461-1472	6.3	28
898	Bone extracts immunomodulate and enhance the regenerative performance of dicalcium phosphates bioceramics. <b>2019</b> , 89, 343-358		21
897	Bone healing dynamics associated with 3 implants with different surfaces: histologic and histomorphometric analyses in dogs. <b>2019</b> , 49, 25-38		8
896	Glucagon like peptide 2 has a positive impact on osteoporosis in ovariectomized rats. <b>2019</b> , 226, 47-56		8
895	Catabolic activity of osteoblast lineage cells contributes to osteoclastic bone resorption. <b>2019</b> , 132,		8

894	MyD88 and IL-1R signaling drive antibacterial immunity and osteoclast-driven bone loss during Staphylococcus aureus osteomyelitis. <b>2019</b> , 15, e1007744	34
893	An Invertible Mathematical Model of Cortical Bone's Adaptation to Mechanical Loading. <b>2019</b> , 9, 5890	4
892	Indoxyl Sulfate and p-Cresyl Sulfate Promote Vascular Calcification and Associate with Glucose Intolerance. <b>2019</b> , 30, 751-766	74
891	Inverse correlation between trabecular bone volume and bone marrow adipose tissue in rats treated with osteoanabolic agents. <b>2019</b> , 123, 211-223	15
890	Histomorphometry in Rodents. <b>2019</b> , 1914, 411-435	10
889	Intrinsic Bone Defects in Cystinotic Mice. <b>2019</b> , 189, 1053-1064	8
888	Regulation of cytoskeleton and adhesion signaling in osteoclasts by tetraspanin CD82. <b>2019</b> , 10, 100196	5
887	Hypoxia-inducible factor 2∄s a negative regulator of osteoblastogenesis and bone mass accrual. <b>2019</b> , 7, 7	18
886	Slc20a2, Encoding the Phosphate Transporter PiT2, Is an Important Genetic Determinant of Bone Quality and Strength. <i>Journal of Bone and Mineral Research</i> , <b>2019</b> , 34, 1101-1114	18
885	Effects of parathyroidectomy on the biology of bone tissue in patients with chronic kidney disease and secondary hyperparathyroidism. <b>2019</b> , 121, 277-283	10
884	Prolonged release of iloprost enhances pulpal blood flow and dentin bridge formation in a rat model of mechanical tooth pulp exposure. <b>2019</b> , 61, 73-81	6
883	Activation of vitamin D in the gingival epithelium and its role in gingival inflammation and alveolar bone loss. <b>2019</b> , 54, 444-452	10
882	Techniques in Histomorphometry. <b>2019</b> , 141-158	
881	Treatment with an inhibitor of fatty acid synthase attenuates bone loss in ovariectomized mice. <b>2019</b> , 122, 114-122	13
880	Effect of the lipoxygenase inhibitor baicalein on bone tissue and bone healing in ovariectomized rats. <b>2019</b> , 16, 4	7
879	Short-term perioperative parecoxib is not detrimental to shaft fracture healing in a rat model. <b>2019</b> , 8, 472-480	3
878	Increased pore size of scaffolds improves coating efficiency with sulfated hyaluronan and mineralization capacity of osteoblasts. <b>2019</b> , 23, 26	16
877	The Importance of Biologically Active Vitamin D for Mineralization by Osteocytes After Parathyroidectomy for Renal Hyperparathyroidism. <b>2019</b> , 3, e10234	4

876	Doxycycline reduces osteopenia in female rats. <b>2019</b> , 9, 15316	5
875	A comparison of the bone and growth phenotype of , and murine models with the C57BL/10 wild-type mouse. <b>2020</b> , 13,	3
874	Lupus-like Disease in FcRIIB Mice Induces Osteopenia. <b>2019</b> , 9, 17342	4
873	Clinical Inference of Serum and Bone Sclerostin Levels in Patients with End-Stage Kidney Disease. <b>2019</b> , 8,	6
872	Author response. <b>2019</b> , 156, 709-710	
871	PTEN Inhibits Inflammatory Bone Loss in Ligature-Induced Periodontitis via IL1 and TNF <b>2019</b> , 2019, 6712591	4
870	Growth Hormone Effects on Bone Loss-Induced by Mild Traumatic Brain Injury and/or Hind Limb Unloading. <b>2019</b> , 9, 18995	3
869	Histomorphometric Evaluation of Critical-Sized Bone Defects Using Osteomeasure and Aperio Image Analysis Systems. <b>2019</b> , 25, 732-741	5
868	Increased COUP-TFII Expression Mediates the Differentiation Imbalance of Bone Marrow-Derived Mesenchymal Stem Cells in Femoral Head Osteonecrosis. <b>2019</b> , 2019, 9262430	3
867	Evidence for Genetic Contribution to Variation in Posttraumatic Osteoarthritis in Mice. <b>2019</b> , 71, 370-381	18
866	The development of bone microstructure, metabolism and biomechanics in lumbar vertebra under short-term glucocorticoid exposure. <b>2019</b> , 29, 687-692	
865	Paradise lost: Evidence for a devastating metabolic bone disease in an insular Pleistocene deer. <b>2019</b> , 24, 213-226	7
864	Osteocytes reflect a pro-inflammatory state following spinal cord injury in a rodent model. <b>2019</b> , 120, 465-475	14
863	Reduction of Cortical Bone Turnover and Erosion Depth After 2 and 3 Years of Denosumab: Iliac Bone Histomorphometry in the FREEDOM Trial. <i>Journal of Bone and Mineral Research</i> , <b>2019</b> , 34, 626-631 <sup>6.3</sup>	8
862	Normal trabecular vertebral bone is formed via rapid transformation of mineralized spicules: A high-resolution 3D ex-vivo murine study. <b>2019</b> , 86, 429-440	3
861	IL-17 Receptor Signaling in Osteoblasts/Osteocytes Mediates PTH-Induced Bone Loss and Enhances Osteocytic RANKL Production. <i>Journal of Bone and Mineral Research</i> , <b>2019</b> , 34, 349-360	31
860	Androgen Receptor in Neurons Slows Age-Related Cortical Thinning in Male Mice. <i>Journal of Bone and Mineral Research</i> , <b>2019</b> , 34, 508-519	8
859	The effect of PPARIInhibition on bone marrow adipose tissue and bone in C3H/HeJ mice. <b>2019</b> , 316, E96-E105	5

858	Lack of Myosin X Enhances Osteoclastogenesis and Increases Cell Surface Unc5b in Osteoclast-Lineage Cells. <i>Journal of Bone and Mineral Research</i> , <b>2019</b> , 34, 939-954	6.3	8
857	Once-Weekly Teriparatide Treatment Prevents Microdamage Accumulation in the Lumbar Vertebral Trabecular Bone of Ovariectomized Cynomolgus Monkeys. <b>2019</b> , 104, 402-410		4
856	Antibiotic Perturbation of Gut Microbiota Dysregulates Osteoimmune Cross Talk in Postpubertal Skeletal Development. <b>2019</b> , 189, 370-390		23
855	HIF-1Emetabolically controls collagen synthesis and modification in chondrocytes. <b>2019</b> , 565, 511-515		86
854	Collagen I-based scaffolds negatively impact fracture healing in a mouse-osteotomy-model although used routinely in research and clinical application. <b>2019</b> , 86, 171-184		18
853	Use of backscattered scanning electron microscopy to quantify the bone tissues of midthoracic human ribs. <b>2019</b> , 168, 262-278		5
852	Weekly teriparatide treatment increases vertebral body strength by improving cortical shell architecture in ovariectomized cynomolgus monkeys. <b>2019</b> , 121, 80-88		5
851	Clodronate-Loaded Liposome Treatment Has Site-Specific Skeletal Effects. <b>2019</b> , 98, 459-467		6
850	Abaloparatide, a novel osteoanabolic PTHrP analog, increases cortical and trabecular bone mass and architecture in orchiectomized rats by increasing bone formation without increasing bone resorption. <b>2019</b> , 120, 148-155		21
849	Reduced Terminal Complement Complex Formation in Mice Manifests in Low Bone Mass and Impaired Fracture Healing. <b>2019</b> , 189, 147-161		5
848	A moderately elevated soy protein diet mitigates inflammatory changes in gut and in bone turnover during chronic TNBS-induced inflammatory bowel disease. <b>2019</b> , 44, 595-605		11
847	Effect of Anti-TGF-Treatment in a Mouse Model of Severe Osteogenesis Imperfecta. <i>Journal of Bone and Mineral Research</i> , <b>2019</b> , 34, 207-214	6.3	25
846	Abietic acid attenuates RANKL induced osteoclastogenesis and inflammation associated osteolysis by inhibiting the NF-KB and MAPK signaling. <b>2018</b> , 234, 443-453		19
845	A novel Bruton's tyrosine kinase inhibitor, acalabrutinib, suppresses osteoclast differentiation and Porphyromonas gingivalis lipopolysaccharide-induced alveolar bone resorption. <b>2019</b> , 90, 546-554		5
844	Induction of Lrp5 HBM-causing mutations in Cathepsin-K expressing cells alters bone metabolism. <b>2019</b> , 120, 166-175		6
843	SF-deferoxamine, a bone-seeking angiogenic drug, prevents bone loss in estrogen-deficient mice. <b>2019</b> , 120, 156-165		12
842	Preventing and Repairing Myeloma Bone Disease by Combining Conventional Antiresorptive Treatment With a Bone Anabolic Agent in Murine Models. <i>Journal of Bone and Mineral Research</i> , <b>2019</b> , 34, 783-796	6.3	14
841	Pre-treatment with Pamidronate Improves Bone Mechanical Properties in Mdx Mice Treated with Glucocorticoids. <b>2019</b> , 104, 182-192		2

840	Systemic bone loss, impaired osteogenic activity and type I muscle fiber atrophy in mice with elastase-induced pulmonary emphysema: Establishment of a COPD-related osteoporosis mouse model. <b>2019</b> , 120, 114-124		12
839	Skeletal and Extraskeletal Actions of Vitamin D: Current Evidence and Outstanding Questions. <b>2019</b> , 40, 1109-1151		304
838	Activating Etatenin/Pax6 axis negatively regulates osteoclastogenesis by selectively inhibiting phosphorylation of p38/MAPK. <b>2019</b> , 33, 4236-4247		10
837	Mechanical loading mitigates osteoarthritis symptoms by regulating endoplasmic reticulum stress and autophagy. <b>2019</b> , 33, 4077-4088		30
836	Bone Matrix Mineralization in Patients With Gain-of-Function Calcium-Sensing Receptor Mutations Is Distinctly Different From that in Postsurgical Hypoparathyroidism. <i>Journal of Bone and Mineral Research</i> , <b>2019</b> , 34, 661-668	6.3	3
835	Skeletal phenotype of the neuropeptide Y knockout mouse. <b>2019</b> , 73, 78-88		14
834	Bone matrix hypermineralization associated with low bone turnover in a case of Nasu-Hakola disease. <b>2019</b> , 123, 48-55		4
833	Findings as a starting point to unravel the underlying mechanisms of in vivo interactions involving Wnt10a in bone, fat and muscle. <b>2019</b> , 120, 75-84		7
832	Androgen receptor SUMOylation regulates bone mass in male mice. <b>2019</b> , 479, 117-122		4
831	The effect of raloxifene on bone marrow adipose tissue and bone turnover in postmenopausal women with osteoporosis. <b>2019</b> , 118, 62-68		24
830	High calcium, phosphate and calcitriol supplementation leads to an osteocyte-like phenotype in calcified vessels and bone mineralisation defect in uremic rats. <b>2019</b> , 37, 212-223		9
829	Comparison of clinical, biochemical and histomorphometric analysis of bone biopsies in dialysis patients with and without fractures. <b>2019</b> , 37, 125-133		13
828	Biomaterial granules used for filling bone defects constitute 3D scaffolds: porosity, microarchitecture and molecular composition analyzed by microCT and Raman microspectroscopy. <b>2019</b> , 107, 415-423		17
827	Imaging methods used to study mouse and human HSC niches: Current and emerging technologies. <b>2019</b> , 119, 19-35		13
826	Histomorphometry and cortical robusticity of the adult human femur. <b>2019</b> , 37, 90-104		14
825	Optimal administration frequency and dose of teriparatide for acceleration of biomechanical healing of long-bone fracture in a mouse model. <b>2019</b> , 37, 256-263		11
824	Generalized Osteosclerotic Condition in the Skeleton of Nanophoca vitulinoides, a Dwarf Seal from the Miocene of Belgium. <b>2019</b> , 26, 517-543		5
823	Mechanical Vibration Associated With Intermittent PTH Improves Bone Microarchitecture in Ovariectomized Rats. <b>2020</b> , 23, 511-519		2

822	Vegetable hierarchical structures as template for bone regeneration: New bio-ceramization process for the development of a bone scaffold applied to an experimental sheep model. <b>2020</b> , 108, 600-611		7	
821	Mechanistic complexities of bone loss in Alzheimer's disease: a review. <b>2020</b> , 61, 4-18		12	
820	Altered gut microbiota ameliorates bone pathology in the mandible of obese-insulin-resistant rats. <b>2020</b> , 59, 1453-1462		14	
819	Dissecting the mechanisms of bone loss in Gorham-Stout disease. <b>2020</b> , 130, 115068		9	
818	Bone Histomorphometry in Young Patients With Type 2 Diabetes is Affected by Disease Control and Chronic Complications. <b>2020</b> , 105,		9	
817	Microimaging. <b>2020</b> , 1833-1856		1	
816	The long noncoding RNA Crnde regulates osteoblast proliferation through the Wnt/Etatenin signaling pathway in mice. <b>2020</b> , 130, 115076		17	
815	Inhibition of tissue-nonspecific alkaline phosphatase protects against medial arterial calcification and improves survival probability in the CKD-MBD mouse model. <b>2020</b> , 250, 30-41		23	
814	Calcium-Sensing Receptors in Chondrocytes and Osteoblasts Are Required for Callus Maturation and Fracture Healing in Mice. <i>Journal of Bone and Mineral Research</i> , <b>2020</b> , 35, 143-154	6.3	4	
813	Nandrolone decanoate in induced fracture nonunion with vascular deficit in rat model: morphological aspects. <b>2020</b> , 104, 303-311		2	
812	Digital radiography as an alternative method in the evaluation of bone density in uremic rats. <b>2020</b> , 42, 8-17			
811	CSF-1 in Osteocytes Inhibits Nox4-mediated Oxidative Stress and Promotes Normal Bone Homeostasis. <b>2020</b> , 4, e10080		8	
810	Preactivation of Eatenin in osteoblasts improves the osteoanabolic effect of PTH in type 1 diabetic mice. <b>2020</b> , 235, 1480-1493		3	
809	Improvement of bone repair with l-PRF and bovine bone in calvaria of rats. histometric and immunohistochemical study. <b>2020</b> , 24, 1637-1650		9	
808	Application of Bone Morphometry and Densitometry by X-Ray Micro-CT to Bone Disease Models and Phenotypes. <b>2020</b> , 49-75		1	
807	X-ray-based quantitative osteoporosis imaging at the spine. <b>2020</b> , 31, 233-250		33	
806	Magnesium prevents vascular calcification in Klotho deficiency. <b>2020</b> , 97, 487-501		27	
805	Mice lacking plastin-3 display a specific defect of cortical bone acquisition. <b>2020</b> , 130, 115062		9	

804	6-Shogaol, an active ingredient of ginger, inhibits osteoclastogenesis and alveolar bone resorption in ligature-induced periodontitis in mice. <b>2020</b> , 91, 809-818		9
803	Histomorphometric analysis of bone remodeling. <b>2020</b> , 445-467		
802	Cellular actions of parathyroid hormone on bone. <b>2020</b> , 775-788		1
801	An Inverse Agonist Ligand of the PTH Receptor Partially Rescues Skeletal Defects in a Mouse Model of Jansen's Metaphyseal Chondrodysplasia. <i>Journal of Bone and Mineral Research</i> , <b>2020</b> , 35, 540-549	6.3	3
800	A xenograft model to evaluate the bone forming effects of sclerostin antibody in human bone derived from pediatric osteogenesis imperfecta patients. <b>2020</b> , 130, 115118		4
799	Osteocytic miR21 deficiency improves bone strength independent of sex despite having sex divergent effects on osteocyte viability and bone turnover. <b>2020</b> , 287, 941-963		2
798	Disorders of Mineral and Bone Metabolism During Pregnancy and Lactation. 2020, 329-370		1
797	Murine Axial Compression Tibial Loading Model to Study Bone Mechanobiology: Implementing the Model and Reporting Results. <b>2020</b> , 38, 233-252		24
796	Influence of Ibuprofen on Bone Healing After Colles' Fracture: A Randomized Controlled Clinical Trial. <b>2020</b> , 38, 545-554		6
795	BMP9 Reduces Bone Loss in Ovariectomized Mice by Dual Regulation of Bone Remodeling. <i>Journal of Bone and Mineral Research</i> , <b>2020</b> , 35, 978-993	6.3	11
794	Trabecula: A Random Generator of Computational Phantoms for Bone Marrow Dosimetry. <b>2020</b> , 118, 53-59		3
793	Rac1 Inhibition Via Srgap2 Restrains Inflammatory Osteoclastogenesis and Limits the Clastokine, SLIT3. <i>Journal of Bone and Mineral Research</i> , <b>2020</b> , 35, 789-800	6.3	9
792	Effects of Long-Term Sclerostin Deficiency on Trabecular Bone Mass and Adaption to Limb Loading Differ in Male and Female Mice. <b>2020</b> , 106, 415-430		6
791	Skeletal impact of 17Eestradiol in T cell-deficient mice: age-dependent bone effects and osteosarcoma formation. <b>2020</b> , 37, 269-281		3
790	Reactive oxygen species-responsive dexamethasone-loaded nanoparticles for targeted treatment of rheumatoid arthritis via suppressing the iRhom2/TNF-BAFF signaling pathway. <b>2020</b> , 232, 119730		36
789	Felodipine blocks osteoclast differentiation and ameliorates estrogen-dependent bone loss in mice by modulating p38 signaling pathway. <b>2020</b> , 387, 111800		5
788	Consensus Nomenclature for Reporting Neovascular Age-Related Macular Degeneration Data: Consensus on Neovascular Age-Related Macular Degeneration Nomenclature Study Group. <b>2020</b> , 127, 616-636		154
787	Bone histomorphometry in rodents. <b>2020</b> , 1899-1922		1

786	Effect of Advanced Glycation End-Products (AGE) Lowering Drug ALT-711 on Biochemical, Vascular, and Bone Parameters in a Rat Model of CKD-MBD. <i>Journal of Bone and Mineral Research</i> , <b>2020</b> , 35, 608-6	517	20
785	Subchondral bone deterioration in femoral heads in patients with osteoarthritis secondary to hip dysplasia: A case-control study. <b>2020</b> , 24, 190-197		4
784	Disuse-induced loss of bone mineral density and bone strength is attenuated by post-lactational bone gain in NMRI mice. <b>2020</b> , 131, 115183		5
783	The deleterious effects of smoking in bone mineralization and fibrillar matrix composition. <b>2020</b> , 241, 117132		9
782	Postoperative Administration of Alpha-tocopherol Enhances Osseointegration of Stainless Steel Implants: An In Vivo Rat Model. <b>2020</b> , 478, 406-419		5
781	Relating mechanical properties of vertebral trabecular bones to osteoporosis. <b>2020</b> , 23, 54-68		1
780	Abaloparatide at the Same Dose Has the Same Effects on Bone as PTH (1-34) in Mice. <i>Journal of Bone and Mineral Research</i> , <b>2020</b> , 35, 714-724	6.3	11
779	Hypophosphatemic rickets accelerate chondrogenesis and cell trans-differentiation from TMJ chondrocytes into bone cells via a sharp increase in Eatenin. <b>2020</b> , 131, 115151		7
778	PARP1 Hinders Histone H2B Occupancy at the NFATc1 Promoter to Restrain Osteoclast Differentiation. <i>Journal of Bone and Mineral Research</i> , <b>2020</b> , 35, 776-788	6.3	1
777	Increased Expression of FGF-21 Negatively Affects Bone Homeostasis in Dystrophin/Utrophin Double Knockout Mice. <i>Journal of Bone and Mineral Research</i> , <b>2020</b> , 35, 738-752	6.3	7
776	Zebrafish: An Emerging Model for Orthopedic Research. <b>2020</b> , 38, 925-936		19
775	Correlation of Micro-Computed Tomography Assessment of Valvular Mineralisation with Histopathological and Immunohistochemical Features of Calcific Aortic Valve Disease. <b>2019</b> , 9,		1
774	Biphasic Calcium Phosphate Sphere Graft Combined with a Double-Layer Non-Crosslinked Collagen Membrane Technique for Ridge Preservation: A Randomized Controlled Animal Study. <b>2019</b> , 13,		2
773	Renoprotective effects of sucroferric oxyhydroxide in a rat model of chronic renal failure. <b>2020</b> , 35, 168	9-169	94
772	Re-thinking the bone remodeling cycle mechanism and the origin of bone loss. <b>2020</b> , 141, 115628		21
771	Peri-implant bone alterations under the influence of abutment screw preload stress. A preclinical vivo study. <b>2020</b> , 31, 1232-1242		O
770	Functionalized Scaffold and Barrier Membrane with Anti-BMP-2 Monoclonal Antibodies for Alveolar Ridge Preservation in a Canine Model. <b>2020</b> , 2020, 6153724		1
769	Hindlimb unloading causes regional loading-dependent changes in osteocyte inflammatory cytokines that are modulated by exogenous irisin treatment. <b>2020</b> , 6, 28		7

768	Increased marrow adipogenesis does not contribute to age-dependent appendicular bone loss in female mice. <b>2020</b> , 19, e13247	10
767	Towards a 2D cortical osseous tissue representation and generation at micro scale. A computational model for bone simulations. <b>2020</b> , 197, 105774	О
766	Unleashing Etatenin with a new anti-Alzheimer drug for bone tissue regeneration. 2020, 51, 2449-2459	2
765	Performance of two bone substitutes of novel cotton-like ETCP/PDLGA and granular ETCP on bone regeneration in the femoral bone defect of the Beagle dogs. <b>2020</b> , 13, 100718	O
764	Hdac3 regulates bone modeling by suppressing osteoclast responsiveness to RANKL. <b>2020</b> , 295, 17713-17723	3
763	Dapagliflozin and Liraglutide Therapies Rapidly Enhanced Bone Material Properties and Matrix Biomechanics at Bone Formation Site in a Type 2 Diabetic Mouse Model. <b>2020</b> , 107, 281-293	4
762	CCN1/Cyr61 Is Required in Osteoblasts for Responsiveness to the Anabolic Activity of PTH. <i>Journal of Bone and Mineral Research</i> , <b>2020</b> , 35, 2289-2300	3
761	Negligible Effect of Estrogen Deficiency on Development of Skeletal Changes Induced by Type 1 Diabetes in Experimental Rat Models. <b>2020</b> , 2020, 2793804	1
760	A novel negative regulatory mechanism of Smurf2 in BMP/Smad signaling in bone. 2020, 8, 41	11
759	Novel 2,7-Diazaspiro[4,4]nonane Derivatives to Inhibit Mouse and Human Osteoclast Activities and Prevent Bone Loss in Ovariectomized Mice without Affecting Bone Formation. <b>2020</b> , 63, 13680-13694	2
758	Effects of Estrogen Receptor and Wnt Signaling Activation on Mechanically Induced Bone Formation in a Mouse Model of Postmenopausal Bone Loss. <b>2020</b> , 21,	6
757	Effect of PTH and corticotomy on implant movement under mechanical force. <b>2020</b> , 20, 315	O
756	Histomorphometric and micro-CT analyses of calvarial bone grafts used to reconstruct the extremely atrophied maxilla. <b>2020</b> , 22, 593-601	5
755	Radiation causes tissue damage by dysregulating inflammasome-gasdermin D signaling in both host and transplanted cells. <b>2020</b> , 18, e3000807	12
754	PDGF Receptor Signaling in Osteoblast Lineage Cells Controls Bone Resorption Through Upregulation of Csf1 Expression. <i>Journal of Bone and Mineral Research</i> , <b>2020</b> , 35, 2458-2469	5
753	Transcriptome Analysis Reveals That Nakai Extract Inhibits RANKL-Mediated Osteoclastogenensis Mainly Through Suppressing Nfatc1 Expression. <b>2020</b> , 9,	1
752	Age-related changes of micro-morphological subchondral bone properties in the healthy femoral head. <b>2020</b> , 28, 1437-1447	3
75 <sup>1</sup>	Low energy irradiation of narrow-range UV-LED prevents osteosarcopenia associated with vitamin D deficiency in senescence-accelerated mouse prone 6. <b>2020</b> , 10, 11892	3

750	Proliferating osteoblasts are necessary for maximal bone anabolic response to loading in mice. <b>2020</b> , 34, 12739-12750	5
749	Comparison of the Efficacy and Renal Safety of Bisphosphonate Between Low-Dose/High-Frequency and High-Dose/Low-Frequency Regimens in a Late-Stage Chronic Kidney Disease Rat Model. <b>2020</b> , 107, 389-402	O
748	Evaluation of the bone morphology around four types of porous metal implants placed in distal femur of ovariectomized rats. <b>2020</b> , 15, 296	2
747	The low-expression programming of 11EHSD2 mediates osteoporosis susceptibility induced by prenatal caffeine exposure in male offspring rats. <b>2020</b> , 177, 4683-4700	7
746	Individuals with type 2 diabetes mellitus show dimorphic and heterogeneous patterns of loss in femoral bone quality. <b>2020</b> , 140, 115556	8
745	Sclerostin expression in trabecular bone is downregulated by osteoclasts. <b>2020</b> , 10, 13751	5
744	The Role of Aqueous Extract as a Bone Protective Agent, a Histomorphometric Study. 2020, 21,	2
743	Effect of Teriparatide on Bone Remodeling and Density in Premenopausal Idiopathic Osteoporosis: A Phase II Trial. <b>2020</b> , 105,	7
742	Structural and Metabolic Assessment of Bone. <b>2020</b> , 262, 369-396	
741	Targeting Bone Cells During Sexual Maturation Reveals Sexually Dimorphic Regulation of Endochondral Ossification. <b>2020</b> , 4, e10413	2
74 <sup>1</sup>		2
	Endochondral Ossification. <b>2020</b> , 4, e10413  High Mineralization Capacity of IDG-SW3 Cells in 3D Collagen Hydrogel for Bone Healing in	
740	Endochondral Ossification. <b>2020</b> , 4, e10413  High Mineralization Capacity of IDG-SW3 Cells in 3D Collagen Hydrogel for Bone Healing in Estrogen-Deficient Mice. <b>2020</b> , 8, 864	2
74° 739	Endochondral Ossification. 2020, 4, e10413  High Mineralization Capacity of IDG-SW3 Cells in 3D Collagen Hydrogel for Bone Healing in Estrogen-Deficient Mice. 2020, 8, 864  The neuropeptide calcitonin gene-related peptide alpha is essential for bone healing. 2020, 59, 102970  Low protein intake during reproduction compromises the recovery of lactation-induced bone loss	2
74° 739 738	Endochondral Ossification. 2020, 4, e10413  High Mineralization Capacity of IDG-SW3 Cells in 3D Collagen Hydrogel for Bone Healing in Estrogen-Deficient Mice. 2020, 8, 864  The neuropeptide calcitonin gene-related peptide alpha is essential for bone healing. 2020, 59, 102970  Low protein intake during reproduction compromises the recovery of lactation-induced bone loss in female mouse dams without affecting skeletal muscles. 2020, 34, 11844-11859  Identification of osteogenic progenitor cell-targeted peptides that augment bone formation. 2020,	2 12 1
74° 739 738 737	High Mineralization Capacity of IDG-SW3 Cells in 3D Collagen Hydrogel for Bone Healing in Estrogen-Deficient Mice. 2020, 8, 864  The neuropeptide calcitonin gene-related peptide alpha is essential for bone healing. 2020, 59, 102970  Low protein intake during reproduction compromises the recovery of lactation-induced bone loss in female mouse dams without affecting skeletal muscles. 2020, 34, 11844-11859  Identification of osteogenic progenitor cell-targeted peptides that augment bone formation. 2020, 11, 4278  B cell acute lymphoblastic leukemia cells mediate RANK-RANKL-dependent bone destruction. 2020,	2 12 1
740 739 738 737 736	Endochondral Ossification. 2020, 4, e10413  High Mineralization Capacity of IDG-SW3 Cells in 3D Collagen Hydrogel for Bone Healing in Estrogen-Deficient Mice. 2020, 8, 864  The neuropeptide calcitonin gene-related peptide alpha is essential for bone healing. 2020, 59, 102970  Low protein intake during reproduction compromises the recovery of lactation-induced bone loss in female mouse dams without affecting skeletal muscles. 2020, 34, 11844-11859  Identification of osteogenic progenitor cell-targeted peptides that augment bone formation. 2020, 11, 4278  B cell acute lymphoblastic leukemia cells mediate RANK-RANKL-dependent bone destruction. 2020, 12,  Zoledronic Acid in a Mouse Model of Human Fibrous Dysplasia: Ineffectiveness on Tissue	2 12 1 7

732	Imaging Techniques for the Assessment of the Bone Osteoporosis-Induced Variations with Particular Focus on Micro-CT Potential. <b>2020</b> , 10, 8939	
731	Division of an Iliac Crest Bone Biopsy Specimen to Allow Histomorphometry, Immunohistochemical, Molecular Analysis, and Tissue Banking: Technical Aspect and Applications. <b>2020</b> , 4, e10424	1
730	The heparan sulfate proteoglycan Syndecan-1 influences local bone cell communication via the RANKL/OPG axis. <b>2020</b> , 10, 20510	2
729	The Efficacy of PTH and Abaloparatide to Counteract Immobilization-Induced Osteopenia Is in General Similar. <b>2020</b> , 11, 588773	6
728	SIX WEEKS OF TREADMILL RUNNING EXERCISE IMPROVE BONE ARCHITECTURE IN ADULT OSTEOPENIC RATS: AN EXPERIMENTAL STUDY TOWARD EXERCISE DOSE PRESCRIPTION. <b>2020</b> , 23, 2050012	
727	Traumatic joint injury induces acute catabolic bone turnover concurrent with articular cartilage damage in a rat model of posttraumatic osteoarthritis. <b>2021</b> , 39, 1965-1976	3
726	Andrographolide modulates OPG/RANKL axis to promote osteoblastic differentiation in MC3T3-E1 cells and protects bone loss during estrogen deficiency in rats. <b>2020</b> , 131, 110763	9
725	Nuclear factor of activated T cells 1 and 2 are required for vertebral homeostasis. <b>2020</b> , 235, 8520-8532	4
724	Disruption of the aldehyde dehydrogenase 2 gene increases the bone anabolic response to intermittent PTH treatment in an ovariectomized mouse model. <b>2020</b> , 136, 115370	3
723	No evidence for alteration in early secondary mineralization by either alendronate, teriparatide or combination of both in transiliac bone biopsy samples from postmenopausal osteoporotic patients. <b>2020</b> , 12, 100253	4
722	regulates the action of nitrogen-containing bisphosphonates on bone. <b>2020</b> , 12,	6
721	Teriparatide improves microarchitectural characteristics of peri-implant bone in orchiectomized rats. <b>2020</b> , 31, 1807-1815	6
720	Mice Carrying a Ubiquitous R235W Mutation of Wnt1 Display a Bone-Specific Phenotype. <i>Journal of Bone and Mineral Research</i> , <b>2020</b> , 35, 1726-1737	3
719	Disruption of the hepcidin/ferroportin regulatory circuitry causes low axial bone mass in mice. <b>2020</b> , 137, 115400	3
718	Biomarkers of Bone Turnover Identify Subsets of Chronic Kidney Disease Patients at Higher Risk for Fracture. <b>2020</b> , 105,	7
717	Quantitative histomorphometric analysis of halved iliac crest bone biopsies yield comparable ROD diagnosis as full 7.5mm wide samples. <b>2020</b> , 138, 115460	6
716	Transient receptor potential vanilloid 1 and 4 double knockout leads to increased bone mass in mice. <b>2020</b> , 12, 100268	7
715	Elevated Bone Hardness Under Denosumab Treatment, With Persisting Lower Osteocyte Viability During Discontinuation. <b>2020</b> , 11, 250	6

714	Gnathodiaphyseal dysplasia is not recapitulated in a respective mouse model carrying a mutation of the Ano5 gene. <b>2020</b> , 12, 100281	1
713	Disruption of BMP Signaling Prevents Hyperthyroidism-Induced Bone Loss in Male Mice. <i>Journal of Bone and Mineral Research</i> , <b>2020</b> , 35, 2058-2069	4
712	Pyk2 deficiency enhances bone mass during midpalatal suture expansion. <b>2020</b> , 23, 501-508	2
711	Effects of diosgenin on the skeletal system in rats with experimental type 1 diabetes. <b>2020</b> , 129, 110342	4
710	Dose-dependent skeletal deficits due to varied reductions in mechanical loading in rats. <b>2020</b> , 6, 15	7
709	The curious fate of bone following bariatric surgery: bone effects of sleeve gastrectomy (SG) and Roux-en-Y gastric bypass (RYGB) in mice. <b>2020</b> , 44, 2165-2176	Ο
708	The Senolytic Drug Navitoclax (ABT-263) Causes Trabecular Bone Loss and Impaired Osteoprogenitor Function in Aged Mice. <b>2020</b> , 8, 354	26
707	The Use of Autogenous Bone Mixed with a Biphasic Calcium Phosphate in a Maxillary Sinus Floor Elevation Procedure with a 6-Month Healing Time: A Clinical, Radiological, Histological and Histomorphometric Evaluation. <b>2020</b> , 10, 462	
706	Pten deletion in Dmp1-expressing cells does not rescue the osteopenic effects of Wnt/Etatenin suppression. <b>2020</b> , 235, 9785-9794	
705	Effect of Botulinum Toxin Type A on Mandibular Fracture Healing: An Experimental Study in Rabbits. <b>2020</b> , 78, 2281.e1-2281.e8	1
704	CRELD2 Is a Novel LRP1 Chaperone That Regulates Noncanonical WNT Signaling in Skeletal Development. <i>Journal of Bone and Mineral Research</i> , <b>2020</b> , 35, 1452-1469	5
703	Male mice with elevated C-type natriuretic peptide-dependent guanylyl cyclase-B activity have increased osteoblasts, bone mass and bone strength. <b>2020</b> , 135, 115320	7
702	Association of parathormone and alkaline phosphatase with bone turnover and mineralization in children with CKD on dialysis: effect of age, gender, and race. <b>2020</b> , 35, 1297-1305	9
701	Cxcl12 Deletion in Mesenchymal Cells Increases Bone Turnover and Attenuates the Loss of Cortical Bone Caused by Estrogen Deficiency in Mice. <i>Journal of Bone and Mineral Research</i> , <b>2020</b> , 35, 1441-1451 <sup>6.3</sup>	3
700	Enteroendocrine K Cells Exert Complementary Effects to Control Bone Quality and Mass in Mice. <i>Journal of Bone and Mineral Research</i> , <b>2020</b> , 35, 1363-1374	6
699	Untargeted metabolomics revealed therapeutic mechanisms of icariin on low bone mineral density in older caged laying hens. <b>2020</b> , 11, 3201-3212	7
698	Administration of allogeneic mesenchymal stem cells in lengthening phase accelerates early bone consolidation in rat distraction osteogenesis model. <b>2020</b> , 11, 129	7
697	Large osteocyte lacunae in iliac crest infantile bone are not associated with impaired mineral distribution or signs of osteocytic osteolysis. <b>2020</b> , 135, 115324	9

696	Ridge Augmentation Using ETricalcium Phosphate and Biphasic Calcium Phosphate Sphere with Collagen Membrane in Chronic Pathologic Extraction Sockets with Dehiscence Defect: A Pilot Study in Beagle Dogs. <b>2020</b> , 13,		3
695	Postnatal Conditional Deletion of Bmal1 in Osteoblasts Enhances Trabecular Bone Formation Via Increased BMP2 Signals. <i>Journal of Bone and Mineral Research</i> , <b>2020</b> , 35, 1481-1493	6.3	4
694	Modeling-Based Bone Formation in the Human Femoral Neck in Subjects Treated With Denosumab. Journal of Bone and Mineral Research, <b>2020</b> , 35, 1282-1288	6.3	15
693	The tethering function of mitofusin2 controls osteoclast differentiation by modulating the Ca-NFATc1 axis. <b>2020</b> , 295, 6629-6640		8
692	Reporting Guidelines, Review of Methodological Standards, and Challenges Toward Harmonization in Bone Marrow Adiposity Research. Report of the Methodologies Working Group of the International Bone Marrow Adiposity Society. <b>2020</b> , 11, 65		21
691	Effects of Odanacatib on Bone Structure and Quality in Postmenopausal Women With Osteoporosis: 5-Year Data From the Phase 3 Long-Term Odanacatib Fracture Trial (LOFT) and its Extension. <i>Journal of Bone and Mineral Research</i> , <b>2020</b> , 35, 1289-1299	6.3	6
690	Skeletal and mineral metabolic effects of risedronate in a rat model of high-turnover renal osteodystrophy. <b>2020</b> , 38, 501-510		3
689	Skeletal restoration by phosphodiesterase 5 inhibitors in osteopenic mice: Evidence of osteoanabolic and osteoangiogenic effects of the drugs. <b>2020</b> , 135, 115305		10
688	Effects of ultraviolet irradiation with a LED device on bone metabolism associated with vitamin D deficiency in senescence-accelerated mouse P6. <b>2020</b> , 6, e03499		4
687	Bone microarchitecture and turnover in the irradiated human mandible. <b>2020</b> , 48, 733-740		2
686	An animal trial to study damage and repair in ovariectomized rabbits. <b>2020</b> , 108, 109866		
685	A molecular basis for neurofibroma-associated skeletal manifestations in NF1. <b>2020</b> , 22, 1786-1793		2
684	Effects of C-Peptide Replacement Therapy on Bone Microarchitecture Parameters in Streptozotocin-Diabetic Rats. <b>2020</b> , 107, 266-280		5
683	A Clinical Perspective on Advanced Developments in Bone Biopsy Assessment in Rare Bone Disorders. <b>2020</b> , 11, 399		3
682	A marine fungus-derived nitrobenzoyl sesquiterpenoid suppresses receptor activator of NF-B ligand-induced osteoclastogenesis and inflammatory bone destruction. <b>2020</b> , 177, 4242-4260		10
681	A FAK/HDAC5 signaling axis controls osteocyte mechanotransduction. <b>2020</b> , 11, 3282		26
680	Combined effect of teriparatide and an anti-RANKL monoclonal antibody on bone defect regeneration in mice with glucocorticoid-induced osteoporosis. <b>2020</b> , 139, 115525		3
679	Effects of abaloparatide and teriparatide on bone resorption and bone formation in female mice. <b>2020</b> , 13, 100291		9

678	Dual X-ray absorptiometry has limited utility in detecting bone pathology in children with hypophosphatasia: A pooled post hoc analysis of asfotase alfa clinical trial data. <b>2020</b> , 137, 115413		4
677	Nephrectomy Does not Exacerbate Cancellous Bone loss in Thalassemic Mice. <b>2020</b> , 10, 7786		1
676	Using histomorphometry for human and nonhuman distinction: A test of four methods on fresh and archaeological fragmented bones. <b>2020</b> , 313, 110369		1
675	Gastrin for prevention of steroid-associated osteonecrosis in rats. <b>2020</b> , 25, 105-114		1
674	Bioactive PLGA/tricalcium phosphate scaffolds incorporating phytomolecule icaritin developed for calvarial defect repair in rat model. <b>2020</b> , 24, 112-120		8
673	Histological scoring system for subchondral bone changes in murine models of joint aging and osteoarthritis. <b>2020</b> , 10, 10077		11
672	Bone Structure and Function. 2020, 233-246		
671	Controversy of physiological vs. pharmacological effects of BMP signaling: Constitutive activation of BMP type IA receptor-dependent signaling in osteoblast lineage enhances bone formation and resorption, not affecting net bone mass. <b>2020</b> , 138, 115513		3
670	Picolinic Acid, a Catabolite of Tryptophan, Has an Anabolic Effect on Bone In Vivo. <i>Journal of Bone and Mineral Research</i> , <b>2020</b> , 35, 2275-2288	6.3	6
669	Osteoporosis Treatments Affect Bone Matrix Maturation in a Rat Model of Induced Cortical Remodeling. <b>2020</b> , 4, e10344		1
668	A microRNA Approach to Discriminate Cortical Low Bone Turnover in Renal Osteodystrophy. <b>2020</b> , 4, e10353		4
667	Osteoinductive potential of highly porous polylactide granules and Bio-Oss impregnated with low doses of BMP-2. <b>2020</b> , 421, 052035		2
666	Resveratrol promotes osteogenesis via activating SIRT1/FoxO1 pathway in osteoporosis mice. <b>2020</b> , 246, 117422		24
665	miR-136-3p targets PTEN to regulate vascularization and bone formation and ameliorates alcohol-induced osteopenia. <b>2020</b> , 34, 5348-5362		13
664	Adult Osteosclerotic Metaphyseal Dysplasia With Progressive Osteonecrosis of the Jaws and Abnormal Bone Resorption Pattern Due to a LRRK1 Splice Site Mutation. <i>Journal of Bone and Mineral Research</i> , <b>2020</b> , 35, 1322-1332	6.3	4
663	Correlation between F-Sodium Fluoride positron emission tomography and bone histomorphometry in dialysis patients. <b>2020</b> , 134, 115267		11
662	GLP-2 administration in ovariectomized mice enhances collagen maturity but did not improve bone strength. <b>2020</b> , 12, 100251		2
661	High bone microarchitecture, strength, and resistance to bone loss in MRL/MpJ mice correlates with activation of different signaling pathways and systemic factors. <b>2020</b> , 34, 789-806		4

660	Specific Commensal Bacterium Critically Regulates Gut Microbiota Osteoimmunomodulatory Actions During Normal Postpubertal Skeletal Growth and Maturation. <b>2020</b> , 4, e10338	8
659	Sclerostin antibody treatment rescues the osteopenic bone phenotype of TGFIInducible early gene-1 knockout female mice. <b>2020</b> , 235, 5679-5688	3
658	PTH induces bone loss via microbial-dependent expansion of intestinal TNF T cells and Th17 cells. <b>2020</b> , 11, 468	42
657	Mechanical sensing protein PIEZO1 regulates bone homeostasis via osteoblast-osteoclast crosstalk. <b>2020</b> , 11, 282	88
656	Skeletal deterioration in COL2A1-related spondyloepiphyseal dysplasia occurs prior to osteoarthritis. <b>2020</b> , 28, 334-343	7
655	Frizzled-4 is required for normal bone acquisition despite compensation by Frizzled-8. <b>2020</b> , 235, 6673-6683	5
654	Subchondral bone dysplasia partly participates in prenatal dexamethasone induced-osteoarthritis susceptibility in female offspring rats. <b>2020</b> , 133, 115245	5
653	Foxf1 knockdown promotes BMSC osteogenesis in part by activating the Wnt/Etatenin signalling pathway and prevents ovariectomy-induced bone loss. <b>2020</b> , 52, 102626	23
652	L-Plastin deficiency produces increased trabecular bone due to attenuation of sealing ring formation and osteoclast dysfunction. <b>2020</b> , 8, 3	7
651	Long-Term Immobilization in Elderly Females Causes a Specific Pattern of Cortical Bone and Osteocyte Deterioration Different From Postmenopausal Osteoporosis. <i>Journal of Bone and Mineral Research</i> , <b>2020</b> , 35, 1343-1351	21
650	Magnesium and vitamin C supplementation attenuates steroid-associated osteonecrosis in a rat model. <b>2020</b> , 238, 119828	33
649	The Rho GTPase RAC1 in Osteoblasts Controls Their Function. <b>2020</b> , 21,	6
648	Enzyme replacement therapy in mice lacking arylsulfatase B targets bone-remodeling cells, but not chondrocytes. <b>2020</b> , 29, 803-816	6
647	Osteoclast-mediated bone resorption is controlled by a compensatory network of secreted and membrane-tethered metalloproteinases. <b>2020</b> , 12,	35
646	Targeted Reduction of Senescent Cell Burden Alleviates Focal Radiotherapy-Related Bone Loss. <i>Journal of Bone and Mineral Research</i> , <b>2020</b> , 35, 1119-1131	40
645	Sclerostin-Antibody Treatment Decreases Fracture Rates in Axial Skeleton and Improves the Skeletal Phenotype in Growing oim/oim Mice. <b>2020</b> , 106, 494-508	9
644	Dietary countermeasure mitigates simulated spaceflight-induced osteopenia in mice. <b>2020</b> , 10, 6484	7
643	Histological, Histomorphometrical, and Biomechanical Studies of Bone-Implanted Medical Devices: Hard Resin Embedding. <b>2020</b> , 2020, 1804630	10

642	Age-Related Increases in Marrow Fat Volumes have Regional Impacts on Bone Cell Numbers and Structure. <b>2020</b> , 107, 126-134		3
641	Pharmacological TNAP inhibition efficiently inhibits arterial media calcification in a warfarin rat model but deserves careful consideration of potential physiological bone formation/mineralization impairment. <b>2020</b> , 137, 115392		10
640	Biomimetic UHMWPE/HA scaffolds with rhBMP-2 and erythropoietin for reconstructive surgery. <b>2020</b> , 111, 110750		15
639	Highly porous PEEK and PEEK/HA scaffolds with Escherichia coli-derived recombinant BMP-2 and erythropoietin for enhanced osteogenesis and angiogenesis. <b>2020</b> , 87, 106518		8
638	FAK Promotes Early Osteoprogenitor Cell Proliferation by Enhancing mTORC1 Signaling. <i>Journal of Bone and Mineral Research</i> , <b>2020</b> , 35, 1798-1811	6.3	3
637	Carbon Monoxide and Exercise Prevents Diet-Induced Obesity and Metabolic Dysregulation Without Affecting Bone. <b>2020</b> , 28, 924-931		2
636	The old sheep: a convenient and suitable model for senile osteopenia. 2020, 38, 620-630		О
635	Antisense oligonucleotides targeting ameliorate the osteopenic phenotype in a mouse model of Hajdu-Cheney syndrome. <b>2020</b> , 295, 3952-3964		7
634	Flufenamic Acid Inhibits Adipogenic Differentiation of Mesenchymal Stem Cells by Antagonizing the PI3K/AKT Signaling Pathway. <b>2020</b> , 2020, 1540905		3
633	Breast cancer bone metastases are attenuated in a Tgif1-deficient bone microenvironment. <b>2020</b> , 22, 34		4
632	Effects of Propranolol on Bone, White Adipose Tissue, and Bone Marrow Adipose Tissue in Mice Housed at Room Temperature or Thermoneutral Temperature. <b>2020</b> , 11, 117		6
631	Brain-Derived Acetylcholine Maintains Peak Bone Mass in Adult Female Mice. <i>Journal of Bone and Mineral Research</i> , <b>2020</b> , 35, 1562-1571	6.3	2
630	A pilot study to investigate the histomorphometric changes of murine maxillary bone around the site of mini-screw insertion in regenerated bone induced by anabolic reagents. <b>2021</b> , 43, 86-93		1
629	Sensitive detection of Cre-mediated recombination using droplet digital PCR reveals Tg(BGLAP-Cre) and Tg(DMP1-Cre) are active in multiple non-skeletal tissues. <b>2021</b> , 142, 115674		4
628	Microcrack surface density in the human otic capsule: An unbiased stereological quantification. <b>2021</b> , 304, 961-967		2
627	Type I Angiotensin II Receptor Blockade Reduces Uremia-Induced Deterioration of Bone Material Properties. <i>Journal of Bone and Mineral Research</i> , <b>2021</b> , 36, 67-79	6.3	5
626	Mandibular biomechanical behavior of rats submitted to chronic intermittent or continuous hypoxia and periodontitis. <b>2021</b> , 25, 519-527		1
625	Quantitative bone imaging biomarkers to diagnose temporomandibular joint osteoarthritis. <b>2021</b> , 50, 227-235		5

624	A Neutralizing Antibody Targeting Oxidized Phospholipids Promotes Bone Anabolism in Chow-Fed Young Adult Mice. <i>Journal of Bone and Mineral Research</i> , <b>2021</b> , 36, 170-185	6.3	4
623	An overview of de novo bone generation in animal models. <b>2021</b> , 39, 7-21		3
622	Regional variation in bone turnover at the iliac crest versus the greater trochanter. <b>2021</b> , 143, 115604		
621	Clinical and Radiological Characterization of Patients with Immobilizing and Progressive Stress Fractures in Methotrexate Osteopathy. <b>2021</b> , 108, 219-230		4
620	Molecular Basis for Craniofacial Phenotypes Caused by Sclerostin Deletion. <b>2021</b> , 100, 310-317		2
619	Calcified cartilage in patients with osteoarthritis of the hip compared to that of healthy subjects. A design-based histological study. <b>2021</b> , 143, 115660		1
618	Mechanically Driven Counter-Regulation of Cortical Bone Formation in Response to Sclerostin-Neutralizing Antibodies. <i>Journal of Bone and Mineral Research</i> , <b>2021</b> , 36, 385-399	6.3	4
617	In vivo osseointegration and erosion of nacre screws in an animal model. <b>2021</b> , 109, 780-788		3
616	Effects of acidosis on the structure, composition, and function of adult murine femurs. <b>2021</b> , 121, 484-4	196	2
615	Glutamine Metabolism in Osteoprogenitors Is Required for Bone Mass Accrual and PTH-Induced Bone Anabolism in Male Mice. <i>Journal of Bone and Mineral Research</i> , <b>2021</b> , 36, 604-616	6.3	10
614	Piezo1 Inactivation in Chondrocytes Impairs Trabecular Bone Formation. <i>Journal of Bone and Mineral Research</i> , <b>2021</b> , 36, 369-384	6.3	17
613	Randomized, controlled trial to assess the safety and efficacy of odanacatib in the treatment of men with osteoporosis. <b>2021</b> , 32, 173-184		O
612	Evaluation of in vitro corrosion resistance and in vivo osseointegration properties of a FeMnSiCa alloy as potential degradable implant biomaterial. <b>2021</b> , 118, 111436		8
611	Surface decoration of development-inspired synthetic N-cadherin motif via Ac-BP promotes osseointegration of metal implants. <b>2021</b> , 6, 1353-1364		5
610	Osteoblastic monocyte chemoattractant protein-1 (MCP-1) mediation of parathyroid hormone's anabolic actions in bone implicates TGF-laignaling. <b>2021</b> , 143, 115762		3
609	Interleukin-6 (IL-6) deficiency enhances intramembranous osteogenesis following stress fracture in mice. <b>2021</b> , 143, 115737		O
608	Chronic Kidney Disease-Induced Vascular Calcification Impairs Bone Metabolism. <i>Journal of Bone and Mineral Research</i> , <b>2021</b> , 36, 510-522	6.3	7
607	Osseointegration of additive manufacturing Ti-6Al-4V and Co-Cr-Mo alloys, with and without surface functionalization with hydroxyapatite and type I collagen. <b>2021</b> , 115, 104262		6

606	Abaloparatide treatment increases bone formation, bone density and bone strength without increasing bone resorption in a rat model of hindlimb unloading. <b>2021</b> , 144, 115801	3
605	Burosumab for the Treatment of Tumor-Induced Osteomalacia. <i>Journal of Bone and Mineral Research</i> , <b>2021</b> , 36, 627-635	29
604	Frequent administration of abaloparatide shows greater gains in bone anabolic window and bone mineral density in mice: A comparison with teriparatide. <b>2021</b> , 142, 115651	6
603	Activin type IIA decoy receptor and intermittent parathyroid hormone in combination overturns the bone loss in disuse-osteopenic mice. <b>2021</b> , 142, 115692	5
602	Ablation of Results in Transient Bone Hypomineralization. <b>2021</b> , 5, e10439	O
601	Osteomalacia and Vitamin D Status: A Clinical Update 2020. <b>2021</b> , 5, e10447	9
600	Osteoporosis and osteoblasts cocultured with adipocytes inhibit osteoblast differentiation by downregulating histone acetylation. <b>2021</b> , 236, 3906-3917	8
599	Co-deletion of Lrp5 and Lrp6 in the skeleton severely diminishes bone gain from sclerostin antibody administration. <b>2021</b> , 143, 115708	5
598	USP7 regulates the proliferation and differentiation of ATDC5 cells through the Sox9-PTHrP-PTH1R axis. <b>2021</b> , 143, 115714	4
597	Iliac crest bone biopsy by interventional radiologists to improve access to bone biopsy in chronic kidney disease populations: technical note and a case series. <b>2021</b> , 34, 901-906	2
596	LncRNA-H19 silencing suppresses synoviocytes proliferation and attenuates collagen-induced arthritis progression by modulating miR-124a. <b>2021</b> , 60, 430-440	8
595	Sclerostin-Neutralizing Antibody Treatment Rescues Negative Effects of Rosiglitazone on Mouse Bone Parameters. <i>Journal of Bone and Mineral Research</i> , <b>2021</b> , 36, 158-169	6
594	Lessons from bone histomorphometry on the mechanisms of action of osteoporosis drugs. <b>2021</b> , 1835-1863	1
593	Magnesium and Calcium Homeostasis Depend on KCTD1 Function in the Distal Nephron. <b>2021</b> , 34, 108616	6
592	1⊉5-Dihydroxyvitamin D3 ameliorates diabetes-induced bone loss by attenuating FoxO1-mediated autophagy. <b>2021</b> , 296, 100287	7
591	The miRNA-15b/USP7/KDM6B axis engages in the initiation of osteoporosis by modulating osteoblast differentiation and autophagy. <b>2021</b> , 25, 2069-2081	5
590	Comparable Effects of Strontium Ranelate and Alendronate Treatment on Fracture Reduction in a Mouse Model of Osteogenesis Imperfecta. <b>2021</b> , 2021, 4243105	O
589	The effect of different irrigation solutions on fracture healing in a rat femur fracture model. <b>2021</b> , 32, 144-151	

588	Chemerin located in bone marrow promotes osteogenic differentiation and bone formation via Akt/Gsk3/Ecatenin axis in mice. <b>2021</b> , 236, 6042-6054	3
587	Early Effects of Abaloparatide on Bone Formation and Resorption Indices in Postmenopausal Women With Osteoporosis. <i>Journal of Bone and Mineral Research</i> , <b>2021</b> , 36, 644-653	9
586	In Vivo and In Vitro Models for the Study of Bone Remodeling and the Role of Immune Cells. <b>2021</b> , 2325, 97-106	
585	Bone marrow adipogenic lineage precursors promote osteoclastogenesis in bone remodeling and pathologic bone loss. <b>2021</b> , 131,	31
584	Maternal High-Fat Diet Induces Long-Lasting Defects in Bone Structure in Rat Offspring Through Enhanced Osteoclastogenesis. <b>2021</b> , 108, 680-692	3
583	'Educated' Osteoblasts Reduce Osteoclastogenesis in a Bone-Tumor Mimetic Microenvironment. <b>2021</b> , 13,	1
582	Effect of a high crude protein content diet during energy restriction and re-alimentation on animal performance, skeletal growth and metabolism of bone tissue in two genotypes of cattle. <b>2021</b> , 16, e0247718	1
581	Progressive loss of implant fixation in a preclinical rat model of cemented knee arthroplasty. <b>2021</b> , 39, 2353-2362	О
580	Assessment of Trabecular Bone During Dental Implant Planning using Cone-beam Computed Tomography with High-resolution Parameters. <b>2021</b> , 15, 57-63	O
579	A comparison of alendronate to varying magnitude PEMF in mitigating bone loss and altering bone remodeling in skeletally mature osteoporotic rats. <b>2021</b> , 143, 115761	6
578	Early bone formation in mini-lateral window sinus floor elevation with simultaneous implant placement: An in vivo experimental study. <b>2021</b> , 32, 448-459	O
577	Bone loss markers in the earliest Pacific Islanders. <b>2021</b> , 11, 3981	1
576	Combination effect of laser diode for photodynamic therapy with doxycycline on a wistar rat model of periodontitis. <b>2021</b> , 21, 80	2
575	Oral Estradiol Impact on Mitigating Unloading-Induced Bone Loss in Ovary-Intact Rats. <b>2021</b> , 92, 65-74	2
574	Selective deletion of the receptor for CSF1, c-fms, in osteoclasts results in a high bone mass phenotype, smaller osteoclasts in vivo and an impaired response to an anabolic PTH regimen. <b>2021</b> , 16, e0247199	О
573	An Unanticipated Role for Sphingosine Kinase-2 in Bone and in the Anabolic Effect of Parathyroid Hormone. <b>2021</b> , 162,	4
572	Skeletal Biology and Disease Modeling in Zebrafish. <i>Journal of Bone and Mineral Research</i> , <b>2021</b> , 36, 436-4.58	12
571	Inhibition of longevity regulator PAPP-A modulates tissue homeostasis via restraint of mesenchymal stromal cells. <b>2021</b> , 20, e13313	1

 $570\,$  Dual targeting of salt inducible kinases and CSF1R uncouples bone formation and bone resorption.

569	Intact Glucocorticoid Receptor Dimerization Is Deleterious in Trauma-Induced Impaired Fracture Healing. <b>2020</b> , 11, 628287		1
568	Treatment with an active vitamin D analogue blocks hypothalamic dysfunction-induced bone loss in mice. <b>2021</b> , 542, 48-53		O
567	Delivery of dimethyloxalylglycine in calcined bone calcium scaffold to improve osteogenic differentiation and bone repair. <b>2020</b> ,		1
566	Duration-Dependent Increase of Human Bone Matrix Mineralization in Long-Term Bisphosphonate Users with Atypical Femur Fracture. <i>Journal of Bone and Mineral Research</i> , <b>2021</b> , 36, 1031-1041	6.3	3
565	Severity of Megakaryocyte-Driven Osteosclerosis in Mpig6b-Deficient Mice Is Sex-Linked. <i>Journal of Bone and Mineral Research</i> , <b>2021</b> , 36, 803-813	6.3	O
564	A histological comparison of non-human rib models suited for sharp force trauma analysis. <b>2021</b> , 319, 110661		1
563	Morusin induces osteogenic differentiation of bone marrow mesenchymal stem cells by canonical Wnt/Ecatenin pathway and prevents bone loss in an ovariectomized rat model. <b>2021</b> , 12, 173		5
562	Omega-3 fatty acid modulation of serum and osteocyte tumor necrosis factor-An adult mice exposed to ionizing radiation. <b>2021</b> , 130, 627-639		О
561	Effect of denosumab on osteolytic lesion activity after total hip arthroplasty: a single-centre, randomised, double-blind, placebo-controlled, proof of concept trial. <b>2021</b> , 3, e195-e203		4
560	Mesenchymal stem cells overexpressing BMP-9 by CRISPR-Cas9 present high in vitro osteogenic potential and enhance in vivo bone formation. <b>2021</b> ,		2
559	Compound Heterozygous Frameshift Mutations in MESD Cause a Lethal Syndrome Suggestive of Osteogenesis Imperfecta Type XX. <i>Journal of Bone and Mineral Research</i> , <b>2021</b> , 36, 1077-1087	6.3	6
558	Cancellous Bone May Have a Greater Adaptive Strain Threshold Than Cortical Bone. <b>2021</b> , 5, e10489		2
557	The role of Zfp467 in mediating the pro-osteogenic and anti-adipogenic effects on bone and bone marrow niche. <b>2021</b> , 144, 115832		3
556	RhoA/Rock activation represents a new mechanism for inactivating Wnt/Etatenin signaling in the aging-associated bone loss. <b>2021</b> , 10, 8		2
555	Deletion of in Preosteoblasts Reveals a Role for the Mammalian Target of Rapamycin Complex 1 (mTORC1) Complex in Dietary-Induced Changes to Bone Mass and Glucose Homeostasis in Female Mice. <b>2021</b> , 5, e10486		
554	EHydroxy-EMethylbutyrate (HMB) Supplementation Prevents Bone Loss during Pregnancy-Novel Evidence from a Spiny Mouse () Model. <b>2021</b> , 22,		1
553	Disparate bone anabolic cues activate bone formation by regulating the rapid lysosomal degradation of sclerostin protein. <b>2021</b> , 10,		6

Osseointegration of two types of titanium cylinders with geometric or trabecular microarchitecture: A nanotomographic and histomorphometric study. **2021**,

551	Syndecan-3 enhances anabolic bone formation through WNT signaling. <b>2021</b> , 35, e21246	2
550	Internet of things image detection and activation of Ecatenin on bone growth. 2021, 81, 103706	
549	Histopathological and Radiographic Features of Osteolysis After Fixation of Osteochondral Fragments Using Poly-L-Lactic Acid Pins for Osteochondral Lesions of the Talus. <b>2021</b> , 49, 1589-1595	1
548	Relevanz der detaillierten skelettalen Analyse durch hochauflßende periphere quantitative Computertomographie (HR-pQCT) in der Orthopßie und Unfallchirurgie. <b>2021</b> , 19, 19-26	
547	Bone quality analysis of jaw bones in individuals with type 2 diabetes mellitus-post mortem anatomical and microstructural evaluation. <b>2021</b> , 25, 4377-4400	3
546	A decrease in NAD contributes to the loss of osteoprogenitors and bone mass with aging. <b>2021</b> , 7, 8	3
545	A cross-sectional study of functional and metabolic changes during aging through the lifespan in male mice. <b>2021</b> , 10,	11
544	Leukemia inhibitory factor treatment attenuates the detrimental effects of glucocorticoids on bone in mice. <b>2021</b> , 145, 115843	5
543	Bone Quality in CKD Patients: Current Concepts and Future Directions - Part I. <b>2021</b> , 7, 268-277	2
542	Periostin loss-of-function protects mice from post-traumatic and age-related osteoarthritis. <b>2021</b> , 23, 104	3
541	Teriparatide and Abaloparatide Have a Similar Effect on Bone in Mice. <b>2021</b> , 12, 628994	6
540	Genomic variants within chromosome 14q32.32 regulate bone mass through MARK3 signaling in osteoblasts. <b>2021</b> , 131,	0
539	A Role for TGFIsignaling in Preclinical Osteolytic Estrogen Receptor-Positive Breast Cancer Bone Metastases Progression. <b>2021</b> , 22,	2
538	Formation Dominates Resorption With Increasing Mineralized Density and Time Postfracture in Cortical but Not Trabecular Bone: A Longitudinal HRpQCT Imaging Study in the Distal Radius. <b>2021</b> , 5, e10493	1
537	Peptidomimetic inhibitor of L-plastin reduces osteoclastic bone resorption in aging female mice. <b>2021</b> , 9, 22	2
536	Short-range UV-LED irradiation in postmenopausal osteoporosis using ovariectomized mice. <b>2021</b> , 11, 7875	1
535	RANKL-Induced Increase in Cathepsin K Levels Restricts Cortical Expansion in a Periostin-Dependent Fashion: A Potential New Mechanism of Bone Fragility. <i>Journal of Bone and Mineral Research</i> , <b>2021</b> , 36, 1636-1645	3 2

534	Effects of treatment with a bone-targeted prostaglandin E2 receptor 4 agonist C3 (Mes-1007) in a mouse model of severe osteogenesis imperfecta. <b>2021</b> , 145, 115867	Ο
533	Adenine-induced chronic kidney disease induces a similar skeletal phenotype in male and female C57BL/6 mice with more severe deficits in cortical bone properties of male mice. <b>2021</b> , 16, e0250438	6
532	The Contribution of Macrophages in Old Mice to Periodontal Disease. <b>2021</b> , 100, 1397-1404	5
531	Effect of load-induced local mechanical strain on peri-implant bone cell activity related to bone resorption and formation in mice: An analysis of histology and strain distributions. <b>2021</b> , 116, 104370	3
530	Insertion Mutation in Tnfrsf11a Causes a Paget's Disease-Like Phenotype in Heterozygous Mice and Osteopetrosis in Homozygous Mice. <i>Journal of Bone and Mineral Research</i> , <b>2021</b> , 36, 1376-1386	2
529	Improving Bone Health by Optimizing the Anabolic Action of Wnt Inhibitor Multitargeting. <b>2021</b> , 5, e10462	2
528	Non-oxidized parathyroid hormone (PTH) measured by current method is not superior to total PTH in assessing bone turnover in chronic kidney disease. <b>2021</b> , 99, 1173-1178	4
527	Lgr4 promotes aerobic glycolysis and differentiation in osteoblasts via the canonical Wnt/Etatenin pathway. <i>Journal of Bone and Mineral Research</i> , <b>2021</b> , 36, 1605-1620	7
526	Changes in the Intestinal Histomorphometry, the Expression of Intestinal Tight Junction Proteins, and the Bone Structure and Liver of Pre-Laying Hens Following Oral Administration of Fumonisins for 21 Days. <b>2021</b> , 13,	0
525	Osteocyte- and late osteoblast-derived NOTUM reduces cortical bone mass in mice. <b>2021</b> , 320, E967-E975	O
524	Bone densitometry versus bone histomorphometry in renal transplanted patients: a cross-sectional study. <b>2021</b> , 34, 1065-1073	1
523	Incorporation of anterior iliac crest or calvarial bone grafts in reconstructed atrophied maxillae: A randomized clinical trial with histomorphometric and micro-CT analyses. <b>2021</b> , 23, 492-502	2
522	PTX3 Effects on Osteogenic Differentiation in Osteoporosis: An In Vitro Study. <b>2021</b> , 22,	2
521	Bone quality in hypoparathyroidism. <b>2021</b> , 46, 325-334	
520	DEC1 deficiency results in accelerated osteopenia through enhanced DKK1 activity and attenuated PI3KCA/Akt/GSK3[signaling. <b>2021</b> , 118, 154730	1
519	Sclerostin and DKK1 circulating levels associate with low bone turnover in patients with chronic kidney disease Stages 3 and 4. <b>2021</b> , 14, 2401-2408	5
518	Bone Marrow Adiposity in Premenopausal Women With Type 2 Diabetes With Observations on Peri-Trabecular Adipocytes. <b>2021</b> , 106, e3592-e3602	1
517	Three-Dimensional Cell Printed Lock-Key Structure for Oral Soft and Hard Tissue Regeneration. <b>2021</b> ,	2

516	The KDM4B-CCAR1-MED1 axis is a critical regulator of osteoclast differentiation and bone homeostasis. <b>2021</b> , 9, 27	2
515	Early B-cell Factor1 (Ebf1) promotes early osteoblast differentiation but suppresses osteoblast function. <b>2021</b> , 146, 115884	1
514	Effects of Osteoporosis on Bone Morphometry and Material Properties of Individual Human Trabeculae in the Femoral Head. <b>2021</b> , 5, e10503	О
513	Mitochondrial Sirt3 contributes to the bone loss caused by aging or estrogen deficiency. <b>2021</b> , 6,	9
512	The TrkA agonist gambogic amide augments skeletal adaptation to mechanical loading. <b>2021</b> , 147, 115908	2
511	Chronic Lead Exposure Alters Mineral Properties in Alveolar Bone. <b>2021</b> , 11, 642	
510	Bisphenol A exposure prenatally delays bone development and bone mass accumulation in female rat offspring via the ER/HDAC5/TGFBignaling pathway. <b>2021</b> , 458, 152830	4
509	Effect of serum 25-hydroxyvitamin D concentrations on skeletal mineralization in black and white women. <b>2021</b> , 39, 843-850	O
508	Sclerostin antibody increases trabecular bone and bone mechanical properties by increasing osteoblast activity damaged by whole-body irradiation in mice. <b>2021</b> , 147, 115918	2
507	Microarchitecture of titanium cylinders obtained by additive manufacturing does not influence osseointegration in the sheep. <b>2021</b> , 8, rbab021	2
506	miR-433-3p suppresses bone formation and mRNAs critical for osteoblast function in mice. <i>Journal of Bone and Mineral Research</i> , <b>2021</b> , 36, 1808-1822	3
505	Disturbance of osteonal bone remodeling and high tensile stresses on the lateral cortex in atypical femoral fracture after long-term treatment with Risedronate and Alfacalcidol for osteoporosis. <b>2021</b> , 14, 101091	4
504	PPARG in osteocytes controls sclerostin expression, bone mass, marrow adiposity and mediates TZD-induced bone loss. <b>2021</b> , 147, 115913	8
503	A functional motif of long noncoding RNA Nron against osteoporosis. <b>2021</b> , 12, 3319	16
502	Bone Histomorphometry and F-Sodium Fluoride Positron Emission Tomography Imaging: Comparison Between only Bone Turnover-based and Unified TMV-based Classification of Renal Osteodystrophy. <b>2021</b> , 109, 605-614	5
501	Short-term glucocorticoid excess blunts abaloparatide-induced increase in femoral bone mass and strength in mice. <b>2021</b> , 11, 12258	3
500	Histopathology of osteogenesis imperfecta bone. Supramolecular assessment of cells and matrices in the context of woven and lamellar bone formation using light, polarization and ultrastructural microscopy. <b>2021</b> , 14, 100734	5
499	FOS/GOS attenuates high-fat diet induced bone loss via reversing microbiota dysbiosis, high intestinal permeability and systemic inflammation in mice. <b>2021</b> , 119, 154767	13

498	Components of the Gut Microbiome That Influence Bone Tissue-Level Strength. <i>Journal of Bone and Mineral Research</i> , <b>2021</b> , 36, 1823-1834	6.3	1
497	Dual targeting of salt inducible kinases and CSF1R uncouples bone formation and bone resorption. <b>2021</b> , 10,		1
496	An variant links aberrant Rac1 function to early-onset skeletal fragility. 2021, 5, e10509		
495	Inhibition of miR-29 Activity in the Myeloid Lineage Increases Response to Calcitonin and Trabecular Bone Volume in Mice. <b>2021</b> , 162,		2
494	A quantitative analysis of bone lamellarity and bone collagen linearity induced by distinct dosing and frequencies of teriparatide administration in ovariectomized rats and monkeys. <b>2021</b> , 70, 498-509		О
493	Phosphate restriction impairs mTORC1 signaling leading to increased bone marrow adipose tissue and decreased bone in growing mice. <i>Journal of Bone and Mineral Research</i> , <b>2021</b> , 36, 1510-1520	6.3	1
492	Effects of risedronate, alendronate, and minodronate alone or in combination with eldecalcitol on bone mineral density, quality, and strength in ovariectomized rats. <b>2021</b> , 14, 101061		1
491	Effect of ErhBMP-2-loaded Etricalcium phosphate on ulna defects in the osteoporosis rabbit model. <b>2021</b> , 14, 100739		1
490	The Beneficial Effect of an Intra-articular Injection of Losartan on Microfracture-Mediated Cartilage Repair Is Dose Dependent. <b>2021</b> , 49, 2509-2521		3
489	Mmp-13 deletion in cells of the mesenchymal lineage increases bone mass, decreases endocortical osteoclast number, and attenuates the cortical bone loss caused by estrogen deficiency in mice.		
488	Strain-specific alterations in the skeletal response to adenine-induced chronic kidney disease are associated with differences in parathyroid hormone levels. <b>2021</b> , 148, 115963		4
487	Liquiritigenin promotes osteogenic differentiation and prevents bone loss via inducing auto-lysosomal degradation and inhibiting apoptosis. <b>2021</b> ,		1
486	The Effect of Early Application of a Combined Therapy of Bone Marrow Mesenchymal Stem Cells and Platelet-Rich Plasma on Blood and Bone Parameters in Ovariectomized Rats. <b>2021</b> , 57, 972-990		
485	Chronic Kidney Disease-Induced Arterial Media Calcification in Rats Prevented by Tissue Non-Specific Alkaline Phosphatase Substrate Supplementation Rather Than Inhibition of the Enzyme. <b>2021</b> , 13,		2
484	Allograft Chip Incorporation in Acetabular Reconstruction: Multiscale Characterization Revealing Osteoconductive Capacity. <b>2021</b> , 103, 1996-2005		2
483	Long-Term Administration of Abacavir and Etravirine Impairs Semen Quality and Alters Redox System and Bone Metabolism in Growing Male Wistar Rats. <b>2021</b> , 2021, 5596090		2
482	Neutralization of oxidized phospholipids attenuates age-associated bone loss in mice. <b>2021</b> , 20, e13442	2	5
481	Loss of function of lysosomal acid lipase (LAL) profoundly impacts osteoblastogenesis and increases fracture risk in humans. <b>2021</b> , 148, 115946		1

480	Notum Deletion From Late-Stage Skeletal Cells Increases Cortical Bone Formation and Potentiates Skeletal Effects of Sclerostin Inhibition. <i>Journal of Bone and Mineral Research</i> , <b>2021</b> ,	2
479	Targeting local lymphatics to ameliorate heterotopic ossification via FGFR3-BMPR1a pathway. <b>2021</b> , 12, 4391	1
478	Inhibition of ACLY Leads to Suppression of Osteoclast Differentiation and Function Via Regulation of Histone Acetylation. <i>Journal of Bone and Mineral Research</i> , <b>2021</b> , 36, 2065-2080	6
477	Aldo-keto reductase family 1 member C1 regulates the osteogenic differentiation of human ASCs by targeting the progesterone receptor. <b>2021</b> , 12, 383	
476	LRRc17 controls BMSC senescence via mitophagy and inhibits the therapeutic effect of BMSCs on ovariectomy-induced bone loss. <b>2021</b> , 43, 101963	7
475	Glucocorticoid-induced dose-related and site-specific bone remodelling, microstructure, and mechanical changes in cancellous and cortical bones. <b>2021</b> , 48, 1421-1429	
474	Osteolineage depletion of mitofusin2 enhances cortical bone formation in female mice. <b>2021</b> , 148, 115941	2
473	Osseointegration evaluation of UHMWPE and PEEK-based scaffolds with BMP-2 using model of critical-size cranial defect in mice and push-out test. <b>2021</b> , 119, 104477	2
472	Biofunctionalization of bioactive ceramic scaffolds to increase the cell response for bone regeneration. <b>2021</b> , 16,	2
47 <sup>1</sup>	Bone microstructure and bone mineral density are not systemically different in Antarctic icefishes and related Antarctic notothenioids. <b>2022</b> , 240, 34-49	1
470	Pathogenic variants in GNPTAB and GNPTG encoding distinct subunits of GlcNAc-1-phosphotransferase differentially impact bone resorption in patients with mucolipidosis type II and III. <b>2021</b> , 23, 2369-2377	O
469	Differential Expression of Alkaline Phosphatase and PHOSPHO1 in Bone from a Murine Model of Chronic Kidney Disease.	
468	Patterns of renal osteodystrophy 1 year after kidney transplantation. <b>2021</b> , 36, 2130-2139	2
467	Wing and leg bone microstructure reflects migratory demands in resident and migrant populations of the Dark-eyed Junco (Junco hyemalis).	O
466	Texturized P(VDF-TrFE)/BT membrane enhances bone neoformation in calvaria defects regardless of the association with photobiomodulation therapy in ovariectomized rats. <b>2021</b> , 1	2
465	Skeletal Effects of Bone-Targeted TGFbeta Inhibition in a Mouse Model of Duchenne Muscular Dystrophy. <b>2021</b> , 11,	O
464	Characterization of Skeletal Phenotype and Associated Mechanisms With Chronic Intestinal Inflammation in the Winnie Mouse Model of Spontaneous Chronic Colitis. <b>2021</b> ,	1
463	Piezoelectric Microvibration Mitigates Estrogen Loss-Induced Osteoporosis and Promotes Piezo1, MicroRNA-29a, and Wnt3a Signaling in Osteoblasts. <b>2021</b> , 22,	1

462	Synergistic effects of magnesium ions and simvastatin on attenuation of high-fat diet-induced bone loss. <b>2021</b> , 6, 2511-2522		6
461	Bone Nanomechanical Properties and Relationship to Bone Turnover and Architecture in Patients With Atypical Femur Fractures: A Prospective Nested Case-Control Study. <b>2021</b> , 5, e10523		
460	Colon epithelial cell-specific Bmal1 deletion impairs bone formation in mice.		
459	Biodegradable magnesium combined with distraction osteogenesis synergistically stimulates bone tissue regeneration via CGRP-FAK-VEGF signaling axis. <b>2021</b> , 275, 120984		11
458	Stimulation of Treg Cells to Inhibit Osteoclastogenesis in Gorham-Stout Disease. <b>2021</b> , 9, 706596		1
457	RSPO3 is important for trabecular bone and fracture risk in mice and humans. <b>2021</b> , 12, 4923		3
456	The Role of Bone Volume, FGF23 and Sclerostin in Calcifications and Mortality; a Cohort Study in CKD Stage 5 Patients. <b>2021</b> , 1		О
455	Activation, development, and attenuation of modeling- and remodeling-based bone formation in adult rats. <b>2021</b> , 276, 121015		1
454	Bone loss after severe spinal cord injury coincides with reduced bone formation and precedes bone blood flow deficits. <b>2021</b> , 131, 1288-1299		О
453	TNF-Polarized Macrophages Produce Insulin-like 6 Peptide to Stimulate Bone Formation in Rheumatoid Arthritis in Mice. <i>Journal of Bone and Mineral Research</i> , <b>2021</b> ,	6.3	2
452	Osteoblast-Specific Wnt Secretion Is Required for Skeletal Homeostasis and Loading-Induced Bone Formation in Adult Mice. <i>Journal of Bone and Mineral Research</i> , <b>2021</b> ,	6.3	3
451	Protective Effects of Water Extract of against Oxidative Stress-Related Osteoporosis In Vivo and In Vitro. <b>2021</b> , 8,		2
450	Identification of candidate regulators of mandibular bone loss in FcRIIB Mice. 2021, 11, 18726		1
449	Myeloid Lineage Ablation of Regulates M-CSF Signaling and Tempers Bone Resorption in Female Mice. <b>2021</b> , 22,		O
448	Bone Quality and Fractures in Women With Osteoporosis Treated With Bisphosphonates for 1 to 14 Years. <b>2021</b> , 5, e10549		2
447	NMUR1 in the NMU-Mediated Regulation of Bone Remodeling. <b>2021</b> , 11,		1
446	Intraosseous Injection of Calcium Phosphate Polymer-Induced Liquid Precursor Increases Bone Density and Improves Early Implant Osseointegration in Ovariectomized Rats. <b>2021</b> , 16, 6217-6229		1
445	Differentiating the causes of adynamic bone in advanced chronic kidney disease informs osteoporosis treatment. <b>2021</b> , 100, 546-558		10

444	Salvianolate Ameliorates Osteopenia and Improves Bone Quality in Prednisone-Treated Rheumatoid Arthritis Rats by Regulating RANKL/RANK/OPG Signaling. <b>2021</b> , 12, 710169		0
443	Conductive Hearing Loss in the Hyp Mouse Model of X-Linked Hypophosphatemia Is Accompanied by Hypomineralization of the Auditory Ossicles. <i>Journal of Bone and Mineral Research</i> , <b>2021</b> ,	6.3	О
442	The SFRP1 Inhibitor WAY-316606 Attenuates Osteoclastogenesis Through Dual Modulation of Canonical Wnt Signaling. <i>Journal of Bone and Mineral Research</i> , <b>2021</b> ,	6.3	О
441	Mice Lacking the Calcitonin Receptor Do Not Display Improved Bone Healing. 2021, 10,		
440	An in vitro / in vivo release test of risedronate drug loaded nano-bioactive glass composite scaffolds. <b>2021</b> , 607, 120989		2
439	Feeding intervention potentiates the effect of mechanical loading to induce new bone formation in mice. <b>2021</b> , 35, e21792		1
438	Tetracycline, an Appropriate Reagent for Measuring Bone-Formation Activity in the Murine Model of the -Induced Bone Loss. <b>2021</b> , 11, 714366		
437	Bone Structural, Biomechanical and Histomorphometric Characteristics of the Postcranial Skeleton of the Marsh Rice Rat (Oryzomys palustris).		
436	Gestational and lactational exposure to BPA or BPS has minimal effects on skeletal outcomes in adult female mice. <b>2021</b> , 15, 101136		O
435	Maternal bone adaptation to mechanical loading during pregnancy, lactation, and post-weaning recovery. <b>2021</b> , 151, 116031		3
434	Static histomorphometry allows for a diagnosis of bone turnover in renal osteodystrophy in the absence of tetracycline labels. <b>2021</b> , 152, 116066		4
433	The impact of airborne endotoxin exposure on rheumatoid arthritis-related joint damage, autoantigen expression, autoimmunity, and lung disease. <b>2021</b> , 100, 108069		3
432	Non-bone metastatic cancers promote osteocyte-induced bone destruction. <b>2021</b> , 520, 80-90		3
431	Inadequate response to treatment reveals persistent osteoclast bone resorption in osteoporotic patients. <b>2021</b> , 153, 116167		О
430	Deletion of the sodium/hydrogen exchanger 6 causes low bone volume in adult mice. <b>2021</b> , 153, 11617	8	O
429	Chloroquine increases osteoclast activity in vitro but does not improve the osteopetrotic bone phenotype of ADO2 mice. <b>2021</b> , 153, 116160		
428	Cdc42 in osterix-expressing cells alters osteoblast behavior and myeloid lineage commitment. <b>2021</b> , 153, 116150		1
427	Hypobaric hypoxia deteriorates bone mass and strength in mice. <b>2022</b> , 154, 116203		1

426	Sclerostin antibody improves phosphate metabolism hormones, bone formation rates, and bone mass in adult Hyp mice. <b>2022</b> , 154, 116201	2
425	Intra-skeletal vascular density in a bipedal hopping macropod with implications for analyses of rib histology. <b>2021</b> , 96, 386-399	1
424	Scaffold-free human mesenchymal stem cell construct geometry regulates long bone regeneration. <b>2021</b> , 4, 89	1
423	Activation of Notch3 in osteoblasts/osteocytes causes compartment-specific changes in bone remodeling. <b>2021</b> , 296, 100583	1
422	Osteolytic effects of tumoral estrogen signaling in an estrogen receptor-positive breast cancer bone metastasis model. <b>2021</b> , 7,	1
421	Enhanced Osseointegration by the Hierarchical Micro-Nano Topography on Selective Laser Melting Ti-6Al-4V Dental Implants. <b>2020</b> , 8, 621601	6
420	Induction of fully stabilized cortical bone defects to study intramembranous bone regeneration. <b>2015</b> , 1226, 183-92	2
419	Growth, Modeling and Remodeling of Bone. <b>2015</b> , 95-173	3
418	Registered Micro-Computed Tomography Data as a Four-Dimensional Imaging Biomarker of Bone Formation and Resorption. <b>2017</b> , 557-586	1
417	Ancient Human Bone Microstructure Case Studies from Medieval England. <b>2019</b> , 35-52	1
416	Overexpression of Fam20C in osteoblast in vivo leads to increased cortical bone formation and osteoclastic bone resorption. <b>2020</b> , 138, 115414	3
415	Inhibition of miR-29-3p isoforms via tough decoy suppresses osteoblast function in homeostasis but promotes intermittent parathyroid hormone-induced bone anabolism. <b>2021</b> , 143, 115779	7
414	SENP3 Suppresses Osteoclastogenesis by De-conjugating SUMO2/3 from IRF8 in Bone Marrow-Derived Monocytes. <b>2020</b> , 30, 1951-1963.e4	8
413	Deletion of protein kinase D1 in osteoprogenitor cells results in decreased osteogenesis inlivitro and reduced bone mineral density inlivivo. <b>2018</b> , 461, 22-31	5
412	The androgen receptor is required for maintenance of bone mass in adult male mice. <b>2019</b> , 479, 159-169	12
411	Arylsulfatase K inactivation causes mucopolysaccharidosis due to deficient glucuronate desulfation of heparan and chondroitin sulfate. <b>2020</b> , 477, 3433-3451	4
410	Conditional deletion of E11/Podoplanin in bone protects against ovariectomy-induced increases in osteoclast formation and activity. <b>2020</b> , 40,	3
409	Traumatic Joint Injury Induces Acute Catabolic Bone Turnover Concurrent with Articular Cartilage Damage in a Rat Model of Post-Traumatic Osteoarthritis.	1

408	Low protein intake compromises the recovery of lactation-induced bone loss in female mouse dams without affecting skeletal muscles.	1
407	Bone marrow adipogenic lineage precursors (MALPs) promote osteoclastogenesis in bone remodeling and pathologic bone loss.	2
406	Osteoclast-derived IGF1 is required for pagetic lesion formation in vivo. <b>2020</b> , 5,	2
405	Protein kinase G1 regulates bone regeneration and rescues diabetic fracture healing. <b>2020</b> , 5,	5
404	Increased FGF-23 levels are linked to ineffective erythropoiesis and impaired bone mineralization in myelodysplastic syndromes. <b>2020</b> , 5,	6
403	Osteocyte RANKL is required for cortical bone loss with age and is induced by senescence. <b>2020</b> , 5,	12
402	Fatty acid oxidation by the osteoblast is required for normal bone acquisition in a sex- and diet-dependent manner. <b>2017</b> , 2,	44
401	Inducible podocyte-specific deletion of CTCF drives progressive kidney disease and bone abnormalities. <b>2018</b> , 3,	10
400	Sclerostin neutralization unleashes the osteoanabolic effects of Dkk1 inhibition. 2018, 3,	39
399	Cathepsin K-deficient osteocytes prevent lactation-induced bone loss and parathyroid hormone suppression. <b>2019</b> , 129, 3058-3071	26
398	Lkb1 deletion in periosteal mesenchymal progenitors induces osteogenic tumors through mTORC1 activation. <b>2019</b> , 129, 1895-1909	20
397	Salt-inducible kinases dictate parathyroid hormone 1 receptor action in bone development and remodeling. <b>2019</b> , 129, 5187-5203	14
396	Parathyroid hormone-dependent bone formation requires butyrate production by intestinal microbiota. <b>2020</b> , 130, 1767-1781	44
395	Osteoclast-secreted CTHRC1 in the coupling of bone resorption to formation. <b>2013</b> , 123, 3914-24	143
394	Sex steroid deficiency-associated bone loss is microbiota dependent and prevented by probiotics. <b>2016</b> , 126, 2049-63	265
393	Osteoclast-secreted SLIT3 coordinates bone resorption and formation. <b>2018</b> , 128, 1429-1441	71
392	Narrowband-autofluorescence imaging for bone analysis. <b>2019</b> , 10, 2367-2382	1
391	Runx2 is essential for the transdifferentiation of chondrocytes into osteoblasts. <b>2020</b> , 16, e1009169	23

## (2016-2013)

390	Inhibition of GSK-3I rescues the impairments in bone formation and mechanical properties associated with fracture healing in osteoblast selective connexin 43 deficient mice. <b>2013</b> , 8, e81399	32
389	Sex and genetic factors determine osteoblastic differentiation potential of murine bone marrow stromal cells. <b>2014</b> , 9, e86757	37
388	Midkine-deficiency delays chondrogenesis during the early phase of fracture healing in mice. <b>2014</b> , 9, e116282	27
387	Bone mass and bone quality are altered by hypoactivity in the chicken. <b>2015</b> , 10, e0116763	29
386	NOD/SCID-GAMMA mice are an ideal strain to assess the efficacy of therapeutic agents used in the treatment of myeloma bone disease. <b>2015</b> , 10, e0119546	27
385	Deletion of histone deacetylase 7 in osteoclasts decreases bone mass in mice by interactions with MITF. <b>2015</b> , 10, e0123843	17
384	A Model for Osteonecrosis of the Jaw with Zoledronate Treatment following Repeated Major Trauma. <b>2015</b> , 10, e0132520	25
383	Fracture Healing Is Delayed in Immunodeficient NOD/scid- IL2R[£null Mice. <b>2016</b> , 11, e0147465	27
382	Treadmill Exercise Improves Fracture Toughness and Indentation Modulus without Altering the Nanoscale Morphology of Collagen in Mice. <b>2016</b> , 11, e0163273	7
381	Nrf2 regulates mass accrual and the antioxidant endogenous response in bone differently depending on the sex and age. <b>2017</b> , 12, e0171161	22
380	Effects of combination treatment with alendronate and raloxifene on skeletal properties in a beagle dog model. <b>2017</b> , 12, e0181750	4
379	Treatment of OPG-deficient mice with WP9QY, a RANKL-binding peptide, recovers alveolar bone loss by suppressing osteoclastogenesis and enhancing osteoblastogenesis. <b>2017</b> , 12, e0184904	19
378	Clinically relevant doses of vitamin A decrease cortical bone mass in mice. 2018, 239, 389-402	13
377	Membrane estrogen receptor Hs essential for estrogen signaling in the male skeleton. <b>2018</b> , 239, 303-312	9
376	Losartan improves alveolar bone dynamics in normotensive rats but not in hypertensive rats. <b>2019</b> , 27, e20180574	2
375	Effect of stem cells combined with a polymer/ceramic membrane on osteoporotic bone repair. <b>2019</b> , 33, e079	4
374	Bone marrow macrophages support prostate cancer growth in bone. <b>2015</b> , 6, 35782-96	39
373	SRC kinase inhibition with saracatinib limits the development of osteolytic bone disease in multiple myeloma. <b>2016</b> , 7, 30712-29	17

C-met inhibition blocks bone metastasis development induced by renal cancer stem cells. 2016, 7, 45525-4553 ½1 372 Standardised Nomenclature, Abbreviations, and Units for the Study of Bone Marrow Adiposity: Report of the Nomenclature Working Group of the International Bone Marrow Adiposity Society. 16 371 2019, 10, 923 A micro-CT study of microstructure change of alveolar bone during orthodontic tooth movement 370 13 under different force magnitudes in rats. 2017, 13, 1793-1798 Short time guided bone regeneration using beta-tricalcium phosphate with and without fibronectin 369 - An experimental study in rats. **2020**, 25, e532-e540 368 Effect of clopidogrel in bone healing-experimental study in rabbits. 2019, 10, 434-445 2 FGF-23 serum levels and bone histomorphometric results in adult patients with chronic kidney 22 disease on dialysis. **2014**, 82, 287-95 Effects of the linagliptin, dipeptidyl peptidase-4 inhibitor, on bone fragility induced by type 2 366 1 diabetes mellitus in obese mice. 2020, 14, 218-225 Reduced expression of C/EBPLIP extends health and lifespan in mice. 2018, 7, 365 11 Stimulation of Piezo1 by mechanical signals promotes bone anabolism. 2019, 8, 364 84 A trans-eQTL network regulates osteoclast multinucleation and bone mass. 2020, 9, 363 10 Irisin directly stimulates osteoclastogenesis and bone resorption in vitro and in vivo. 2020, 9, 362 25 Cortical bone adaptation and mineral mobilization in the subterranean mammal (Rodentia: 8 361 Bathyergidae): effects of age and sex. 2018, 6, e4944 Acceleration of Fracture Healing in Mouse Tibiae Using Intramedullary Nails Composed of Type 360 4 TiNbSn Alloy with Low Young's Modulus. 2021, 255, 135-142 Femoral DCT Analysis, Mechanical Testing and Immunolocalization of Bone Proteins in Hydroxy EMethylbutyrate (HMB) Supplemented Spiny Mouse in a Model of Pregnancy and 359 Lactation-Associated Osteoporosis. 2021, 10, Novel Preosteoclast Populations in Obesity-Associated Periodontal Disease. 2021, 220345211040729 358 3 Clinical Prediction of High-Turnover Bone Disease After Kidney Transplantation. 2021, 1 357 Stochastic parametric skeletal dosimetry model for humans: General approach and application to 356 1 active marrow exposure from bone-seeking beta-particle emitters. 2021, 16, e0257605 Neoadjuvant teriparatide therapy targeting the osteoporotic spine: influence of administration 355 period from the perspective of bone histomorphometry. 2021, 1-11

354	Sparse dose-dependent difference in skeletal effects of short-term glucocorticoid excess in outbred Swiss mice. <b>2021</b> , 5, 100114	1
353	Methylsulfonylmethane Increases the Alveolar Bone Density of Mandibles in Aging Female Mice. <b>2021</b> , 12, 708905	0
352	In premenopausal women with idiopathic osteoporosis, lower bone formation rate is associated with higher body fat and higher IGF-1. <b>2021</b> , 1	1
351	Regulatory Perspectives on Juvenile Animal Toxicologic Pathology. <b>2021</b> , 49, 1393-1404	
350	Extracellular vesicles derived from the periodontal pathogen Filifactor alocis induce systemic bone loss through Toll-like receptor 2. <b>2021</b> , 10, e12157	4
349	Antimicrobial-induced oral dysbiosis exacerbates naturally occurring alveolar bone loss. <b>2021</b> , 35, e22015	
348	Diagnostic Accuracy of Noninvasive Bone Turnover Markers in Renal Osteodystrophy. 2021,	4
347	Low bone turnover is associated with plain X-ray vascular calcification in predialysis patients. <b>2021</b> , 16, e0258284	2
346	Renal osteodystrophy. <b>2015</b> , 1692-1697	
345	Registered Micro-Computed Tomography Data as a Four-Dimensional Imaging Biomarker of Bone Formation and Resorption. <b>2015</b> , 1-30	
344	The Reproductive System. <b>2015</b> , 206-227	
343	Diagnostik von Knochenerkrankungen. <b>2018</b> , 45-81	
342	Effects of Parathyroid Hormone, Alendronate and Odanacatib on the mineralisation process in intracortical and endocortical Haversian bone of ovariectomized rabbits.	
341	ATRAID regulates the action of nitrogen-containing bisphosphonates on bone.	O
340	Naproxen impairs load-induced bone formation, reduces bone toughness, and delays stress fracture repair in mice.	
339	Osteocyte death and bone overgrowth in mice lacking Fibroblast Growth Factor Receptors 1 and 2 in mature osteoblasts and osteocytes.	
338	Diagnosis of Osteosarcopenia Biochemistry and Pathology. <b>2019</b> , 265-321	
337	[Biocompatibility and osteoinductive properties of collagen and fibronectin hydrogel impregnated with rhBMP-2]. <b>2019</b> , 98, 5-11	O

Mineral and Bone Disorders Following Renal Transplantation. 2019, 243-261 336 Pathology of Bone, Skeletal Muscle, and Tooth. 2019, 571-618 335 Stroke prevents exercise-induced gains in bone microstructure but not composition in mice.  $\circ$ 334 High Fat Diet-Induced Obesity Negatively Affects Whole Bone Bending Strength but not Cortical 333 Structure in the Femur. Stroke Prevents Exercise-induced Gains in Bone Microstructure But Not Composition in Mice. 2019, 332 The heparan sulfate proteoglycan Syndecan-1 influences local bone cell communication via the 331 RANKL/OPG axis. Syndecan-3 enhances anabolic bone formation through WNT signalling. 330 A trans-eQTL network regulates osteoclast multinucleation and bone mass. 329 Effects of the combined administration of risedronate and menatetrenone on bone loss induced by 328 tacrolimus in rats. 2020, 14, 77-83 Effects of N-methyl-d-aspartate receptor antagonist MK-801 (dizocilpine) on bone homeostasis in 327 mice. 2020, 62, 131-138 Characterization, pharmacokinetics, and pharmacodynamics of anti-Siglec-15 antibody and its potency for treating osteoporosis and as follow-up treatment after parathyroid hormone use. 2021 326 O , 155, 116241 Simulated Galactic Cosmic Rays Modify Mitochondrial Metabolism in Osteoclasts, Increase 325  $\circ$ Osteoclastogenesis and Cause Trabecular Bone Loss in Mice. 2021, 22, Chronic Ethanol Consumption Induces Osteopenia via Activation of Osteoblast Necroptosis. 2021, 324 4 2021, 3027954 Bone Growth is Influenced by Fructose in Adolescent Male Mice Lacking Ketohexokinase (KHK). 323 2020, 106, 541-552 Renal Osteodystrophy and Bone Biopsy. 2020, 19, 215-225 322 Skeletal muscle mitochondrial dysfunction in mice is linked to bone loss via the bone marrow 321 immune microenvironment. Feeding intervention potentiates the effect of mechanical loading to induce new bone formation in 320 mice.

The Method But cylinderIfor Approximation Round and Cylindrical Shape Objects and Its

Comparison with Other Methods. 2020, 50-58

318	Effects of C-peptide replacement therapy on bone microarchitecture parameters in streptozotocin-diabetic rats.	
317	Propranolol promotes bone formation and limits resorption through novel mechanisms during anabolic parathyroid hormone treatment in female C57BL/6J mice.	
316	Pharmacological inhibition of longevity regulator PAPP-A restrains mesenchymal stromal cell activity.	
315	The Thyroid Hormone Transporter MCT10 Is a Novel Regulator of Trabecular Bone Mass and Bone Turnover in Male Mice. <b>2022</b> , 163,	O
314	Gestational and lactational exposure to BPA, but not BPS, negatively impacts trabecular microarchitecture and cortical geometry in adult male offspring. <b>2021</b> , 15, 101147	О
313	Hairy and enhancer of split 1 is a primary effector of NOTCH2 signaling and induces osteoclast differentiation and function. <b>2021</b> , 297, 101376	1
312	Decreased Trabecular Bone Mass in -Deficient Mice. <b>2021</b> , 10,	O
311	Bone microstructure in healthy men measured by HR-pQCT: Age-related changes and their relationships with DXA parameters and biochemical markers. <b>2022</b> , 154, 116252	1
310	Bone grafted with GTCP granules in the rabbit: A microcomputed tomographic, histologic, Raman microspectrometric, and Raman imaging study. <b>2020</b> , 51, 2435-2446	О
309	Disparate Bone Anabolic Cues Activate Bone Formation by Regulating the Rapid Lysosomal Degradation of Sclerostin Protein.	
308	PPARG in osteocytes is essential for sclerostin expression, bone mass, marrow adiposity and TZD-induced bone loss.	
307	Mandible Aseptic Osteonecrosis Caused by admission of the Narcotic Substances Containing Aminophosphonic Impurities: Levelling with Trilon B. <b>2020</b> ,	
306	Osteocytic connexin 43 is not required for the increase in bone mass induced by intermittent PTH administration in male mice. <b>2016</b> , 16, 45-57	10
305	Comparison between quantitative X-ray imaging, dual energy X-ray absorptiometry and microCT in the assessment of bone mineral density in disuse-induced bone loss. <b>2015</b> , 15, 42-52	13
304	Effect of local application of biphosphonates on improving peri-implant osseointegration in type-2 diabetic osteoporosis. <b>2019</b> , 11, 5417-5437	4
303	Treatment with soluble bone morphogenetic protein type 1A receptor fusion protein alleviates irradiation-induced bone loss in mice through increased bone formation and reduced bone resorption. <b>2020</b> , 12, 743-757	1
302	Gender differences in tibial fractures healing in normal and muscular dystrophic mice. <b>2020</b> , 12, 2640-2651	4
301	Using virtual microscopy for the development of sampling strategies in quantitative histology and design-based stereology. <b>2021</b> ,	1

300	Myeloid-specific PTP1B deficiency attenuates inflammation- and ovariectomy-induced bone loss in mice by inhibiting osteoclastogenesis. <i>Journal of Bone and Mineral Research</i> , <b>2021</b> ,	1
299	Bone targeting antioxidative nano-iron oxide for treating postmenopausal osteoporosis <b>2022</b> , 14, 250-261	6
298	Inhibition of TGF-Bignaling attenuates disuse-induced trabecular bone loss after spinal cord injury in male mice. <b>2021</b> ,	O
297	The WNT1 mutation specifically affects skeletal integrity in a mouse model of osteogenesis imperfecta type XV. <b>2021</b> , 9, 48	2
296	Osteoblast-specific inactivation of p53 results in locally increased bone formation. <b>2021</b> , 16, e0249894	O
295	Iron deficiency and high-intensity running interval training do not impact femoral or tibial bone in young female rats. <b>2021</b> , 1-8	1
294	Analysis of histomorphometric variables: Proposal and validation of osteon definitions. 2021,	
293	Perspective of the GEMSTONE Consortium on Current and Future Approaches to Functional Validation for Skeletal Genetic Disease Using Cellular, Molecular and Animal-Modeling Techniques <b>2021</b> , 12, 731217	1
292	Osteoinductive Moldable and Curable Bone Substitutes Based on Collagen, BMP-2 and Highly Porous Polylactide Granules, or a Mix of HAP/ETCP. <b>2021</b> , 13,	2
291	Mechanism Reversing Bone Resorption to Formation During Bone Remodeling. <b>2022</b> , 89-99	
<b>2</b> 90	Effects of Once-Weekly Teriparatide Treatment on Trabecular Bone Microdamage Accumulation and Cortical Structure in the Lumbar Vertebrae of Ovariectomized Cynomolgus Monkeys. <b>2022</b> , 361-376	
289	Bone Minimodeling, Modeling-Based Bone Formation in Trabecular, Endocortical and Periosteal Bone. <b>2022</b> , 67-87	
288	Mineralization Impairment Due to Vitamin D Deficiency in Bone Histomorphometry. 2022, 273-281	
287	Bone Phenotyping Approaches in Human, Mice and Zebrafish - Expert Overview of the EU Cost Action GEMSTONE ("GEnomics of MusculoSkeletal traits TranslatiOnal NEtwork") <b>2021</b> , 12, 720728	O
286	Disturbance of Osteonal Remodeling in Atypical Femoral Fracture: A Short Review of Pathogenesis and a Case Report: Histomorphometric Analysis of Fracture Site. <b>2022</b> , 243-270	
285	Bone Histomorphometry in Miscellaneous Metabolic Diseases: Hepatic C-Associated Osteosclerosis, IgG4-Related Disease, and EhlersDanlos Syndrome. <b>2022</b> , 305-313	
284	Iron-based phosphorus chelator: Risk of iron deposition and action on bone metabolism in uremic rats. <b>2021</b> , 15353702211057280	
283	[F] Sodium Fluoride PET Kinetic Parameters in Bone Imaging <b>2021</b> , 7, 843-854	O

282 Histomorphometry of Remodeling and Modeling-Based Mineral Apposition. **2022**, 47-65

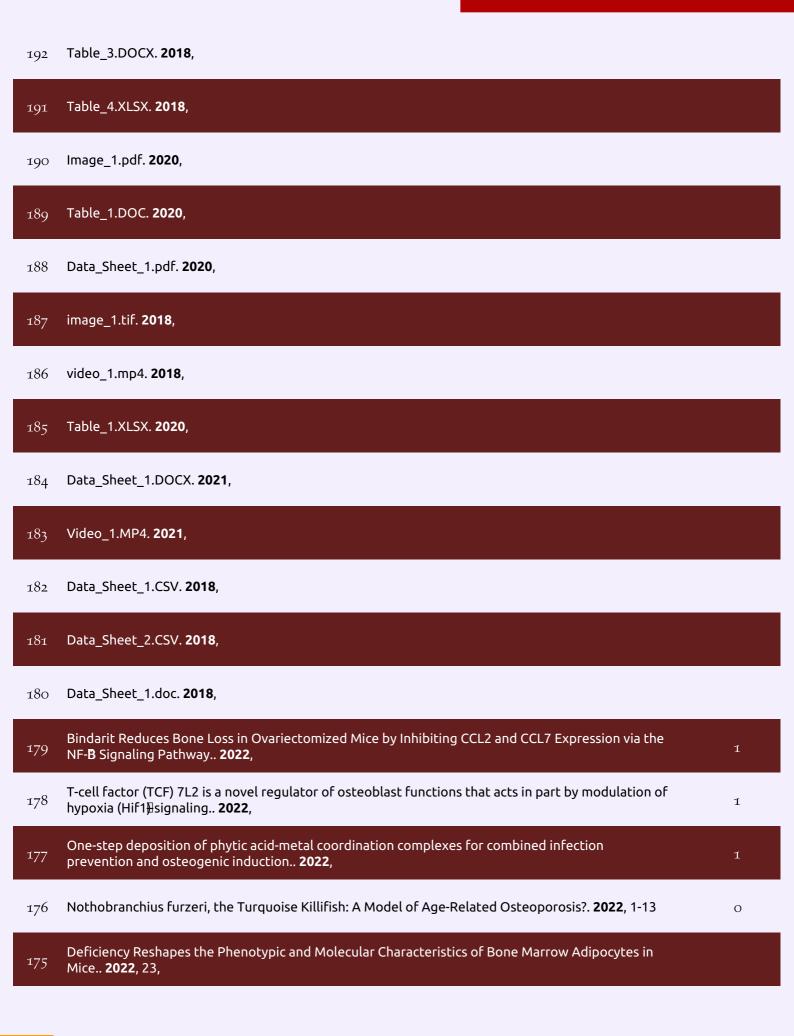
281	Significance of Reversal-Resorption Phase in Bone Loss. <b>2022,</b> 101-110		O
201	Significance of Neversac Nesot peront mase in Bone 2003. 2022, 101 110		O
280	Nanostring technology on Fibrous Dysplasia bone biopsies. A pilot study suggesting different histology-related molecular profiles <b>2022</b> , 16, 101156		1
279	[Morphological features of jaw osteonecroses in injectable drug abuse]. <b>2021</b> , 83, 20-26		
278	Dmp1 Lineage Cells Contribute Significantly to Periosteal Lamellar Bone Formation Induced by Mechanical Loading But Are Depleted from the Bone Surface During Rapid Bone Formation <b>2022</b> , 6, e10593		0
277	P2RX7 inhibition reduces breast cancer induced osteolytic lesions - implications for bone metastasis.		Ο
276	Impaired bone quality in the superolateral femoral neck occurs independent of hip geometry and bone mineral density <b>2022</b> , 141, 233-233		0
275	Improved biomechanics in experimental chronic rotator cuff repair after shockwaves is not reflected by bone microarchitecture <b>2022</b> , 17, e0262294		1
274	Association between bone mineral metabolism and vascular calcification in end-stage renal disease <b>2022</b> , 23, 12		2
273	Cortical bone density by quantitative computed tomography mirrors disorders of bone structure in bone biopsy of non-dialysis CKD patients <b>2022</b> , 16, 101166		
272	Lack of berberine effect on bone mechanical properties in rats with experimentally induced diabetes <b>2022</b> , 146, 112562		1
271	A mouse model of disuse osteoporosis based on a movable noninvasive 3D-printed unloading device <b>2022</b> , 33, 1-12		О
270	Sex-specific differences in direct osteoclastic indirect osteoblastic effects underlay the low bone mass of Pannexin1 deletion in TRAP-expressing cells in mice <b>2022</b> , 16, 101164		О
269	Housing in the Animal Enclosure Module Spaceflight Hardware Increases Trabecular Bone Mass in Ground-Control Mice. <b>2013</b> , 1, 2-19		3
268	Effect of resistance training on osteopenic rat bones in neonatal streptozotocin-induced diabetes: Analysis of GLUT4 content and biochemical, biomechanical, densitometric, and microstructural evaluation. <b>2021</b> , 287, 120143		0
267	Short Cyclic Regimen with Parathyroid Hormone (PTH) Results in Prolonged Anabolic Effect Relative to Continuous Treatment Followed by Discontinuation in Ovariectomized Rats <i>Journal of Bone and Mineral Research</i> , <b>2021</b> ,	6.3	1
266	Impaired ERK MAPK activation in mature osteoblasts enhances bone formation via the mTOR pathway.		0
265	Evaluation of an Ionic Calcium Fiber Supplement and Its Impact on Bone Health Preservation in a Dietary Calcium Deficiency Mice Model <b>2022</b> , 14,		1

264	Could Bone Biomarkers Predict Bone Turnover after Kidney Transplantation?-A Proof-of-Concept Study <b>2022</b> , 11,	О
263	Lipocalin 2 Influences Bone and Muscle Phenotype in the Mouse Model of Duchenne Muscular Dystrophy <b>2022</b> , 23,	3
262	Histone H3K27 demethylase, Utx, regulates osteoblast-to-osteocyte differentiation <b>2021</b> , 590, 132-138	1
261	Treatment with Soluble Activin Type IIB Receptor Ameliorates Ovariectomy-Induced Bone Loss and Fat Gain in Mice <b>2022</b> ,	
260	Commensal oral microbiota induces osteoimmunomodulatory effects separate from systemic microbiome in mice <b>2022</b> ,	О
259	The osteoprotective role of USP26 in coordinating bone formation and resorption 2022,	1
258	Natural History of Bone Disease Following Kidney Transplantation 2022,	1
257	PTH 1-34-functionalized bioactive glass improves peri-implant bone repair in orchiectomized rats: Microscale and ultrastructural evaluation <b>2022</b> , 112688	1
256	Bone architecture, bone material properties, and bone turnover in non-osteoporotic post-menopausal women with fragility fracture <b>2022</b> , 33, 1125	О
255	The altered osteocytic expression of connexin 43 and sclerostin in human cadaveric donors with alcoholic liver cirrhosis: Potential treatment targets <b>2022</b> ,	O
254	Generalized Uncoupled Bone Remodeling Associated With Delayed Healing of Fatigue Fractures <b>2022</b> , 6, e10598	
253	Bone Structural, Biomechanical and Histomorphometric Characteristics of the Hindlimb Skeleton in the Marsh Rice Rat (Oryzomys palustris) <b>2022</b> ,	O
252	Effects of teriparatide and loading modality on modeling-based and remodeling-based bone formation in the human femoral neck <b>2022</b> , 116342	О
251	Age-Progressive and Gender-Dependent Bone Phenotype in Mice Lacking Both Ebf1 and Ebf2 in Prrx1-Expressing Mesenchymal Cells <b>2022</b> , 1	O
250	Propranolol promotes bone formation and limits resorption through novel mechanisms during anabolic parathyroid hormone treatment in female C57BL/6J mice <i>Journal of Bone and Mineral Research</i> , <b>2022</b> ,	О
249	Inhibition of Cdk5 Ameliorates Skeletal Bone Loss in Glucocorticoid-Treated Mice 2022, 10,	O
248	Wnt/Eatenin Signaling Controls Maxillofacial Hyperostosis <b>2022</b> , 220345211067705	0
247	Effect of Acetazolamide and Zoledronate on Simulated High Altitude-Induced Bone Loss <b>2022</b> , 13, 831369	O

246	A neomorphic variant in SP7 alters sequence specificity and causes a high-turnover bone disorder <b>2022</b> , 13, 700	2
245	Assessment of trabecular and cortical parameters using high-resolution peripheral quantitative computed tomography, histomorphometry and microCT of iliac crest bone core in hemodialysis patients <b>2022</b> , 16, 101173	Ο
244	Contemporary kidney transplantation has a limited impact on bone microarchitecture 2022, 16, 101172	О
243	Loading-Induced Bone Formation is Mediated by Wnt1 Induction in Osteoblast-Lineage Cells.	
242	Regulation of sclerostin by the SIRT1 stabilization pathway in osteocytes 2022,	1
241	Single Application of Low-Dose, Hydroxyapatite-Bound BMP-2 or GDF-5 Induces Long-Term Bone Formation and Biomechanical Stabilization of a Bone Defect in a Senile Sheep Lumbar Osteopenia Model <b>2022</b> , 10,	O
240	Skeletal muscle mitoribosomal defects are linked to low bone mass caused by bone marrow inflammation in male mice <b>2022</b> ,	0
239	Bone volume, mineral density, and fracture risk after kidney transplantation <b>2022</b> , 17, e0261686	Ο
238	Conditional loss of IKKIIn Osterix + cells has no effect on bone but leads to age-related loss of peripheral fat <b>2022</b> , 12, 4915	Ο
237	Role of nuclear factor of activated T cells in chondrogenesis osteogenesis and osteochondroma formation <b>2022</b> , 1	
236	Lonafarnib Inhibits Farnesyltransferase via Suppressing ERK Signaling Pathway to Prevent Osteoclastogenesis in Titanium Particle-Induced Osteolysis <b>2022</b> , 13, 848152	
235	Asarone Attenuates Osteoclastogenesis and Prevents Against Oestrogen-Deficiency Induced Osteoporosis <b>2022</b> , 13, 780590	1
234	Low Turnover Renal Osteodystrophy With Abnormal Bone Quality and Vascular Calcification in Patients With Mild-to-Moderate CKD <b>2022</b> , 7, 1016-1026	0
233	Dronabinol inhibits alveolar bone remodeling in tooth movement of rats 2021,	Ο
232	Bone Mass and Osteoblast Activity Are Sex-Dependent in Mice Lacking the Estrogen Receptor <del>I</del> In Chondrocytes and Osteoblast Progenitor Cells <b>2022</b> , 23,	1
231	TET2 regulates osteoclastogenesis by modulating autophagy in OVX-induced bone loss 2022,	Ο
230	Mice with Targeted Knockout of Tetraspanin 3 Exhibit Reduced Trabecular Bone Mass Caused by Decreased Osteoblast Functions <b>2022</b> , 11,	О
229	Exercise history predicts focal differences in bone volume fraction, mineral density and microdamage in the proximal sesamoid bones of Thoroughbred racehorses <b>2022</b> ,	O

228	Improvement of Mineral and Bone Disorders After Renal Transplantation 2022,	О
227	Inferring longevity from advanced rib remodelling in insular dwarf deer.	
226	Deletion of the scavenger receptor Scarb1 in osteoblast progenitors does not affect bone mass <b>2022</b> , 17, e0265893	О
225	Puerarin specifically disrupts osteoclast activation via blocking integrin-B Pyk2/Src/Cbl signaling pathway <b>2022</b> , 33, 55-69	1
224	Lysine-Specific Demethylase 1 (LSD1) epigenetically controls osteoblast differentiation <b>2022</b> , 17, e0265027	2
223	Drinking Natural Mineral Water Maintains Bone Health in Young Rats With Metabolic Acidosis <b>2022</b> , 9, 813202	
222	Plumbagin is a NF- <b>B</b> -Inducing Kinase Inhibitor with Dual Anabolic and Anti-Resorptive Effects that Prevents Menopausal-Related Osteoporosis in Mice <b>2022</b> , 101767	O
221	Genetic Deletion of Menin in Mouse Mesenchymal Stem Cells: An Experimental and Computational Analysis <b>2022</b> , 6, e10622	O
220	Acod1 negatively impacts osteoclastogenesis via GPR91-mediated NFATc1 activation.	
219	Anti-sclerostin antibodies and abaloparatide have additive effects when used as a countermeasure against disuse osteopenia in female rats <b>2022</b> , 116417	O
218	The CMS19 disease model specifies a pivotal role for collagen XIII in bone homeostasis <b>2022</b> , 12, 5866	1
217	A cholinergic neuroskeletal interface promotes bone formation during postnatal growth and exercise <b>2022</b> ,	1
216	Combined growth hormone and insulin-like growth factor 1 rescues growth retardation in glucocorticoid-treated mdx mice but does not prevent osteopenia <b>2022</b> ,	О
215	Tetracyclines and bone: Unclear actions with potentially lasting effects <b>2022</b> , 159, 116377	1
214	2D size of trabecular bone structure units (BSU) correlate more strongly with 3D architectural parameters than age in human vertebrae <b>2022</b> , 160, 116399	О
213	Evidence for the major contribution of remodeling-based bone formation in sclerostin-deficient mice <b>2022</b> , 160, 116401	О
212	Estrogen Receptor Bignaling in Osteoblasts is Required for Mechanotransduction in Bone Fracture Healing <b>2021</b> , 9, 782355	1
211	Increased bone resorption by long-term cigarette smoke exposure in animal model <b>2021</b> , 7, e08587	

210	Commensal gut bacterium critically regulates alveolar bone homeostasis 2021,	1
209	Micro-CT Study of Mongolian Gerbil Humeral Bone After Prolonged Spaceflight Based on a New Algorithm for Delimitation of Long-Bone Regions <b>2021</b> , 12, 752893	O
208	Bones and Teeth. <b>2021</b> , 520-540	
207	Liraglutide Inhibits Osteoclastogenesis and Improves Bone Loss by Downregulating Trem2 in Female Type 1 Diabetic Mice: Findings From Transcriptomics <b>2021</b> , 12, 763646	1
206	The role of forkhead box class O1 during implant osseointegration. 2021,	
205	Micropetrosis in hemodialysis patients <b>2021</b> , 15, 101150	1
204	Effect of Topical PTH 1-34 Functionalized to Biogran in the Process of Alveolar Repair in Rats Submitted to Orchiectomy <b>2021</b> , 15,	2
203	Particle Radiation Side-Effects: Intestinal Microbiota Composition Shapes Interferon-Induced Osteo-Immunogenicity <b>2022</b> , 197, 184-192	
202	Reduced bone mass in collagen prolyl 4-hydroxylase P4ha1 +/-; P4ha2 -/- compound mutant mice.	0
201	Sustained morphine delivery suppresses bone formation and alters metabolic and circulating miRNA profiles in male C57BL/6J mice.	
200	Accelerated bone regeneration through rational design of magnesium phosphate cements 2022,	1
199	Image_1.TIF. <b>2018</b> ,	
198	Image_2.TIF. <b>2018</b> ,	
197	Image_3.TIF. <b>2018</b> ,	
196	Image_4.TIF. <b>2018</b> ,	
195	Image_5.tif. <b>2018</b> ,	
194	Table_1.DOCX. <b>2018</b> ,	
193	Table_2.DOCX. <b>2018</b> ,	



174	Effects of ferric citrate and intravenous iron sucrose on markers of mineral, bone, and iron homeostasis in a rat model of CKD-MBD <b>2022</b> ,		1
173	Effects of Korean red ginseng on three-dimensional trabecular bone microarchitecture and strength in growing rats: Comparison with changes due to jump exercise <b>2022</b> , 17, e0267466		
172	BMP9 reduces age-related bone loss in mice by inhibiting osteoblast senescence through Smad1-Stat1-P21 axis <b>2022</b> , 8, 254		О
171	TREM2 R47H variant causes distinct age- and sex-dependent musculoskeletal alterations in mice <i>Journal of Bone and Mineral Research</i> , <b>2022</b> ,	6.3	1
170	Reversing the imbalance in bone homeostasis via sustained release of SIRT-1 agonist to promote bone healing under osteoporotic condition <b>2023</b> , 19, 429-443		О
169	Roxadustat promotes osteoblast differentiation and prevents estrogen deficiency-induced bone loss by stabilizing HIF-1 activating the Wnt/Etatenin signaling pathway. 2022, 17,		1
168	3D-Printed composite scaffolds based on poly( $\bar{\mu}$ -caprolactone ) filled with poly(glutamic acid)-modified cellulose nanocrystals for improved bone tissue regeneration.		2
167	High phosphate intake induces bone loss in nephrectomized thalassemic mice. <b>2022</b> , 17, e0268732		O
166	Alterations of bone material properties in growing Ifitm5/BRIL p.S42 knock-in mice, a new model for atypical type VI osteogenesis imperfecta. <b>2022</b> , 116451		О
165	Intracortical remodelling increases in highly-loaded bone after exercise cessation.		O
164	Effects of Dietary Protein Source and Quantity on Bone Morphology and Body Composition Following a High-Protein Weight-Loss Diet in a Rat Model for Postmenopausal Obesity. <b>2022</b> , 14, 2262		
163	Absence of P2Y2 Receptor Does Not Prevent Bone Destruction in a Murine Model of Muscle Paralysis-Induced Bone Loss. <b>2022</b> , 13,		
162	Toll-like receptor 9 deficiency induces osteoclastic bone loss via gut microbiota-associated systemic chronic inflammation. <b>2022</b> , 10,		3
161	LAMELLAR THICKNESS MEASUREMENTS IN NORMAL AND OSTEOGENESIS IMPERFECTA HUMAN BONE, with development of a method of automated thickness averaging to simplify quantitation.		
160	Mechanical forces couple bone matrix mineralization with inhibition of angiogenesis to limit adolescent bone growth. <b>2022</b> , 13,		2
159	EPLINIs Involved in the Assembly of Cadherin-catenin Complexes in Osteoblasts and Affects Bone Formation. <b>2022</b> ,		
158	Manual Therapy Facilitates Homeostatic Adaptation to Bone Microstructural Declines Induced by a Rat Model of Repetitive Forceful Task. <b>2022</b> , 23, 6586		
157	Comparison of the 3D-Microstructure Between Alveolar and Iliac Bone for Enhanced Bioinspired Bone Graft Substitutes. 10,		O

156	Foxf2 represses bone formation via Wnt2b/Etatenin signaling.		О
155	Pim-2 regulates bone resorptive activity of osteoclasts via V-ATPase a 3 isoform expression in periodontal disease.		O
154	Prevention of Hypomineralization In Auditory Ossicles of Vitamin D Receptor (Vdr) Deficient Mice. 13,		
153	Mmp13 deletion in mesenchymal cells increases bone mass and may attenuate the cortical bone loss caused by estrogen deficiency. <b>2022</b> , 12,		O
152	Mouse models of type 1 diabetes and their use in skeletal research. Publish Ahead of Print,		O
151	Altered type I collagen networking in osteoporotic human femoral head revealed by histomorphometric and Fourier transform infrared imaging correlated analyses.		2
150	Low bone mass and impaired fracture healing in mouse models of Trisomy21 (Down syndrome). <b>2022</b> , 162, 116471		0
149	Nutritional Calcium Supply Dependent Calcium Balance, Bone Calcification and Calcium Isotope Ratios in Rats. <b>2022</b> , 23, 7796		O
148	Intestinal inflammation promotes MDL-1+ osteoclast precursor expansion to trigger osteoclastogenesis and bone loss. <b>2022</b> ,		0
147	A Novel Inhibitor INF 39 Promotes Osteogenesis via Blocking the NLRP3/IL-1[Axis. <b>2022</b> , 2022, 1-12		
146	Bone remodeling: an operational process ensuring survival and bone mechanical competence. <b>2022</b> , 10,		7
145	Osteocytes regulate organismal senescence of bone and bone marrow.		
144	Impaired bone strength and bone microstructure in a novel early-onset osteoporotic rat model with a clinically relevant PLS3 mutation.		
143	Clinical Spectrum of Hereditary Hypophosphatemic Rickets With Hypercalciuria (HHRH). <i>Journal of Bone and Mineral Research</i> ,	6.3	
142	Mesenchymal cell-derived Wnt1 signaling regulates subchondral bone remodeling but has no effects on the development of growth plate or articular cartilage in mice. <b>2022</b> , 116497		
141	An in silico model for woven bone adaptation to heavy loading conditions in murine tibia.		O
140	Bone histology in a fossil elephant (Elephas maximus) from Pulau Bangka, Indonesia. 1-12		
139	Induction of a NOTCH3 Lehman syndrome mutation in osteocytes causes osteopenia in male C57BL/6J mice. <b>2022</b> , 162, 116476		O

138	A combined treatment with selective androgen and estrogen receptor modulators prevents bone loss in orchiectomized rats.	O
137	Targeted Deletion of the Claudin12 Gene in Mice Increases Articular Cartilage and Inhibits Chondrocyte Differentiation. 13,	O
136	Prevalence of low bone formation in untreated patients with osteoporosis. 2022, 17, e0271555	O
135	Development of a first-in-class unimolecular dual GIP/GLP-2 analogue, GL-0001, for the treatment of bone fragility.	
134	VEGFA from osteoblasts is not required for lamellar bone formation following tibial loading. <b>2022</b> , 163, 116502	О
133	Effect of fluoride on bone and growth plate cartilage. <b>2021</b> , 39, 388-399	O
132	Effect of Administration of Azithromycin and/or Probiotic Bacteria on Bones of Estrogen-Deficient Rats. <b>2022</b> , 15, 915	
131	Interest of Bone Histomorphometry in Bone Pathophysiology Investigation: Foundation, Present, and Future. 13,	O
130	Csf1 from marrow adipogenic precursors is required for osteoclast formation and hematopoiesis in bone.	
129	GsR201C and estrogen reveal different subsets of bone marrow adiponectin expressing osteogenic cells. <b>2022</b> , 10,	O
128	Loading-induced bone formation is mediated by Wnt1 induction in osteoblast-lineage cells. <b>2022</b> , 36,	0
127	Bone marrow transplantation as a therapy for autosomal dominant osteopetrosis type 2 in mice. <b>2022</b> , 36,	O
126	MicroRNA-101a enhances trabecular bone accrual in male mice. <b>2022</b> , 12,	
125	FOXO1 differentially regulates bone formation in young and aged mice. 2022, 110438	O
124	A TrkB agonist prodrug prevents bone loss via inhibiting asparagine endopeptidase and increasing osteoprotegerin. <b>2022</b> , 13,	1
123	Reactivation of Bone Lining Cells are Attenuated Over Repeated Anti-sclerostin Antibody Administration.	
122	Toll-like receptor 4 signaling in osteoblasts is required for load-induced bone formation in mice.	
121	Periodontitis may impair the homeostasis of systemic bone through regulation of gut microbiota in ApoE //Imice.	O

120	A Novel Nanostructured Surface on Titanium Implants Increases Osseointegration in a Sheep Model. <b>2022</b> , Publish Ahead of Print,	0
119	Biphasic regulation of osteoblast development via the ERK MAPKhTOR pathway. 11,	1
118	Ano5 modulates calcium signaling during bone homeostasis in gnathodiaphyseal dysplasia. <b>2022</b> , 7,	
117	Milk kefir therapy improves the skeletal response to resistance exercise in rats submitted to glucocorticoid-induced osteoporosis. <b>2022</b> , 167, 111921	O
116	Mussaendoside O, a N-triterpene cycloartane saponin, attenuates RANKL-induced osteoclastogenesis and inhibits lipopolysaccharide-induced bone loss. <b>2022</b> , 105, 154378	
115	Unfavorable effects of sodium-glucose cotransporter 2 (SGLT2) inhibitors on the skeletal system of nondiabetic rats. <b>2022</b> , 155, 113679	1
114	A novel murine model of combined insulin-dependent diabetes and chronic kidney disease has greater skeletal detriments than either disease individually. <b>2022</b> , 165, 116559	0
113	Distinct Responses of Modeling- and Remodeling-Based Bone Formation to the Discontinuation of Intermittent Parathyroid Hormone Treatment in Ovariectomized Rats.	O
112	Inhibition of Neddylation Suppresses Osteoclast Differentiation and Function In Vitro and Alleviates Osteoporosis In Vivo. <b>2022</b> , 10, 2355	1
111	Low energy availability reduces bone mass and gonadal function in male mice.	O
110	FlexMetric bone marrow aspirator yields laboratory and clinically improved results from mesenchymal stem and progenitor cells without centrifugation.	0
109	Loss of early B cell protein B decreases bone mass and accelerates skeletal aging. 13,	O
108	Bone characteristics in condylar hyperplasia of the temporomandibular joint: a microcomputed tomography, histology, and Raman microspectrometry study. <b>2022</b> ,	0
107	Loss of Vhl alters trabecular bone loss during S. aureus osteomyelitis in a cell-specific manner. 12,	O
106	Immediate to short-term inflammatory response to biomaterial implanted in calvarium of mice.	0
105	Complement receptor C5aR1 on osteoblasts regulates osteoclastogenesis in experimental postmenopausal osteoporosis. 13,	O
104	Sustained Morphine Delivery Suppresses Bone Formation and Alters Metabolic and Circulating miRNA Profiles in Male C57BL / 6J Mice.	0
103	MiR-539-3p impairs osteogenesis by suppressing Wnt interaction with LRP-6 co-receptor and subsequent inhibition of Akap-3 signaling pathway. 13,	O

102	Validating Causal Diagrams of Human Health Risks for Spaceflight: An Example Using Bone Data from Rodents. <b>2022</b> , 10, 2187	1
101	Leptin and environmental temperature as determinants of bone marrow adiposity in female mice. 13,	O
100	Beta tricalcium phosphate, either alone or in combination with antimicrobial photodynamic therapy or doxycycline, prevents medication-related osteonecrosis of the jaw. <b>2022</b> , 12,	0
99	Mesenchymal cell TRPM7 expression is required for bone formation via the regulation of chondrogenesis. <b>2022</b> , 116579	3
98	A neuronal action of sirtuin 1 suppresses bone mass in young and aging mice.	О
97	Roxadustat improves renal osteodystrophy by dual regulation of bone remodeling.	O
96	Contact ratio and adaptations in the maxillary and mandibular dentoalveolar joints in rats and human clinical analogs. <b>2022</b> , 136, 105485	О
95	Bone fragility: conceptual framework, therapeutic implications, and COVID-19-related issues. <b>2022</b> , 14, 1759720X2211334	1
94	The concept of robusticity in (palaeo-) anthropology and its broad range of application: a short review. <b>2022</b> , 34,	O
93	Context-Dependent Roles for Toll-Like Receptors 2 and 9 in the Pathogenesis of Staphylococcus aureus Osteomyelitis.	O
92	IL6 gene polymorphism association with calcific aortic valve stenosis and influence on serum levels of interleukin-6. 9,	О
91	Contemporary Advances in Computer-Assisted Bone Histomorphometry and Identification of Bone Cells in Culture.	1
90	Osteocytes regulate senescence of bone and bone marrow. 11,	1
89	Bone vitality and vascularization of mandibular and maxillary bone grafts in maxillary sinus floor elevation: A retrospective cohort study.	O
88	Different Requirements of CBFB and RUNX2 in Skeletal Development Among Calvaria, Limbs, Vertebrae and Ribs. <b>2022</b> , 23, 13299	1
87	Inflammaging and Bone Loss in a Rat Model of Spinal Cord Injury.	O
86	Increased osteoclastogenesis contributes to bone loss in the Costello syndrome Hras G12V mouse model. 10,	O
85	Dysfunction of Caveolae-mediated Endocytic TRI Degradation Results in Hypersensitivity of TGF-ISmad Signaling in Osteogenesis Imperfecta.	O

84	R-spondin 3 deletion induces Erk phosphorylation to enhance Wnt signaling and promote bone formation in the appendicular skeleton. 11,	O
83	Conditional Loss of Nmp4 in Mesenchymal Stem Progenitor Cells Enhances PTH-Induced Bone Formation.	O
82	Low-density lipoprotein receptor deficiency reduced bone mass in mice via the c-fos/NFATc1 pathway. <b>2022</b> , 310, 121073	O
81	Validation of Mct8/Oatp1c1 dKO mice as a model organism for the Allan-Herndon-Dudley Syndrome. <b>2022</b> , 66, 101616	O
80	Collagen cross-link profiles and mineral are different between the mandible and femur with site specific response to perturbed collagen. <b>2022</b> , 17, 101629	0
79	Bone mass loss in chronic heart failure is associated with sympathetic nerve activation. <b>2023</b> , 166, 116596	O
78	Female bone physiology resilience in a past Polynesian Outlier community. 2022, 12,	0
77	VDR activation attenuates osteoblastic ferroptosis and senescence by stimulating the Nrf2/GPX4 pathway in age-related osteoporosis. <b>2022</b> ,	O
76	Protein Kinase G2 Is Essential for Skeletal Homeostasis and Adaptation to Mechanical Loading in Male but not Female Mice.	0
75	Targeting Sclerostin and Dkk1 at Optimized Proportions of Low-Dose Antibody Achieves Similar Skeletal Benefits to Higher-Dose Sclerostin Targeting in the Mature Adult and Aged Skeleton. <b>2022</b> , 13, 1891	O
74	Effect of vitamin D metabolites on bone histomorphometry in healthy black and white women: An attempt to unravel the so-called vitamin D paradox in blacks. <b>2023</b> , 18, 101650	0
73	MORPHOGENESIS OF THE ZERO-STAGE OSTEONECROSIS FORMATION OF THE LOWER JAW BASED ON THE USE OF AMINOBISPHOSPHONATES. <b>2022</b> , 18, 235	O
72	Why do State-of-the-art Super-Resolution Methods not work well for Bone Microstructure CT Imaging?. <b>2022</b> ,	0
71	Is Adynamic Bone Always a Disease? Lessons from Patients with Chronic Kidney Disease. <b>2022</b> , 11, 7130	O
70	Comparative Efficiency of Gene-Activated Matrices Based on Chitosan Hydrogel and PRP Impregnated with BMP2 Polyplexes for Bone Regeneration. <b>2022</b> , 23, 14720	1
69	Osteoblast/osteocyte-derived interleukin-11 regulates osteogenesis and systemic adipogenesis. <b>2022</b> , 13,	O
68	Abaloparatide has the same catabolic effects on bones of mice when infused as PTH (1-34).	0
67	Bone loss is ameliorated by fecal microbiota transplantation through SCFA/GPR41/IGF1 pathway in sickle cell disease mice. <b>2022</b> , 12,	1

66	Downregulation of the Autism Spectrum Disorder Gene Shank2 Decreases Bone Mass in Male Mice.	0
65	Juvenile Bone Toxicity: Study Considerations, Regulations, and Techniques for Assessment. 109158182	2114530
64	Muscle-derived extracellular vesicles improve disuse-induced osteoporosis by rebalancing bone formation and bone resorption. <b>2022</b> ,	0
63	Differential Expression of Dickkopf 1 and Periostin in Mouse Strains with High and Low Bone Mass. <b>2022</b> , 11, 1840	O
62	Orally administrable peptides derived from egg yolk promote skeletal repair and ameliorate degenerative skeletal disorders in mouse models. <b>2022</b> , 21, 584-595	0
61	Renal osteodystrophy: A historical review of its origins and conceptual evolution. 2022, 17, 101641	Ο
60	Trabecular Bone Volume Is Reduced, With Deteriorated Microstructure, With Aging in a Rat Model of Duchenne Muscular Dystrophy. <b>2022</b> , 44, 323-330	O
59	Neutralization of Staphylococcus aureus Protein A Prevents Exacerbated Osteoclast Activity and Bone Loss during Osteomyelitis.	Ο
58	Bone Turnover Markers: Basic Biology to Clinical Applications.	1
57	Hematopoietic Cytoplasmic Adaptor Protein Hem1 Promotes Osteoclast Fusion and Bone Resorption in Mice. <b>2022</b> , 102841	O
56	Fragile X Messenger Ribonucleoprotein 1 (FMR1), a novel inhibitor of osteoblast/osteocyte differentiation, regulates bone formation, mass, and strength in young and aged male and female mice	0
55	Histological assessment of cortical bone changes in diabetic rats. <b>2022</b> , 17,	O
54	Cissus quadrangularis (Hadjod) Inhibits RANKL-Induced Osteoclastogenesis and Augments Bone Health in an Estrogen-Deficient Preclinical Model of Osteoporosis Via Modulating the Host Osteoimmune System. <b>2023</b> , 12, 216	0
53	Bone Regeneration Guided by a Magnetized Scaffold in an Ovine Defect Model. <b>2023</b> , 24, 747	1
52	Pycnodysostosis in children and adults. <b>2023</b> , 116674	0
51	MarrowQuant 2.0: a digital pathology workflow assisting bone marrow evaluation in experimental and clinical hematology. <b>2023</b> , 100088	Ο
50	Multifunctional barrier membranes promote bone regeneration by scavenging H2O2, generating O2, eliminating inflammation, and regulating immune response. <b>2023</b> , 222, 113147	О
49	Vasohibin-1 promotes osteoclast differentiation in periodontal disease by stimulating the expression of RANKL in gingival fibroblasts. <b>2023</b> , 1869, 166632	O

48	HIF-1Imediates osteoclast-induced disuse osteoporosis via cytoophidia in the femur of mice. <b>2023</b> , 168, 116648	O
47	Colon epithelial cell-specific Bmal1 deletion impairs bone formation in mice. 2023, 168, 116650	O
46	LAMELLAR THICKNESS MEASUREMENTS IN CONTROL AND OSTEOGENESIS IMPERFECTA HUMAN BONE, with development of a method of automated thickness averaging to simplify quantitation <b>2022</b> ,	0
45	Osteocytic Sclerostin Expression as an Indicator of Altered Bone Turnover. <b>2023</b> , 15, 598	O
44	Enhanced Antitumor Efficacy of Radium-223 and Enzalutamide in the Intratibial LNCaP Prostate Cancer Model. <b>2023</b> , 24, 2189	0
43	Dissociation of clinical, laboratory, and bone biopsy findings in adult X-linked hypophosphatemia: altase report.	O
42	The Dietary Fermentable Fiber Inulin Alters the Intestinal Microbiome and Improves Chronic Kidney Disease Mineral-Bone Disorder in a Rat Model of CKD.	0
41	Mitochondrial B-oxidation of adipose-derived fatty acids by osteoblast fuels parathyroid hormone-induced bone formation.	O
40	Deletion of the scavenger receptor Scarb1 in myeloid cells does not affect bone mass. <b>2023</b> , 170, 116702	0
39	Passive Cycle Training Promotes Bone Recovery after Spinal Cord Injury without Altering Resting-State Bone Perfusion. <b>2023</b> , 55, 813-823	O
38	Exposure of suckling rats to hexavalent chromium (CrVI) alters bone formation at the base of the alveolus causing a delay in tooth eruption. <b>2023</b> ,	O
37	Mild Chronic Kidney Disease Associated with Low Bone Formation and Decrease in Phosphate Transporters and Signaling Pathways Gene Expression. <b>2023</b> , 24, 7270	O
36	FBXO11 regulates bone development. <b>2023</b> , 170, 116709	0
35	C3a-C3aR signaling is a novel modulator of skeletal homeostasis. <b>2023</b> , 18, 101662	O
34	Reambulation following hindlimb unloading attenuates disuse-induced changes in murine fracture healing. <b>2023</b> , 172, 116748	0
33	Myricitrin: A Promising Herbal Therapy for Periodontitis in Immunosuppressed Status. 2023,	O
32	Human femur morphology and histology variation with ancestry and behaviour in an ancient sample from Vietnam. <b>2023</b> , 247, 152054	0
31	Advanced Glycation End Products and Bone Metabolism in Patients with Chronic Kidney Disease. <b>2023</b> , 7,	О

30	USP53 Regulates Bone Homeostasis by Controlling Rankl Expression in Osteoblasts and Bone Marrow Adipocytes. <b>2023</b> , 38, 578-596	0
29	Differentiated embryonic chondrocyte expressed gene-1 is a central signaling component in the development of collagen-induced rheumatoid arthritis. <b>2023</b> , 299, 102982	O
28	Periosteal Bone Formation Varies with Age in Periostin Null Mice. 2023, 112, 463-471	0
27	Csf1 from marrow adipogenic precursors is required for osteoclast formation and hematopoiesis in bone. 12,	Ο
26	HSV1716 Prevents Myeloma Cell Regrowth When Combined with Bortezomib In Vitro and Significantly Reduces Systemic Tumor Growth in Mouse Models. <b>2023</b> , 15, 603	0
25	Unexpected Absence of Skeletal Responses to Dietary Magnesium Depletion: Basis for Future Perspectives?. <b>2023</b> , 11, 655	O
24	A Zeb1/MtCK1 metabolic axis controls osteoclast activation and skeletal remodeling. 2023, 42,	0
23	Toll-like receptor 4 signaling in osteoblasts is required for load-induced bone formation in mice. <b>2023</b> , 26, 106304	O
22	Development of a First-in-Class Unimolecular Dual GIP / GLP -2 Analogue, GL -0001, for the Treatment of Bone Fragility.	0
21	Osteocyte-Derived CaMKK2 Regulates Osteoclasts and Bone Mass in a Sex-Dependent Manner through Secreted Calpastatin. <b>2023</b> , 24, 4718	O
20	Quantitative morphometric analysis in tibiofemoral joint osteoarthritis imaging: A literature review. <b>2023</b> , 3, 100088	0
19	Osteocyte apoptosis and cellular micropetrosis signify skeletal aging in type 1 diabetes. 2023,	0
18	Discordant growth of nasal cartilage and bone contributes to phenotypic variability of the skull in a mouse model.	O
17	Exploration of the skeletal phenotype of the Col1a1+/Mov13 mouse model for haploinsufficient osteogenesis imperfecta type 1. 14,	O
16	Sostdc1 Suppression in the Absence of Sclerostin Potentiates Anabolic Action of Cortical Bone in Mice.	0
15	Mouse Models of Mineral Bone Disorders Associated with Chronic Kidney Disease. <b>2023</b> , 24, 5325	O
14	Lrp5 p. Val667Met Variant Compromises Bone Mineral Density and Matrix Properties in Osteoporosis.	О
13	Activated FGFR3 suppresses bone regeneration and bone mineralization in an ovariectomized mouse model. <b>2023</b> , 24,	1

12	Low energy availability reduces bone mass and gonadal function in male mice. 2023, 41, 182-192	0
11	Lactobacillus plantarum LP45 inhibits the RANKL/OPG signaling pathway and prevents glucocorticoid-induced osteoporosis. 67,	O
10	Effect of sclerostin inactivation in a mouse model of severe dominant osteogenesis imperfecta. <b>2023</b> , 13,	0
9	Bone Tissue Evaluation Indicates Abnormal Mineralization in Patients with Autoimmune Polyendocrine Syndrome Type I: Report on Three Cases.	O
8	Resolving trabecular metaphyseal bone profiles downstream of the growth plate adds value to bone histomorphometry in mouse models. 14,	O
7	CCL12 induces trabecular bone loss by stimulating RANKL production in BMSCs during acute lung injury.	O
6	EArrestin 2 knockout prevents bone loss in response to continuous parathyroid hormone stimulation in male and female mice. 1-12	O
5	Osteocytes contribute via nuclear receptor PPAR-alpha to maintenance of bone and systemic energy metabolism. 14,	O
4	Reversal of the diabetic bone signature with anabolic therapies in mice. 2023, 11,	О
3	Iliac bone biopsy and analysis: A clinical, translational, and cadaveric review. <b>2023</b> , 100245	O
2	Effect of aluminum accumulation on bone and cardiovascular risk in the current era. 2023, 18, e0284123	0
1	Delayed cortical bone healing due to impaired nuclear Nrf2 translocation in COPD mice. <b>2023</b> , 173, 116804	O